



**Universidade de Aveiro** Departamento de Química  
2010

**Ana Filipa  
Martins Cláudio  
Da Silva**

**Extracção de Compostos Fenólicos com Sistemas  
Aquosos Bifásicos**

**Extraction of Phenolic Compounds with Aqueous  
Two- Phase Systems**



**Universidade de Aveiro** Departamento de Química  
2010

**Ana Filipa  
Martins Cláudio  
Da Silva**

**Extracção de Compostos Fenólicos com Sistemas  
Aquosos Bifásicos**

**Extraction of Phenolic Compounds with Aqueous  
Two Phase Systems**

Dissertação apresentada à Universidade de Aveiro para cumprimento dos requisitos necessários à obtenção do grau de Mestre em Engenharia Química, realizada sob a orientação científica do Professor Dr. João Manuel da Costa e Araújo Pereira Coutinho, Professor Associado com agregação do Departamento de Química da Universidade de Aveiro, e co-orientação de Dra. Mara Guadalupe Freire Martins, Estagiária de Pós-Doutoramento no Instituto de Tecnologia Química e Biológica, ITQB2, Universidade Nova de Lisboa.

Dedico este trabalho às pessoas mais importantes da minha vida: à minha mãe, ao meu pai, ao Paulo e à mana.

## **o júri**

presidente

**Prof. Doutor Dmitry Victorovitch Evtuygin**  
Professor Associado com Agregação da Universidade de Aveiro

**Prof. Doutor João Manuel da Costa e Araújo Pereira Coutinho**  
Professor Associado com Agregação da Universidade de Aveiro

**Doutor José Manuel da Silva Simões Esperança**  
Investigador Auxiliar no Instituto de Tecnologia Química e Biológica, ITQB2,  
Universidade Nova de Lisboa

**Doutora Mara Guadalupe Freire Martins**  
Estagiária de Pós-Doutoramento no Instituto de Tecnologia Química e Biológica,  
ITQB2, Universidade Nova de Lisboa

## **Agradecimentos**

Antes de mais, um especial agradecimento ao Professor João Coutinho, por acreditar em mim e me ter convidado para o mundo da investigação que desde o início tanto me fascinou, e contribuiu para o meu crescimento profissional e pessoal. Agradeço a todos os membros dos Path (Pedro Carvalho, Maria Jorge, Sónia Ventura, Mariana Belo, Bernd, Luciana, Mara Freire e Jorge Pereira) e mini Path (Rita Teles, Anabel, Rute, Marta, Vanda, Catarina Neves, Catarina Varanda, Samuel, Joel, Sílvia, Francisca, Rita Brites e Ana Maria) pelos lanches, cafezinhos, apoio, ensinamentos e pelo espírito de inter-ajuda. Não posso deixar de dizer um obrigado especial à Luciana, por ter sido a primeira pessoa do grupo a trabalhar comigo; à Mara, pelo tanto que me ensinou, corrigiu, apoiou, incentivou, e me fez pensar, bem como pela maneira fantástica como vê as coisas, mesmo quando todos os resultados parecem estar mal! Muito obrigado também à Sónia e ao Jorge pelo apoio incondicional, pelas dicas, pelos almoços, jantares, gargalhadas e ajuda a todos os níveis. Obrigado Rita Teles e Anabel pela amizade e apoio. Um especial obrigado também à Ana Maria pelo que me ajudou. Não posso deixar de agradecer aos “amigos de Aveiro” (Filipe, Susana, Joana, Ana Catarina,...), aos “amigos de Ovar” e aos “amigos mais crescidos” que foram muito importantes para mim, neste ano, devido à compreensão, amizade e demonstração de carinho que tiveram para comigo. Por último, e por serem as pessoas mais especiais da minha vida, tenho que agradecer muito à minha mãe por ter aturado o meu mau-humor, pelo apoio incondicional e por acreditar em mim; À Inês por ser a mana mais fantástica e dedicada, e pela loiça que lavou na minha vez; Ao meu pai e à Maria José pelo apoio e compreensão; aos meus “futuros sogros” pelo carinho e ajuda incansável; à tia Bélinha pelas perguntas que me faziam pensar, pelo apoio e pelos risos que me ajudavam a descontrair. Ao meu querido namorado pelo apoio total e absoluto, por compreender todas as minhas decisões, por nunca me ter deixado desistir, pelos choros que aguentou, pelas gargalhadas que fez dar, pelas horas ao computador a ajudar-me a trabalhar, por tudo! Obrigado do fundo de coração a todas estas pessoas, ao resto da família e a outras que se cruzaram comigo neste ano cheio de emoções que tanto me ajudou a crescer a nível profissional e pessoal.

**Palavras-chave** Sistemas aquosos bifásicos, líquidos iônicos, compostos fenólicos, vanilina, ácido gálico, extração, coeficientes de partição, diagramas de fase.

**Resumo** Nos últimos anos, os sistemas aquosos bifásicos (ATPS), utilizando líquidos iônicos, têm revelado um enorme potencial no desenvolvimento de novas técnicas de separação e purificação de biomoléculas, mantendo as suas características funcionais intactas.

Neste trabalho, os coeficientes de partição da vanilina e ácido gálico, dois compostos fenólicos com aplicações e propriedades antioxidantes bem conhecidas, foram determinados recorrendo a ATPS envolvendo líquidos iônicos. Foram avaliadas três condições no processo de partição da vanilina: natureza catiónica e aniónica do líquido iónico (LI), a temperatura de equilíbrio e a concentração de vanilina adicionada ao sistema. Todos os parâmetros demonstraram influenciar a partição da vanilina entre as duas fases aquosas. Para obter informação termodinâmica sobre o processo de partição, foram determinadas as funções termodinâmicas molares de transferência da vanilina. Os resultados indicaram que a partição da vanilina resulta essencialmente de um balanço de contribuições entálpicas e entrópicas, onde aniões e catiões mais complexos do LI desempenham um papel crucial. Foram também determinadas duas propriedades termofísicas para estes sistemas, viscosidade e densidade, às mesmas composições às quais se determinaram os coeficientes de partição.

Na partição do ácido gálico, foram avaliados diferentes LIs e a influência do pH do meio aquoso por adição de sais inorgânicos distintos. Estes dois parâmetros demonstraram influenciar fortemente a capacidade de extração dos ATPS estudados. Dada a escassez dos diagramas de fase envolvendo sistemas aquosos de LIs e  $\text{Na}_2\text{SO}_4$ , os diagramas ternários correspondentes a cada LI, e respectivas tie-lines e comprimentos destas, foram também determinados a 298 K. Em todos os sistemas estudados e em todas as condições testadas, tanto a vanilina como o ácido gálico, mostraram sofrer uma migração preferencial para a fase rica em LI. Com base neste trabalho, pode-se afirmar que os novos ATPS propostos apresentam uma elevada eficiência de extração para compostos fenólicos constituindo assim uma nova plataforma para processos de separação.

**Keywords**

Aqueous two-phase systems, ionic liquids, phenolic compounds, vanillin, gallic acid, extraction, partition coefficients, phase diagrams.

**Abstract**

In recent years, ionic-liquid-based aqueous two-phase systems (ATPS) have been object of great interest due to their potential for the design of new “green” separation processes, in particular for the purification and separation of biomolecules, maintaining their functional characteristics unchanged.

In this work, the partition coefficients of vanillin and gallic acid, two well known phenolic compounds, were determined using improved ionic-liquid-based ATPS. Three parameters were evaluated in the vanillin partitioning process: the ionic liquid (IL) cation and anion nature, the temperature of equilibrium and the concentration of vanillin in the system. All parameters have shown to influence the vanillin partitioning. In an attempt to elucidate the thermodynamics of the partitioning process, the standard molar thermodynamic functions of transfer of vanillin were also determined. The results indicated that the partition of vanillin results from an interplay between enthalpic and entropic contributions where both the IL anion and more complex cations play an essential role. Moreover, viscosities and densities of both aqueous phases were experimentally measured at the mass fraction compositions for which the partition coefficients were determined.

Regarding the partitioning of gallic acid, different ILs and the influence of the aqueous medium pH, achieved by the addition of distinct inorganic salts, were evaluated. These two parameters have shown to strongly influence the extraction ability by IL-based ATPS. Due to the lack of the ternary phase diagrams compositions containing ILs and the salt  $\text{Na}_2\text{SO}_4$ , the respective individual phase diagrams, tie-lines and tie-line lengths, were additionally determined at 298 K.

In all systems and conditions tested, both vanillin and gallic acid preferentially migrated to the IL-rich phase. The new proposed ATPS present large extraction efficiencies for phenolic compounds and represent a new platform for separation techniques.

## Contents

Contents.....	I
List of Tables.....	III
List of Figures.....	IV
Notation.....	VI
List of symbols.....	VI
List of Abbreviations.....	VII
1. Introduction.....	1
1.1. Scopes and Objectives.....	2
1.2. Ionic Liquids.....	3
1.3. Extraction of Biomolecules Using Aqueous Two-Phase Systems (ATPS).....	6
1.4. Phenolic compounds (PhCs).....	8
2. Extraction of vanillin in ATPS with ILs.....	12
2.1. Vanillin.....	13
2.2. Experimental Section.....	17
2.2.1. Materials.....	17
2.2.2. Experimental procedure.....	19
2.3. Results and Discussion.....	21
2.3.1. Effect of IL Ions in Vanillin Partitioning.....	21
2.3.2. Effect of Temperature in Vanillin Partitioning.....	24
2.3.3. Effect of Concentration in Vanillin Partitioning.....	27
2.3.4. Density and Viscosity.....	28
2.4. Conclusions.....	36
3. Extraction of gallic acid in ATPS with ILs.....	37
3.1. Gallic Acid.....	38
3.2. Experimental section.....	40
3.2.1. Chemicals.....	40

3.2.2.	3.2.2. <i>Experimental procedure</i> .....	42
3.3.	Results and Discussion.....	45
3.3.1.	Phase Diagrams.....	45
3.3.2.	Effect of IL ions and pH in the acid gallic partitioning .....	51
3.4.	Conclusions.....	56
4.	Future work.....	57
5.	References .....	59
	List of Publications .....	67
	Appendix A .....	69
	A.1. Calibration curve for vanillin .....	70
	A.2. Calibration curve for gallic acid.....	71
	Appendix B.....	72
	Experimental data for the vanillin partition coefficients, density and viscosity .....	73
	Appendix C.....	79
	van't Hoff plots.....	80
	Appendix D .....	81
	Experimental binodal curve mass fraction compositions .....	82
	Appendix E.....	87
	Experimental data of TL .....	88
	Appendix F.....	89
	Experimental data for the gallic acid partition coefficients .....	90

## List of Tables

Table 1: Thermophysical properties of vanillin. <sup>[89, 92]</sup> .....	13
Table 2: Standard molar thermodynamic functions of transfer of vanillin at 298.15 K. ....	26
Table 3: Thermophysical properties of gallic acid. <sup>[92, 117]</sup> .....	38
Table 4: Initial weight fraction compositions for the determination of the phase diagrams and indication of the possibility of existing liquid-liquid equilibrium. ....	46
Table 5: Adjusted Parameters used to describe the experimental binodal data by Equation 5. ....	49
Table 6: pH values as function the different systems performed.....	54

## List of Figures

Figure 1: Number of articles published <i>per</i> year concerning ILs. Data taken from IsiWeb of Knowledge in 9 <sup>th</sup> May, 2010.....	3
Figure 2: Cationic structures of nitrogen-based ILs. ....	4
Figure 3: Structure of some phenolic compounds. ....	8
Figure 4: Chemical structure of vanillin. ....	13
Figure 5: Production of vanillin from eugenol. ....	14
Figure 6: Production of vanillin from sulfonated lignin fragments. ....	14
Figure 7: Lignin precursors: alcohols <i>p</i> -coumaryl, coniferyl and sinapyl, respectively. ....	15
Figure 8: Chemical structure of the studied ILs: (i) [C <sub>2</sub> mim]Cl; (ii) [C <sub>4</sub> mim]Cl; (iii) [C <sub>6</sub> mim]Cl; (iv) [C <sub>7</sub> mim]Cl; (v) [C <sub>10</sub> mim]Cl; (vi) [amim]Cl; (vii) [C <sub>7</sub> H <sub>7</sub> mim]Cl; (viii) [OHC <sub>2</sub> mim]Cl; (ix) [C <sub>4</sub> mim]Br; (x) [C <sub>4</sub> mim][CH <sub>3</sub> SO <sub>3</sub> ]; (xi) [C <sub>4</sub> mim][CH <sub>3</sub> CO <sub>2</sub> ]; (xii) [C <sub>4</sub> mim][CH <sub>3</sub> SO <sub>4</sub> ]; (xiii) [C <sub>4</sub> mim][CF <sub>3</sub> SO <sub>3</sub> ]; (xiv) [C <sub>4</sub> mim][N(CN) <sub>2</sub> ]. ....	18
Figure 9: ATPS formed by IL + K <sub>3</sub> PO <sub>4</sub> + H <sub>2</sub> O.....	19
Figure 10: Partition coefficients of vanillin in chloride-based ILs + K <sub>3</sub> PO <sub>4</sub> ATPS at 298.15 K.....	22
Figure 11: Partition coefficients of vanillin in [C <sub>4</sub> mim]-based ILs + K <sub>3</sub> PO <sub>4</sub> ATPS at 298.15 K.....	23
Figure 12: Partition coefficients of vanillin in IL + K <sub>3</sub> PO <sub>4</sub> ATPS as a function of temperature for the ILs: [C <sub>4</sub> mim]Cl, [C <sub>4</sub> mim][CH <sub>3</sub> SO <sub>4</sub> ], [C <sub>7</sub> H <sub>7</sub> mim]Cl and [amim]Cl.....	25
Figure 13: Partition coefficients of vanillin in IL + K <sub>3</sub> PO <sub>4</sub> ATPS as a function of initial vanillin concentration for the ILs: [C <sub>4</sub> mim]Cl, [C <sub>4</sub> mim][CH <sub>3</sub> SO <sub>4</sub> ] and [C <sub>7</sub> H <sub>7</sub> mim]Cl. ....	27
Figure 14: Experimental viscosity ( $\eta$ ) for the IL-rich phase (full symbols) and K <sub>3</sub> PO <sub>4</sub> -rich phase (open symbols) for systems composed by chloride-based ILs + K <sub>3</sub> PO <sub>4</sub> + H <sub>2</sub> O as a function of temperature. ....	29
Figure 15: Experimental viscosity ( $\eta$ ) for the IL-rich phase (full symbols) and K <sub>3</sub> PO <sub>4</sub> -rich phase (open symbols) for systems composed by [C <sub>4</sub> mim]-based ILs + K <sub>3</sub> PO <sub>4</sub> + H <sub>2</sub> O as a function of temperature. ....	31
Figure 16: Experimental density ( $\rho$ ) for the IL-rich phase (full symbols) and K <sub>3</sub> PO <sub>4</sub> -rich phase (open symbols) for systems composed by chloride-based ILs + K <sub>3</sub> PO <sub>4</sub> + H <sub>2</sub> O as a function of temperature. ....	33
Figure 17: Experimental density ( $\rho$ ) for the IL-rich phase (full symbols) and K <sub>3</sub> PO <sub>4</sub> -rich phase (open symbols) for systems composed by [C <sub>4</sub> mim]-based ILs + K <sub>3</sub> PO <sub>4</sub> + H <sub>2</sub> O as a function of temperature. ....	34

Figure 18: Chemical structure of gallic acid. ....	38
Figure 19: Chemical structure of the studied ILs: (i) [C <sub>7</sub> mim]Cl; (ii) [C <sub>8</sub> mim]Cl; (iii) [C <sub>4</sub> mim]Br; (iv) [C <sub>4</sub> mim][CH <sub>3</sub> SO <sub>4</sub> ]; (v) [C <sub>4</sub> mim][CF <sub>3</sub> SO <sub>3</sub> ]; (vi) [C <sub>4</sub> mim][N(CN) <sub>2</sub> ]; (vii) [C <sub>2</sub> mim][CF <sub>3</sub> SO <sub>3</sub> ]; (viii) [C <sub>7</sub> H <sub>7</sub> mim] [C <sub>2</sub> H <sub>5</sub> SO <sub>4</sub> ]; (ix) [C <sub>4</sub> mim][TOS]; (x) [C <sub>4</sub> mim] [C <sub>2</sub> H <sub>5</sub> SO <sub>4</sub> ]; (xi) [C <sub>8</sub> py][N(CN) <sub>2</sub> ]; (xii) [C <sub>7</sub> H <sub>7</sub> mim]Cl. ....	41
Figure 20: Experimental determination of the binodal curves for the aqueous systems IL-Na <sub>2</sub> SO <sub>4</sub> : in the first picture it is shown a limpid and clear solution while in the second picture it denotes a cloudy solution. ....	42
Figure 21: Ternary phase diagrams for all the ILs studied at 298 K and atmospheric pressure.....	47
Figure 22: Phase diagrams for the different ternary systems composed by IL+ Na <sub>2</sub> SO <sub>4</sub> + H <sub>2</sub> O at 298 K and atmospheric pressure: ♦, experimental binodal data; □, TL data; — fitting of experimental data by the method proposed by Merchuck et al. <sup>[127]</sup> .....	51
Figure 23: Partition coefficients of gallic acid for different ILs + Na <sub>2</sub> SO <sub>4</sub> ATPS at 298.15 K.....	52
Figure 24: Partition coefficients of gallic acid in IL + different inorganic salt ATPS for the ILs: [C <sub>2</sub> mim][CF <sub>3</sub> SO <sub>3</sub> ], [C <sub>4</sub> mim][CF <sub>3</sub> SO <sub>3</sub> ] and [C <sub>7</sub> mim]Cl. ....	53
Figure 25: Partition coefficients of gallic acid in IL + K <sub>2</sub> HPO <sub>4</sub> /KH <sub>2</sub> PO <sub>4</sub> ATPS for [C <sub>4</sub> mim][CF <sub>3</sub> SO <sub>3</sub> ] at 25 wt % and 30 wt %. ....	54

## Notation

### List of symbols

$\Delta_{\text{tr}}G_{\text{m}}^0$	Standard molar Gibbs energy of transfer
$\Delta_{\text{tr}}H_{\text{m}}^0$	Standard molar enthalpy of transfer
$\Delta_{\text{tr}}S_{\text{m}}^0$	Standard molar entropy of transfer
wt %	Weight percentage
$K_{\text{GA}}$	Partition coefficient of gallic acid
$K_{\text{Van}}$	Partition coefficient of vanillin
$R$	Universal gas constant
$R^2$	Correlation coefficient
$T$	Temperature
$X_{\text{B}}$	Inorganic salt weight percentage in the bottom phase
$X_{\text{M}}$	Inorganic salt weight percentage in the mixture
$X_{\text{T}}$	Inorganic salt weight percentage in the top phase
$Y_{\text{B}}$	Ionic liquid weight percentage in the bottom phase
$Y_{\text{M}}$	Ionic liquid weight percentage in the mixture
$Y_{\text{T}}$	Ionic liquid weight percentage in the top phase
$\alpha$	Ratio between the mass of the top phase and the total mass of the mixture
$\eta_{\text{B}}$	Viscosity of the bottom phase
$\eta_{\text{T}}$	Viscosity of the top phase
$\rho_{\text{B}}$	Density of the bottom phase
$\rho_{\text{T}}$	Density of the top phase
$\sigma$	Standard deviation
$w_1$	Mass fraction composition of IL
$w_2$	Mass fraction composition of Na <sub>2</sub> SO <sub>4</sub>

### *List of Abbreviations*

ATPS	Aqueous two-phase systems
BOD	Biochemical oxygen demand
DNA	Desoxyribonucleic acid
ILs	Ionic liquids
LLE	Liquid-liquid equilibrium
PEG	Polyethylene glycol
PhCs	Phenolic compounds
TL	Tie-line
TLC	Thin layer chromatography
TLL	Tie-line length
UV	Ultra-violet
VOCs	Volatile organic compounds
[GA]	Concentration of gallic acid
[GA] <sub>IL</sub>	Concentration of gallic acid in the IL-rich aqueous phase
[GA] <sub>X</sub>	Concentration of gallic acid in the inorganic salt-rich aqueous phase
[Van]	Concentration of vanillin
[Van] <sub>IL</sub>	Concentration of vanillin in the IL- rich aqueous phase
[Van] <sub>K<sub>3</sub>PO<sub>4</sub></sub>	Concentration of vanillin in the K <sub>3</sub> PO <sub>4</sub> -rich aqueous phase
[C <sub>2</sub> mim]Cl	1-ethyl-3-methylimidazolium chloride
[C <sub>2</sub> mim][CH <sub>3</sub> SO <sub>4</sub> ]	1-ethyl-3-methylimidazolium methylsulfate
[C <sub>2</sub> mim][CF <sub>3</sub> SO <sub>3</sub> ]	1-ethyl-3-methyl-imidazolium trifluoromethanesulfonate
[C <sub>4</sub> mim]Cl	1-butyl-3-methylimidazolium chloride
[C <sub>4</sub> mim][CH <sub>3</sub> SO <sub>3</sub> ]	1-butyl-3-methylimidazolium methanesulfonate
[C <sub>4</sub> mim][CF <sub>3</sub> SO <sub>3</sub> ]	1-butyl-3-methyl-imidazolium trifluoromethanesulfonate

[C <sub>4</sub> mim][CH <sub>3</sub> SO <sub>4</sub> ]	1-butyl-3-methylimidazolium methylsulfate
[C <sub>4</sub> mim][C <sub>2</sub> H <sub>5</sub> SO <sub>4</sub> ]	1-butyl-3-methylimidazolium ethylsulfate
[C <sub>4</sub> mim][N(CN) <sub>2</sub> ]	1-butyl-3-methylimidazolium dicyanamide
[C <sub>4</sub> mim][CH <sub>3</sub> CO <sub>2</sub> ]	1-butyl-3-methylimidazolium acetate
[C <sub>4</sub> mim]Br	1-butyl-3-methylimidazolium bromide
[C <sub>4</sub> mim][HSO <sub>4</sub> ]	1-butyl-3-methylimidazolium hydrogensulfate
[C <sub>4</sub> mim][TOS]	1-butyl-3-methylimidazolium tosylate
[C <sub>6</sub> mim][Cl]	1-hexyl-3-methylimidazolium chloride
[C <sub>7</sub> mim]Cl	1-heptyl-3-methylimidazolium chloride
[C <sub>8</sub> mim]Cl	1-octyl-3-methylimidazolium chloride
[C <sub>10</sub> mim]Cl	1-decyl-3-methylimidazolium chloride
[amim]Cl	1-allyl-3-methylimidazolium chloride
[amim][C <sub>2</sub> H <sub>5</sub> SO <sub>4</sub> ]	1-allyl-3-methylimidazolium ethylsulfate
[OHC <sub>2</sub> mim]Cl	1-hydroxyethyl-3-methylimidazolium chloride
[C <sub>7</sub> H <sub>7</sub> mim]Cl	1-benzyl-3-methylimidazolium chloride
[C <sub>7</sub> H <sub>7</sub> mim][C <sub>2</sub> H <sub>5</sub> SO <sub>4</sub> ]	1-benzyl-3-methylimidazolium ethylsulfate
[C <sub>4</sub> mpy]Cl	1-butyl-3-methylpyridinium chloride
[C <sub>4</sub> mpip]Cl	1-butyl-3-methylpiperidinium chloride
[C <sub>4</sub> mpyrr]Cl	1-butyl-3-methylpyrrolidinium chloride
[C <sub>8</sub> py][N(CN) <sub>2</sub> ]	1-octylpyridinium dicyanamide

# **1. Introduction**

## **1.1. Scopes and Objectives**

This work aims at studying the extraction of phenolic compounds (PhCs). Trying to develop more benign extraction techniques than those used nowadays, in this work, a study was conducted using aqueous two phase systems (ATPS) composed by ionic liquids (ILs) and typical inorganic salts. The PhCs studied as partitioning molecules, and as examples of this general group, were vanillin and gallic acid. PhCs present general attractive properties, such as their antioxidant, anti-inflammatory, anti-microbial and anticarcinogenic capacities, among others.<sup>[1-4]</sup> Due to these interesting properties, PhCs have gained a special importance in food, wine, dietary and pharmaceutical industries.<sup>[5-6]</sup>

The use of conventional volatile organic compounds (VOC's) in extraction procedures brings up some associated problems such as toxicity, volatility and flammability, and implies additional environmental hazards. Moreover, some of these solvents can denature biomolecules and thus influence their quality and purity.<sup>[7-8]</sup> Currently ILs appear as a potential and alternative replacement for VOC's due to their negligible vapor pressures and intrinsic character of "designer solvents". The properties of ILs can be tuned by the proper choice of the cation and/or anion, allowing the optimization of the physical and chemical characteristics that best adapt to a particular process. The negligible vapor pressures makes also of ILs excellent candidates as alternatives to VOC's by decreasing atmospheric pollution concerns.<sup>[9-10]</sup>

Concerning the vanillin extraction, several parameters that could affect the solute extraction were studied in ternary systems composed by imidazolium-based ILs, water and  $K_3PO_4$ , namely the influence of the IL cation and anion nature, the temperature of extraction and the accessible concentration of vanillin. Moreover, viscosities and densities of both the  $K_3PO_4$ -rich phase and the IL-rich phase were measured in the temperature range from (298.15 to 318.15) K to evaluate the additional advantages of using IL-based ATPS.

The extraction of gallic acid was studied in ternary systems composed by imidazolium-based ILs,  $Na_2SO_4$  and water. Due to the lack in literature of ternary phase diagrams containing ILs and the salt  $Na_2SO_4$ , the individual phase diagrams, tie-lines and tie-line lengths were additionally determined at 298 K. Both IL cation and anion nature were evaluated through the partitioning of gallic acid. It is well known that the partitioning of an acidic solute is largely affected by the pH of the system, and as a result, further partition coefficients were also determined in aqueous systems formed by IL- $K_3PO_4$  and IL- $K_2HPO_4/KH_2PO_4$ . The pH of each equilibrated phase was measured and reported.

## 1.2. Ionic Liquids

Ionic liquids (ILs) are compounds usually constituted by large and organic cations and organic or inorganic anions with their melting points, by general definition, below 100 °C.<sup>[11-13]</sup> The low symmetry, weak intermolecular interactions and a large distribution of charge in the ions is the cause of the low melting points.<sup>[14-15]</sup>

ILs were first reported at the beginning of the 20<sup>th</sup> century by Paul Walden,<sup>[16]</sup> when testing new explosive compounds with the aim of replacing nitroglycerin. Walden synthesized ethylammonium nitrate, [EtNH<sub>3</sub>][NO<sub>3</sub>] and found that it had a melting point around 13-14 °C.<sup>[15]</sup> The discovery of a liquid salt did not received much attention at that time. In 1934, Charles Graenacher<sup>[17]</sup> filled the first patent for an industrial application for ILs regarding the preparation of cellulose solutions. Later, during the World War II, ILs were again investigated and new patents were filled<sup>[18-19]</sup> concerning the application of mixtures of aluminium chloride (III) and 1-ethylpyridinium bromide to the electrodeposition of aluminium. Despite these findings, only in a recent past these compounds have been extensively studied, and as can be seen in Figure 1, publications regarding ILs exponentially increased from 1990 to 2009.

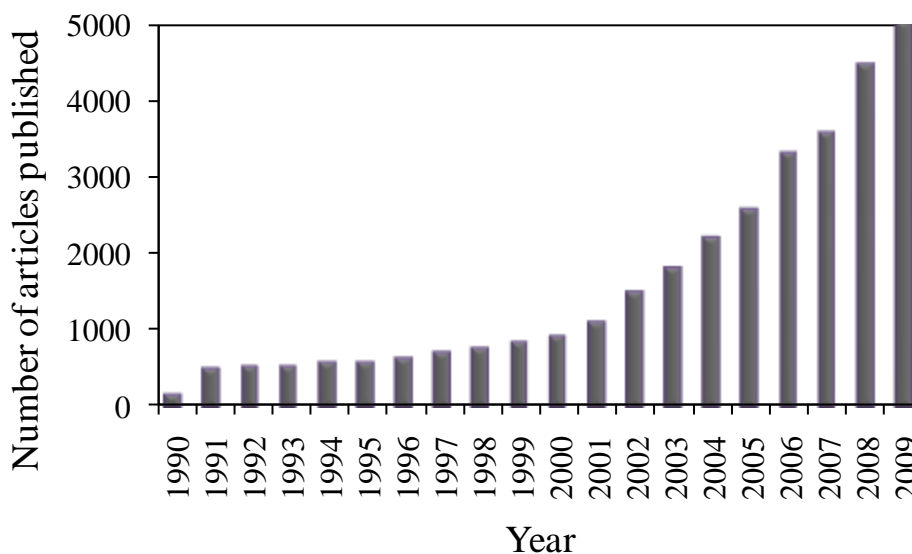


**Figure 1:** Number of articles published *per* year concerning ILs. Data taken from IsiWeb of Knowledge in 9<sup>th</sup> May, 2010.

Among a large range of ILs that can be synthesized the most commonly studied are the nitrogen-based ILs, namely pyrrolidinium-, imidazolium-, piperidinium-, pyridirium-, and ammonium-based ILs, with their general cationic structures depicted in Figure 2. The cation can be highly complex with different sizes for the alkyl side chains, different substitution positions and also additional functional groups.<sup>[20]</sup>

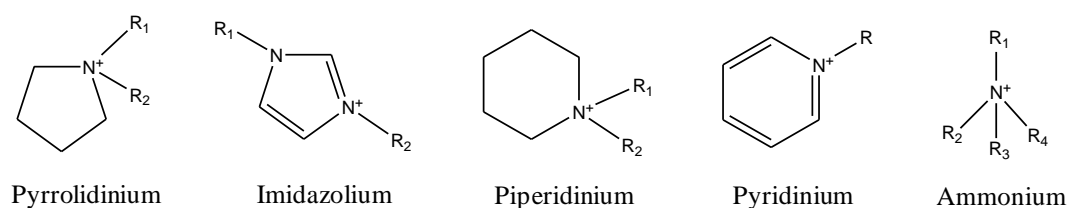


**Figure 2:** Cationic structures of nitrogen-based ILs.

Due to the ionic nature of ILs, they present several physical and chemical advantages over conventional and molecular organic solvents, namely negligible flammability and vapour pressure, high solvation ability, high chemical stability, high selectivity, excellent microwave-absorbing ability, and easiness in recovery and recycling.<sup>[5, 9, 21-24]</sup> Apart from these advantages, many organic, organometallic and inorganic compounds can be dissolved in ILs.<sup>[25]</sup> ILs have also been increasingly applied in catalysis<sup>[26]</sup>, organic synthesis<sup>[21]</sup>, chemical reactions<sup>[14]</sup>, multiphase bioprocess operations<sup>[27]</sup>, electrochemistry<sup>[28]</sup>, chromatographic separations<sup>[29]</sup>, mass spectrometry analysis<sup>[30]</sup>, batteries and in fuel cells investigation<sup>[31]</sup> and in the separation of biomolecules.<sup>[32]</sup> Beyond these applications, ILs have also been used in liquid-liquid extractions of metal ions<sup>[33-34]</sup> and organic compounds.<sup>[35-37]</sup> Indeed, there are great interest on the application of ILs for the removal of organic contaminants from aqueous solutions and in the use of ILs as solvents for multiphase biotransformation reactions.<sup>[37-38]</sup>

It was already shown that most ILs do not inactivate enzymes ensuring their structural integrity and enzymatic activity, and therefore ILs represent a good alternative to the usual solvents in biocatalysis.<sup>[7, 22]</sup> The ILs may allow an improved recovery of biomolecules when carrying liquid-liquid extractions while reducing solvent emissions.

Since the ILs physicochemical properties are strongly dependent on the IL nature, the possibility of changing their properties through the manipulation of the ions that compose them, represents an important and supplementary advantage. This property - the “tunnability” - makes of ILs singular compounds that can be designed with precise conditions for a particular process, as well as to manipulate their extraction capabilities for specific biomolecules.<sup>[14, 23, 32]</sup>

In spite of the ILs potential environmental benefits as “green” replacements over conventional volatile organic solvents, their toxicity must also be here discussed. Several studies<sup>[39-44]</sup> were conducted to evaluate the toxicity of ILs, combining different anions and cations, as well as changing the alkyl group chain length and number of alkyl groups substituted at the cation ring. These studies revealed that ILs toxicity is primordially determined by the cation nature and it is directly correlated with the length of the side alkyl chain and number of alkyl groups. Commonly,

the anion has a smaller influence than the cation, and generally short cation alkyl chains or hydrophilic ILs present low or no toxicity.<sup>[41]</sup>

Usually, the ILs aqueous solubility decrease with the alkyl chain length increase, which for its turn is positive because the more toxic ILs (higher alkyl chain lengths) are poorly water soluble at room temperature, minimizing thus the environmental impact of ILs in aquatic streams.<sup>[41]</sup> The choice of the IL anion and cation determines the thermophysical properties of such fluids, and it was already shown that the anion strongly influences their water miscibility.<sup>[41, 45]</sup> The influence of the cation alkyl chain length in the water solubility was also observed, but it can be considered minor when compared with the anion influence.<sup>[45]</sup>

### **1.3. Extraction of Biomolecules Using Aqueous Two-Phase Systems (ATPS)**

There are two main processes commonly used to extract (bio)compounds from a liquid phase to another: liquid-liquid extraction using immiscible solvents and aqueous two-phase systems (ATPS). These are formed when two mutually incompatible, though both miscible with water, are dissolved in water.

Liquid-liquid extraction processes are used for the purification of biomolecules due to their high effectiveness, high yield, improved purity degree, proper selectivity, technological simplicity and low cost, and also to a good combination between the recovery and purification steps.<sup>[7, 32, 46]</sup> The extraction of biomolecules is usually carried out using organic solvents because of their immiscibility with aqueous media.<sup>[47]</sup> The most common organic solvents used present some disadvantages, such as high volatility and toxicity and the possibility of denaturing biomolecules, which in turn may influence the quality and purity of these to be recovered.<sup>[7]</sup>

Aiming at avoiding the use of organic solvents as the extractive phase, several attempts have been carried out employing ATPS. Separation of biological molecules and particles using ATPS dates to 1958 and were introduced by P. A. Albertsson.<sup>[48]</sup> ATPS consist in two aqueous-rich phases containing polymer/polymer, polymer/salt or salt/salt combinations.<sup>[49]</sup> The basis of separation of (bio)molecules in a two-phase system results from their equilibration and selective distribution between the two liquid aqueous phases.<sup>[50]</sup>

For a while ATPS were used only in laboratories but by their simplicity, biocompatibility, and ease of scale-up operations, their use has expanded to large-scale (bio)separations.<sup>[50]</sup> Furthermore, it was already shown that it is possible to recover and separate a wide range of biomaterials using ATPS, such as plant and animal cells, microorganisms, proteins, among others.<sup>[48, 51-54]</sup> From the industrial point view, ATPS extraction represent no major problems because engineering and existing equipments are easily adapted to the requirements. Indeed, a number of proteins are purified by this process at an industrial level.<sup>[50]</sup>

Common ATPS are usually formed by polyethylene glycol (PEG) because it easily forms a biphasic system with inorganic salts and neutral polymers in aqueous solutions. Some hydrophilic polymers are immiscible among them. The separation of phases coexists in the equilibrium between them, and with each phase containing predominantly water and one of the polymers. The water mixed with polymers acts as the major solvent and can establish non-covalent bonds with them. These interactions increase with the molecular weight of the polymers, and phase separation can occur at very low polymer concentrations due to the loss of entropy in the demixing process.<sup>[55-56]</sup> On the other hand, the presence of an inorganic salt in critical concentrations in a

single polymer-water system can also lead to the formation of two distinct aqueous phases, where usually the lower phase is rich in the inorganic salt, while the upper phase is rich in polymer. The phase separation certainly depends on the type of inorganic salt and respective concentration (for example,  $K_2HPO_4$ ,  $K_3PO_4$ ,  $K_2CO_3$ ,  $KOH$ ,  $Na_2HPO_4$  and  $Na_2SO_4$  are typical inorganic salts employed).<sup>[53, 56]</sup> In general, both phases are composed by approximately 70-90 % of water, which means that biomolecules are not easily denatured, constituting therefore an important advantage when the goal is to extract proteins and/or enzymes.<sup>[50, 57]</sup> It should be pointed out that the partitioning of a biomolecule in ATPS can vary depending on the biomolecule size, surface properties, molecular weight, temperature, pH, net charge, among others.<sup>[58]</sup> In both type of ATPS mentioned, the interactions between a biomolecule and the distinct phases could involve hydrogen bonds, van der Waals-, dispersive-, and electrostatic-interactions, as well as steric-, and conformational effects.<sup>[32, 53]</sup>

To improve the extraction efficiency, the replacement of ordinary organic solvents by ILs has been suggested as a promising alternative. Organic solvents may be substituted directly using hydrophobic ILs as a second immiscible liquid phase with aqueous media<sup>[59]</sup> or by the use of ATPS incorporating hydrophilic ILs.<sup>[8, 32, 49, 60-61]</sup> The second approach is more used because ATPS containing hydrophilic ILs have shown to be more effective in extracting biomolecules.<sup>[32, 59]</sup>

Gutowski et al.<sup>[60]</sup> were the first to show that aqueous solutions of imidazolium-based ILs can form ATPS in presence of aqueous solutions of certain inorganic salts, such as  $K_3PO_4$ . Since then, the equilibrium properties of systems comprising ILs, for the development of specific extraction and isolation procedures, have been investigated.<sup>[41-42, 59, 61-65]</sup> It was already shown that ATPS formed by  $K_3PO_4$  and ILs are extremely advantageous for the partitioning of several biomolecules yielding larger partition coefficients than those conventionally obtained with polymers-inorganic salts or polymers-polysaccharides ATPS.<sup>[32, 49, 61]</sup> The extractive potential of biomolecules using IL-based ATPS was previously studied for distinct compounds, such as testosterone and epitestosterone, alkaloids, antibiotics, bovine serum albumin, penicillin G, L-tryptophan and food colorants<sup>[12, 32, 49, 57, 61, 66-68]</sup>. These results clearly indicated an attractive prospective of IL-based ATPS for biomolecules separation and purification.<sup>[32, 49]</sup> The effect of inorganic salts on ATPS formation has already been widely studied<sup>[12, 57, 60, 69-70]</sup> while demonstrating to follow the Hofmeister series<sup>[71]</sup> (classification of ions based on their salting-out/-in ability). Concerning the ILs in a previous work<sup>[32]</sup> it was shown that the ability of an IL to form ATPS is related with the decrease in the hydrogen bond accepting strength or the increase in the hydrogen bond basicity of the IL anion.

## 1.4. Phenolic compounds (PhCs)

Phenolic compounds, PhCs, are compounds constituted by at least one phenol group, *i.e.*, a benzene ring with a hydroxyl group (-OH). Examples of these compounds are vanillic, gallic, protocatechuic, ellagic, syringic, caffeic, gentisic and ferulic acids, and quercetin, vanillin and resveratrol, among others. These compounds may be present in natural sources such as wood, fruits and vegetables.<sup>[1-2, 6, 72-73]</sup> Some of these examples are depicted in Figure 3.

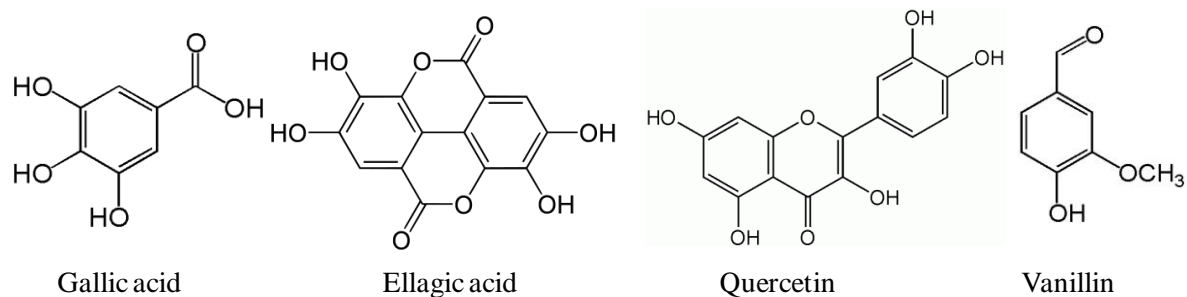


**Figure 3:** Structure of some phenolic compounds.

PhCs present redox properties that allow them to act as hydrogen donors and singlet oxygen quenchers. Since redox reactions involve the transport of electrons, PhCs present antimicrobial action.<sup>[73]</sup> The oxidation of unsaturated fats by free radicals, such as reactive oxygen species, can cause biological changes inside the human body, namely heart disease, arthritis, cellular degeneration related to aging, changes in DNA and even cancer. The antioxidant action of PhCs protects cells by neutralizing free radicals as oxygen free radicals and by decomposing peroxides.<sup>[74-75]</sup> Indeed, in literature,<sup>[76-77]</sup> it was already shown the ability of PhCs to protect cells from oxidative stress.

PhCs have particular characteristics of utmost importance. Besides their high antioxidant capacity, they are also phytotoxic and toxic to bacteria, and used thus in biological wastewater treatments, and present toxicity against human promyelocytic leukemia cells.<sup>[1-2, 4]</sup> A previous study<sup>[73]</sup> revealed that the antimicrobial action of PhCs is independent of pH. PhCs can also act as prooxidants rather than antioxidants, depending on their concentration and free radical source. Therefore, the cytotoxicity of PhCs is linked to their prooxidant properties.<sup>[4]</sup>

The presence of PhCs in plants represents the major source of these compounds from biomass, and some benefits, besides the antioxidant activity, are attributed to them, such as the ability of lowering cholesterol, depression of hypertension, protection against cardiovascular disease, among others.<sup>[78]</sup>

Due to these properties PhCs have been object of special interest in food, wine, dietary and pharmaceutical industries.<sup>[5-6]</sup>

Wood is composed by cellulose, hemicelluloses, lignin and extractables. It is a renewable raw material resource (biomass) and can be used for the production of new materials, energy and several chemical products. Nowadays, wood plays a key role in the production of various commodities and have progressively replaced some products from the petrochemical industry. The PhCs present in the extractables play an important role in the protection of wood against microbiological harm or insect attacks. Moreover, PhCs also contribute to the natural color of wood. Main products such as gallic and ellagic acid, and sugars can be produced from hydrolysable tannins.<sup>[79]</sup>

Besides the presence of PhCs in wood and plants, they can also be found in many residues from the industrial or agricultural activities, such as wastewaters from olive mills. These residues may contain 4-16 % of organic matter, and from which PhCs represent 2-15 %.<sup>[1]</sup>

To decrease the load of organic compounds in effluents, and at the same time add value to the process, there is a growing interest in their extraction both from natural sources and industrial or agricultural waste.<sup>[1]</sup> Concerning this subject, there are some published studies regarding the extraction of phenolic compounds.<sup>[5, 72, 80-90]</sup> It is important to note that depending on the phenolic compound to be extracted, the improved technique or optimum solvent may be quite different. Brudi et al.<sup>[81]</sup> studied the partition coefficients of some aromatic organic substances, such as vanillin and phenol, in a two-phase mixture of water and carbon dioxide. The partition coefficients were determined by the ratio between the mole fraction solubilities between the carbon dioxide and the water phases. The experiments were carried out at high temperature and pressure conditions using carbon dioxide as a supercritical fluid.<sup>[81]</sup> The attained partition coefficients for phenol varied between 0.2 and 1.5.<sup>[81]</sup> On the other hand, the partition coefficients of vanillin ranged between 0.2 and 3. An increase in temperature was found to decrease the partition coefficients.<sup>[81]</sup> Adrian et al.<sup>[80]</sup> investigated the partition coefficients of vanillin and caffeine in an high pressure multiphase equilibrium system. The system was composed by carbon dioxide, water, propanol and a small concentration of the partitioning solute.<sup>[80]</sup> The authors reported that vanillin preferentially migrates for the organic phase ( $K_{\text{van}} \geq 1$ ) and that an increase in pressure increases the partition coefficients of both solutes.<sup>[80]</sup> Following the approach of high pressure systems, also Kim et al.<sup>[87]</sup> studied the extraction of phenolic compounds (*p*-hydroxybenzaldehyde, vanillic acid, syringic acid, vanillin, acetovanillone, and feruric acid) by pressurized low-polarity water (PLPW).

Regarding organic-aqueous two phases systems and to evaluate the PhCs environmental impact, Noubigh et al.<sup>[72]</sup> recently determined the partition coefficients between octanol and water ( $K_{\text{OW}}$ ) for PhCs such as protocatechuic acid, vanillic acid, and vanillin, as a function of temperature, using the slow-stirring method. The  $K_{\text{OW}}$  values of protocatechuic acid, vanillic acid, and vanillin varied between 6.03 and 4.07, 28.84 and 26.18, and 17.78 and 9.77, respectively. In addition, Tarabanko

et al.<sup>[89]</sup> used octylamine-based systems for the extraction of vanillin and found that the distribution ratios increased with the octylamine concentration and in a pH range between 8 and 10. Octylamine provided high distribution ratios, and when using moderate concentrations of octylamine and high pH values, high extraction selectivities could be achieved.<sup>[89]</sup> Moreover it was also found that the extraction of vanillin decreases with the use of additional anti-solvents, such as hexane, toluene, benzene, dichloroethane and chloroform.<sup>[89]</sup>

Horax et al.<sup>[85]</sup> extracted phenolics compounds from pericarp and seeds of bitter melons with ethanol and water systems. The extraction efficiency of PhCs was found to change with the ethanol concentration.<sup>[85]</sup> Moreover, Trabelsi et al.<sup>[90]</sup> investigated several solvents and/or mixtures of solvents on the phenolic compounds extraction efficiencies. The extraction ability of solvents for the extraction of phenolic compounds from leaves decreased in following order: methanol > ethanol/water > acetone/water > methanol/water > methanol/HCl  $\approx$  acetone >> methanol/ethanol/acetone  $\approx$  water > hexane > ethanol.<sup>[90]</sup> In this study it was found that more polar solvents are more efficient in the extraction of PhCs compounds.<sup>[90]</sup> These results are in agreement with others in literature<sup>[84, 88]</sup>, where it was shown that methanol is an improved extractive phase compared to ethanol. In addition, others authors<sup>[83]</sup> investigated the extraction of PhCs from different natural sources using water and organic solvents mixtures, namely acetone/water/acetic acid and ethyl acetate/methanol/water. The authors concluded that the solvent employed has a substantial influence through the extraction of PhCs compounds from *Quercus coccifera* L. and *Juniperus phoenicea* L.<sup>[83]</sup> Following the same type of studies, Khokhar<sup>[91]</sup> postulated that water is the best extracting solvent for PhCs from tea catechins when compared with solutions of 80 % (v/v) of methanol or 70 % (v/v) of ethanol.

Jadhav et al.<sup>[86]</sup> performed a study with the goal of comparing conventional soxhlet and ultrasound-assisted extraction of vanillin from vanilla pods. Also the solvent influence was assessed and it was found that the extraction of vanillin decreases in the following rank: ethanol > methanol > acetone > acetonitrile > chloroform > hexane.<sup>[86]</sup> Again the results obtained revealed that polar solvents are more indicated for the extraction of PhCs.<sup>[86]</sup> Comparing both techniques, the ultrasound-assisted extraction was found to be more efficient.<sup>[86]</sup> In addition to the extractions with pure solvents, mixtures of water–ethanol were also studied.<sup>[86]</sup> The results indicated that the extraction of vanillin from cured vanilla beans was greatly influenced by the mixture composition, where a maximum in extraction was achieved with a mixture composed by 50 % (v/v) of ethanol.<sup>[86]</sup>

Hasmann et al.<sup>[82]</sup> have used aqueous two-phase systems composed by two thermoseparating copolymers (ethylene oxide and propylene oxide) to remove phenolic compounds from hemicellulosic hydrolysate (from rice straw). In this study<sup>[82]</sup> several parameters were evaluated, such as the copolymer molecular weight and the mass fraction compositions of the system. The

thermoseparation was carried out resulting in the formation of a two-phases system consisting of a top copolymer-rich phase and a bottom hydrolysate-rich phase.<sup>[82]</sup> The extraction efficiencies of PhCs varied from 6 % to 80 % depending on the copolymer employed. Curiously, in a system containing 50 wt % of the copolymer with the higher molecular mass, it was not observed the extraction of PhCs due to an high increase in the viscosity of the system. Also, higher mass fraction contents of copolymer (more than 35 wt %) were found unfavorable for PhCs extraction in the studied ATPS.<sup>[82]</sup> Moreover, the use of ILs for the extraction of PhCs from medicinal plants was already studied by Du et al.<sup>[5]</sup> using microwave-assisted extraction (MAE). When comparing the extraction efficiencies between ILs aqueous solutions and pure water, the extraction yields of polyphenolic compounds are greatly improved by the addition of ILs.<sup>[5]</sup> Indeed, no major differences were found in the extraction efficiencies between methanol and ILs aqueous solutions. In the optimized conditions, the extraction yields of the polyphenolic compounds varied between 79.5 % and 93.8 % in an one-step extraction. Using different ILs it was also concluded that cations, and especially the anions of ILs, affect the extraction efficiencies of polyphenolic compounds.

## **2. Extraction of vanillin in ATPS with ILs**

## 2.1. Vanillin

Vanillin, 3-methoxy-4-hydroxybenzaldehyde, presents the chemical formula  $\text{CH}_3\text{O}(\text{OH})\text{C}_6\text{H}_3\text{CHO}$ , and its appearance is a white crystalline powder with an intense and pleasant odor. This biomolecule is relatively soluble in chloroform, ether and water at room temperature. The properties of vanillin are reported in Table 1.

**Table 1:** Thermophysical properties of vanillin.<sup>[89, 92]</sup>

Molar mass ( $\text{g}\cdot\text{mol}^{-1}$ )	Density ( $\text{g}\cdot\text{cm}^{-3}$ )	Melting point (K)	Boiling point (K)	Solubility in water ( $\text{g}\cdot\text{dm}^{-3}$ )	$\text{pK}_a$
152.15	2.056 at 298 K	353-354	558	10 at 298 K	8.2 at 298 K

Vanillin, Figure 4, is a biomolecule relevant for several purposes, whose recovery and purification by cost-effective and environmentally-safe processes is still of major interest. In 1858, Goble<sup>[93-96]</sup> isolated all the components of vanilla detecting that vanillin is the major compound and that confers to it the well known organoleptic properties. Therefore, vanillin is one of the mostly appreciated fragrant substances aiming at creating artificial aromas in a wide range of commercial products. Vanillin or vanilla are currently used in foods, beverages, livestock fodder and pharmaceutical products, as well as in the fragrance industry with the aim of creating perfumes, or masking unpleasant odors, and cleaning products.<sup>[97]</sup> Beyond these aroma and fragrance applications, vanillin is also used as a chemical intermediate in the production of pharmaceuticals and fine chemicals for use in biocides (due to its phenolic character) and specialty chemicals in technical applications, such as TLC (thin layer chromatography).<sup>[72, 98]</sup>

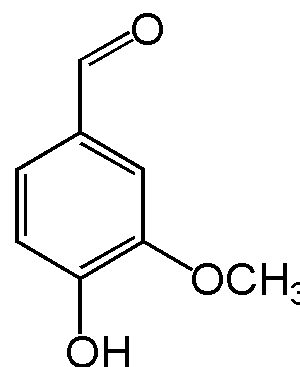


**Figure 4:** Chemical structure of vanillin.

Due to the scarcity of vanillin in natural sources, the synthesis and complex routes for the extraction of this compound were explored.<sup>[98]</sup> Initially, between 1874 and 1920<sup>[98-99]</sup>, the synthesis of vanillin resulted from the reaction involving eugenol compounds taken from oil of cloves. The reaction<sup>[98]</sup> that occurs to generate vanillin from eugenol is given by:

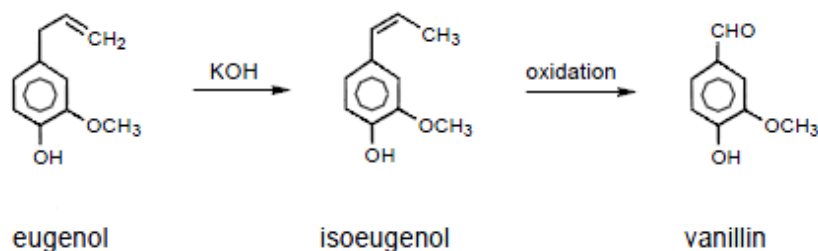


**Figure 5:** Production of vanillin from eugenol.

Other later alternatives relayed on the synthesis of vanillin from guaiacol and/or lignin.<sup>[98]</sup> In the paper production, lignin is withdrawn and so, it is a byproduct of the paper industry. Lignin is a component of wood and typically represents 30 % of its constitution.<sup>[79]</sup> The first signs of producing vanillin from lignin-containing wastes date to 1875 through an anonymous report.<sup>[100]</sup> Years later, Grafe<sup>[101]</sup> confirmed such point through the pyrolysis of dried waste sulfite liquor.<sup>[98]</sup> After this report,<sup>[100]</sup> this method of synthesizing vanillin was further explored by several researchers. Howard,<sup>[102]</sup> and other researchers from the United States, patented some methods in order to concentrate the lignin present in the pulping waste. Tomlinson and Hibbert<sup>[103]</sup> revealed that the yield of vanillin obtained depends on the source of the liquor and on the degree of lignin sulfonation. The authors<sup>[103]</sup> were able to demonstrate that vanillin can be recovered up to 2.6 g·dm<sup>-3</sup> (5.9 % of the lignin content) from waste sulfite liquor. Later, Freudenberg<sup>[104]</sup> proved that the oxidation of lignin from softwoods results in the formation of vanillin, and yielding 10 % using air, or 20–30 % using nitrobenzene as oxidant.<sup>[79]</sup> Despite the higher yield that was obtained with the use of nitrobenzene, these findings were unappealing from the commercial point of view because of the need to deal with the co-produced nitrobenzene.<sup>[98]</sup>

To reaction for synthesizing vanillin from the sulfonated lignin fragment from the purified liquors can be described by:<sup>[98]</sup>

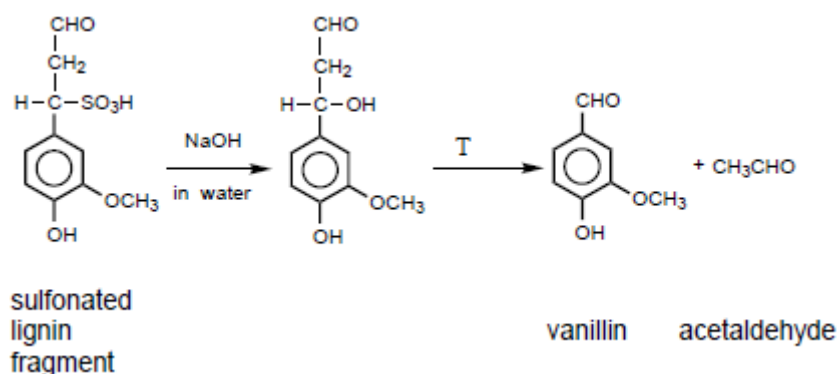


**Figure 6:** Production of vanillin from sulfonated lignin fragments.

In 1936, in North America, the production of vanillin from the lignin-containing waste liquor ("brown liquor"), acquired at the sulfite process, was largely explored using the methodology proposed by Howard.<sup>[105]</sup> Consequently, in the following years, two production-scale plants were built in Ontario, Canada.<sup>[98]</sup> In 1937 it was built the Howard Smith Paper Mills Ltd., in Cornwall, Ontario, based on the study developed the McGill University<sup>[106]</sup>. In 1945, in Thorold, Ontario, it has been created another vanillin-from-lignin production unit through the study conducted by Ontario Pulp and Paper in the 1940s.<sup>[98]</sup> By this implementation at the industrial scale, vanillin became more abundant and less expensive. Indeed, in 1981, a single plant of pulp in Ontario produced 60 % of worldwide vanillin consumed. In this plant, the synthesis of vanillin results from an initial fermentation that uses some fermentable sugars usually present in spent acid sulfite pulping. During the fermentation black liquor alkaline oxidation, the oxidation product stream is extracted with toluene and further back-extracted with aqueous sodium hydroxide. These steps generate an aqueous solution of crude sodium vanillate which is further purified *via* the carbonyl sulfite by the addition of aqueous sulfur dioxide. The soluble additional compounds are separated from acetovanillone and other insoluble phenolic impurities by filtration. In order to produce a product for typical use in the food industry it is also necessary to reprecipitate vanillin from this aqueous solution.<sup>[98]</sup>

The vanillin synthesized through the appropriate treatment of sulfite liquor waste is produced from guaiacyl units of lignin, which is sulfonated and solubilized in the process of transforming wood into chemical pulp to produce paper. To have a high yield of vanillin, the wood used in the chemical process must be of the softwood type (this type of wood is the main precursor of coniferyl alcohol and thus has more guaiacyl units to produce vanillin - called the G lignin (Guaiacyl lignin)). In hardwood the precursor coniferyl and sinapyl alcohol create the GS lignin (Syringyl-Guaiacyl lignin), whose percentage of units of guaiacyl is very low when compared to softwoods.<sup>[79, 98]</sup> The lignin precursors are shown in Figure 7.

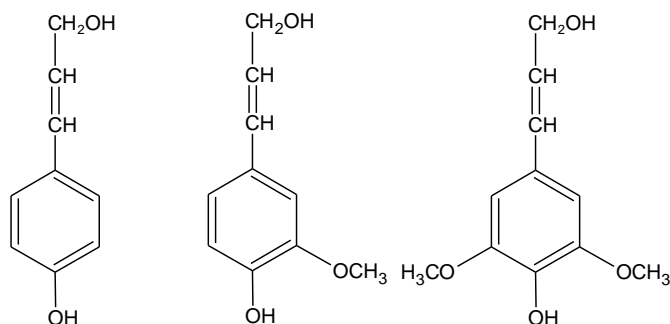


**Figure 7:** Lignin precursors: alcohols *p*-coumaryl, coniferyl and sinapyl, respectively.

After alkaline oxidation, in liquor pulping, vanillin is majorly obtained from softwoods (25 %), unlike to what happens for hardwoods, where the alkaline oxidation leads mainly to the production of syringic aldehyde and to a lower percentage of vanillin.

Although the previous approaches have indicated the synthesis of vanillin from the purified liquor (without sugars) from the acid sulfite method, it should be pointed out that it is also possible to obtain vanillin performing an extraction with an alcohol from the pre-concentrated spent black liquor of kraft (sodium hydroxide and sodium sulfide based).<sup>[107]</sup>

As main disadvantage, lignin-based vanilla is believed to have a richer flavor than the vanilla-based oil. This fact results from the presence of acetovanillone in the lignin-derived products. This compound is an impurity that is not present in vanillin synthesized *via* guaiacol.<sup>[97]</sup>

Initially, the development of methods for the synthesis of vanillin from waste sulfite liquor presented main advantages due to the low contents of solubilized sugars and lignin content (biochemical oxygen demand or BOD properties) of the spent liquor. Nevertheless, after the vanillin recovery process there is the further need of removing  $\approx 160$  kg of "liquid caustic" *per* each kilogram of vanillin produced, making therefore the process not sustainable as it was seemed *a priori*. As a result, residual vanillin-from-lignin plants in Canada and United States, such as the Thorold plant, were closed.<sup>[98]</sup> However, this practice is still under operation in a number of small plants.<sup>[98]</sup> On the other hand, vanillin from guaiacol-based routes is gaining an increasing interest albeit guaiacol is not a renewable source.

The development of new techniques for vanillin separation and purification from several matrices, while maintaining their functional characteristics unchanged, is still ongoing. New and more benign approaches for the selective extraction of vanillin from lignin-containing waste liquor or agricultural or industrial residues should be explored. It should be pointed out that the results presented hereinafter represent a proof of principle of the potential use of IL-based ATPS to carry out such extractions.

## **2.2. Experimental Section**

Attempting at understanding the molecular mechanisms behind the partition of biomolecules in ATPS containing ILs, and to identify the improved ILs for the extraction of PhCs, in this work an extensive study was conducted using vanillin, a phenolic aldehyde, as the partitioning molecule. For that purpose, several extraction parameters were studied in ternary systems composed by imidazolium-based ILs, water and  $K_3PO_4$ , namely the influence of the IL cation and anion, the temperature of extraction and the concentration of vanillin. Moreover, viscosities and densities of both the inorganic salt-rich phase and the IL-rich phase were measured in the temperature range from (298.15 to 318.15) K to evaluate the advantage of using IL-based ATPS.

In this study, the inorganic salt employed for the extractions was  $K_3PO_4$  that confers an alkaline pH to the aqueous system. In the industrial process, based on the lignosulfonate oxidation to originate vanillin, the pH of the medium is also highly alkaline.<sup>[89]</sup>

### **2.2.1. Materials**

Since it is highly difficult to perform measurements through all the possible combinations between cations and anions in ILs it is thus crucial to perform measurements on selective systems aiming at providing results that can be further used as optimized extractions procedures. Therefore, this work evaluated the extraction ability of several IL-based ATPS for vanillin. All ILs studied are based on the imidazolium cation: 1-ethyl-3-methylimidazolium chloride,  $[C_2mim]Cl$ ; 1-butyl-3-methylimidazolium chloride,  $[C_4mim]Cl$ ; 1-hexyl-3-methylimidazolium chloride,  $[C_6mim]Cl$ ; 1-heptyl-3-methylimidazolium chloride,  $[C_7mim]Cl$ ; 1-decyl-3-methylimidazolium chloride,  $[C_{10}mim]Cl$ ; 1-allyl-3-methylimidazolium chloride,  $[amim]Cl$ ; 1-benzyl-3-methylimidazolium chloride,  $[C_7H_7mim]Cl$ ; 1-hydroxyethyl-3-methylimidazolium chloride,  $[OHC_2mim]Cl$ ; 1-butyl-3-methylimidazolium bromide,  $[C_4mim]Br$ ; 1-butyl-3-methylimidazolium methanesulfonate,  $[C_4mim][CH_3SO_3]$ ; 1-butyl-3-methylimidazolium acetate,  $[C_4mim][CH_3CO_2]$ ; 1-butyl-3-methylimidazolium methylsulfate  $[C_4mim][CH_3SO_4]$ ; 1-butyl-3-methylimidazolium trifluoromethanesulfonate,  $[C_4mim][CF_3SO_3]$ ; 1-butyl-3-methylimidazolium dicyanamide,  $[C_4mim][N(CN)_2]$ . The ILs were supplied by Iolitec. To reduce the water and volatile compounds content to negligible values, ILs individual samples were dried under constant agitation at vacuum and moderate temperature ( $\approx 343$  K) for a minimum of 24 hours. After this procedure, the purity of each IL was further checked by  $^1H$ ,  $^{13}C$  and  $^{19}F$  NMR spectra and found to be  $> 99$  wt % for all samples. The inorganic salt  $K_3PO_4$  was from Sigma with a purity level  $> 98$  wt %. Vanillin,  $> 99$  wt % pure, was from Aldrich. The molecular structures of the studied ILs are depicted in Figure 8. The

water employed was double distilled, passed across a reverse osmosis system and further treated with a Milli-Q plus 185 water purification apparatus.

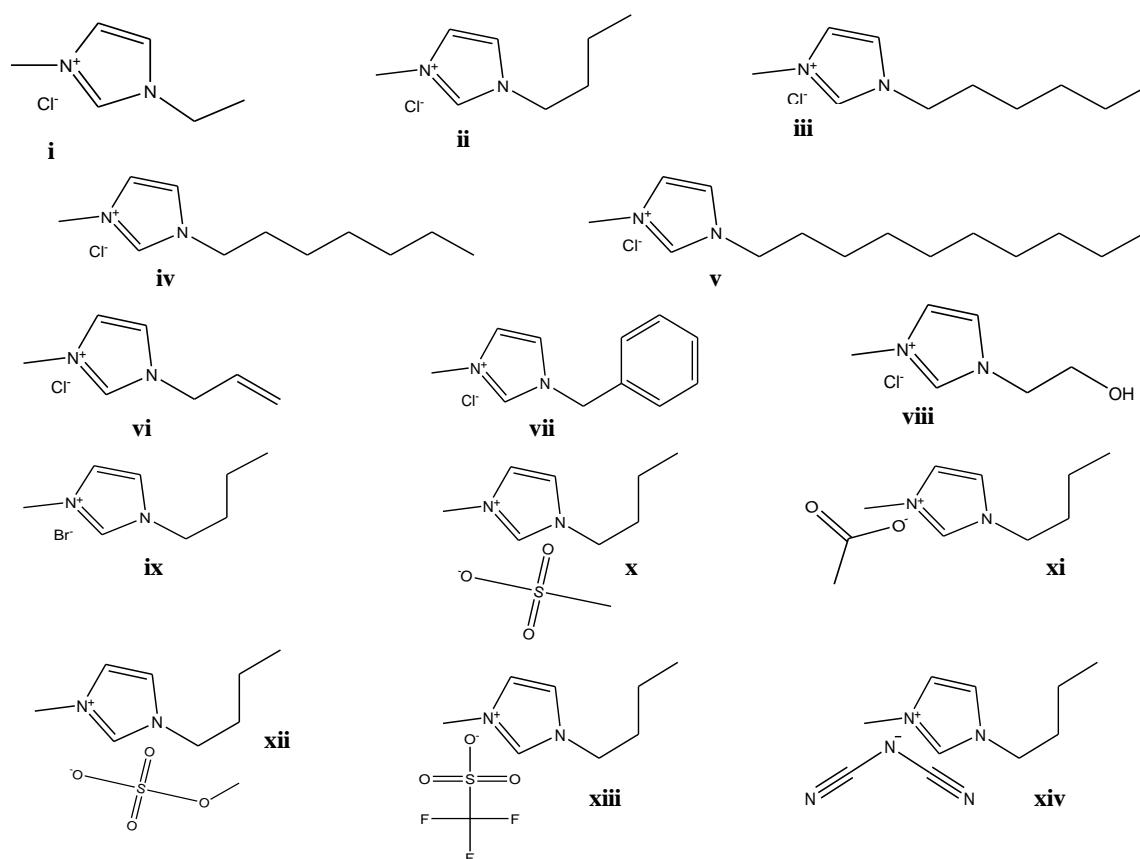


**Figure 8:** Chemical structure of the studied ILs: (i) [C<sub>2</sub>mim]Cl; (ii) [C<sub>4</sub>mim]Cl; (iii) [C<sub>6</sub>mim]Cl; (iv) [C<sub>7</sub>mim]Cl; (v) [C<sub>10</sub>mim]Cl; (vi) [amim]Cl; (vii) [C<sub>7</sub>H<sub>7</sub>mim]Cl; (viii) [OHC<sub>2</sub>mim]Cl; (ix) [C<sub>4</sub>mim]Br; (x) [C<sub>4</sub>mim][CH<sub>3</sub>SO<sub>3</sub>]; (xi) [C<sub>4</sub>mim][CH<sub>3</sub>CO<sub>2</sub>]; (xii) [C<sub>4</sub>mim][CH<sub>3</sub>SO<sub>4</sub>]; (xiii) [C<sub>4</sub>mim][CF<sub>3</sub>SO<sub>3</sub>]; (xiv) [C<sub>4</sub>mim][N(CN)<sub>2</sub>].

## 2.2.2. Experimental procedure

### 2.2.2.1. Vanillin Partitioning

A ternary mixture was prepared within the biphasic region containing 15 wt % of  $K_3PO_4$ , 60 wt % of an aqueous solution of vanillin and 25 wt % of all above mentioned ILs. Only for  $[OHC_2mim]Cl$  a different composition (15 wt % of  $K_3PO_4$ , 40 wt % of IL and 45 wt % of the aqueous solution of vanillin) was used due to the smaller two-phase region obtained within this IL. The ternary mixtures compositions were chosen based on the phase diagrams of each IL- $K_3PO_4$  system reported in previous works.<sup>[32, 49]</sup> For all the ternary mixtures evaluated, and at the compositions used, the top layer is the IL-rich phase while the bottom phase is the  $K_3PO_4$ -rich phase, and as can be seen in Figure 9.

The ternary compositions were prepared by weight with an uncertainty of  $\pm 10^{-5}$  g. The vanillin content influence was studied using different concentrations of the compound at the aqueous phase composition ( $0.5 \text{ g}\cdot\text{dm}^{-3}$ ,  $1.0 \text{ g}\cdot\text{dm}^{-3}$ ,  $2.5 \text{ g}\cdot\text{dm}^{-3}$ ,  $5.0 \text{ g}\cdot\text{dm}^{-3}$  and  $7.5 \text{ g}\cdot\text{dm}^{-3}$  which correspond to  $3.3 \times 10^{-3} \text{ mol}\cdot\text{dm}^{-3}$ ,  $6.6 \times 10^{-3} \text{ mol}\cdot\text{dm}^{-3}$ ,  $1.6 \times 10^{-2} \text{ mol}\cdot\text{dm}^{-3}$ ,  $3.3 \times 10^{-2} \text{ mol}\cdot\text{dm}^{-3}$  and  $4.9 \times 10^{-2} \text{ mol}\cdot\text{dm}^{-3}$ , respectively).

Each mixture (IL,  $K_3PO_4$  and aqueous solution of vanillin) was vigorously stirred and allowed to reach equilibrium by the separation of both phases for 12 h and at the temperature of interest using small ampoules ( $10 \text{ cm}^3$ ) especially built for such extraction procedures. A preliminary study showed that the equilibration of vanillin was attained after a period of 12 h. The time required to establish the equilibrium of vanillin was experimentally determined by measuring the concentration of vanillin in each phase at different times until reproducible data were obtained. The temperatures evaluated were 288.15 K, 298.15 K, 308.15 K, 318.15 K and 328.15 K within an uncertainty of  $\pm 0.01$  K, and attained using an air bath equipped with a Pt 100 probe and a temperature controller or making use of a refrigerated water bath, Julabo F34. After a careful separation of both phases, the amount of vanillin at each aqueous phase was quantified through UV-spectroscopy, using a SHIMADZU UV-1700, Pharma-Spec Spectrometer, at wavelength of 280 nm. Calibration curves were properly established and are reported in Appendix A. At least three individual samples of each phase were quantified in order to determine the vanillin partition coefficients and the respective standard deviations. Possible interferences of both  $K_3PO_4$  and all ILs with the analytical method were investigated and found to be not significant at the working conditions used.

The partition coefficients of vanillin,  $K_{Van}$ , were determined as the ratio of the concentration of vanillin in the IL and in the inorganic salt ( $K_3PO_4$ ) aqueous-rich phases, accordingly to:



**Figure 9:** ATPS formed by IL +  $K_3PO_4$  +  $H_2O$ .

$$K_{\text{Van}} = \frac{[\text{Van}]_{\text{IL}}}{[\text{Van}]_{\text{K}_3\text{PO}_4}} \quad (1)$$

where  $[\text{Van}]_{\text{IL}}$  and  $[\text{Van}]_{\text{K}_3\text{PO}_4}$  are the concentration of vanillin in the IL and in the inorganic salt aqueous rich phases, respectively.

#### **2.2.2.2. Density and Viscosity**

Density and viscosity of the phases formed during the vanillin extraction were measured using an automated SVM 3000 Anton Paar rotational Stabinger viscometer-densimeter in the temperature range from (298.15 to 318.15) K, within  $\pm 0.02$  K. The dynamic viscosity has a relative uncertainty within 0.35 %, while the absolute uncertainty in density is  $\pm 5 \times 10^{-4} \text{ g}\cdot\text{cm}^{-3}$ .

## **2.3. Results and Discussion**

The extraction of a molecule with ATPS strongly depends on the ability to manipulate the physical/chemical properties of the phases aiming at obtaining high partition coefficients and specific selectivity for the biomolecules of interest. Several advances can be used to control the molecules partitioning, such as the chemical nature of the system, temperature of equilibrium, system composition and inclusion of antisolvents, co-solvents or amphiphilic structures. Three process variables were evaluated in this work: the IL cation and anion nature, the temperature of extraction, and the initial concentration of vanillin. To optimize the ILs to be used and operating conditions for the vanillin extraction, it is of high importance to understand the physicochemical issues that rule the biomolecule partitioning between the two equilibrated aqueous-rich phases. The values of the partition coefficients between the two phases result from a complex balance between IL-vanillin,  $K_3PO_4$ -vanillin and water-vanillin interactions and are determined by the relative strengths of the interactions of the biomolecule with each of the compounds present on the system. Taking into account the vanillin and ILs molecular structures depicted in Figure 4 and Figure 8, these interactions may result from dispersive forces, electrostatic interactions, hydrogen-bonding, steric and conformational effects, molecular size and  $\pi \cdots \pi$  stacking between.<sup>[32, 53, 108]</sup> The partitioning of vanillin into one phase requires the disruption of interactions between its components to create a cavity where the solute can be accommodated. It is thus expected that vanillin will partition to a phase where less energy is required to create a cavity and that the new interaction formed between vanillin and its solvation neighbors are indeed more favorable. For all the studied systems it was observed that vanillin preferentially migrates for the IL-rich phase ( $K_{Van} > 1$ ) resulting from the favorable interactions between vanillin and imidazolium-based ILs, and from the lower energy required to create a cavity in the IL-rich phase due to the lower surface tension of this phase.<sup>[109]</sup> The mass fraction compositions used for the determination of each partition coefficient, as well as the partition coefficients values and respective standard deviations, are presented in Appendix B.

### **2.3.1. Effect of IL Ions in Vanillin Partitioning**

In order to evaluate the IL ions influence in the extraction of vanillin several combinations were performed. For the cation influence study, the chloride anion was kept, while combined with the following cations:  $[C_2mim]^+$ ,  $[C_4mim]^+$ ,  $[C_6mim]^+$ ,  $[C_7mim]^+$ ,  $[C_{10}mim]^+$ ,  $[amim]^+$ ,  $[OHC_2mim]^+$  and  $[C_7H_7mim]^+$ . The selected ILs allow the study of the alkyl side chain length effect, as well as the study of additional functional groups. The influence of the IL anion was evaluated through the

use of the  $[C_4mim]^+$  cation combined with the following anions:  $Cl^-$ ,  $Br^-$ ,  $[CH_3CO_2]^-$ ,  $[CH_3SO_3]^-$ ,  $[CF_3SO_3]^-$ ,  $[CH_3SO_4]^-$  and  $[N(CN)_2]^-$ . All of these studies were performed at 298.15 K.

The partition coefficients measured at 298.15 K are presented in Figures 10 and 11 and show that  $K_{Van}$  ranges between 2.72 and 49.59 (at approximately the same mass fraction compositions of IL and inorganic salt).

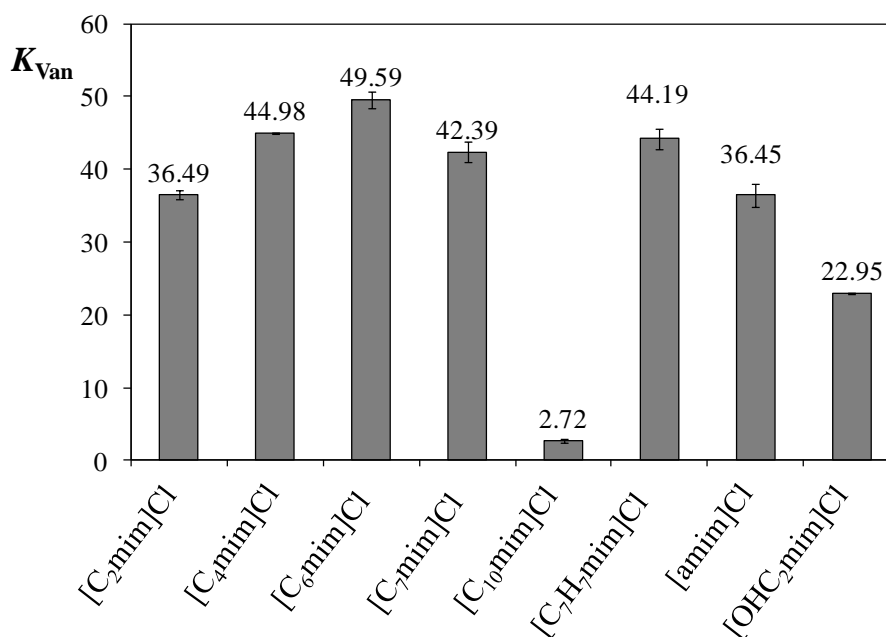


**Figure 10:** Partition coefficients of vanillin in chloride-based ILs +  $K_3PO_4$  ATPS at 298.15 K.

Regarding the IL cation influence, the ability of ILs to extract vanillin follows the order:  $[C_6mim]Cl > [C_4mim]Cl > [C_7H_7mim]Cl > [C_7mim]Cl > [C_2mim]Cl \approx [amim]Cl > [OHC_2mim]Cl \gg [C_{10}mim]Cl$ . Increasing the alkyl side chain of the imidazolium cation there is an increase on the vanillin partition coefficients, reaching a maximum with  $[C_6mim]Cl$ , followed by a decrease until  $[C_{10}mim]Cl$ . Indeed, the lowest partition coefficient of vanillin was observed for the IL with the longest cation alkyl chain length,  $[C_{10}mim]Cl$ . Increasing the size of the alkyl side chain increases the IL free volume, while decreasing the surface tension of the system,<sup>[109]</sup> and thus decreasing the energy of cavity formation to accommodate a vanillin molecule. However, the increase of the alkyl side chain length generates the formation of ILs aggregates in aqueous solutions increasing thus the ILs affinity for water.<sup>[110]</sup> This increase of the alkyl side chain length also promotes a steric hindrance effect that leads to a decrease on the coulombic and polar interactions, while increasing the dispersion interactions, between the IL ions.<sup>[42, 111]</sup> Therefore, these two contributions will act in different directions leading to the observed maximum value on the partition coefficients at about  $[C_6mim]Cl$ .

The presence of a double bond, an aromatic or an hydroxyl group at the imidazolium alkyl chain increases the IL hydrophilicity or the IL affinity for water.<sup>[49]</sup> Nevertheless, the partition coefficients of vanillin were not significantly enhanced using [C<sub>7</sub>H<sub>7</sub>mim]Cl, [amim]Cl or [OHC<sub>2</sub>mim]Cl when compared with the values obtained for [C<sub>7</sub>mim]Cl, [C<sub>4</sub>mim]Cl and [C<sub>2</sub>mim]Cl. Although differences are observed with the IL cation, especially with the alkyl side chain length, the addition of functional groups does not have a particular effect on the partitioning of vanillin. Indeed, only for [C<sub>7</sub>H<sub>7</sub>mim]Cl the partition coefficient increases slightly compared to [C<sub>7</sub>mim]Cl, although they are not statistically different taking into account the associated standard deviations. The results indicate that an increase in the IL cation hydrophilic character by the inclusion of additional functional groups does not improve the vanillin extraction. It seems thus that the cation-anion interaction strengths are the major forces driving the partitioning of vanillin. Weaker coulombic forces allow an easy access of vanillin to interact both with the IL cation and anion.

Regarding the IL anions effect on the vanillin extraction, shown in Figure 11, the following rank was observed: [C<sub>4</sub>mim]Cl > [C<sub>4</sub>mim][N(CN)<sub>2</sub>] > [C<sub>4</sub>mim]Br > [C<sub>4</sub>mim][CH<sub>3</sub>SO<sub>4</sub>] > [C<sub>4</sub>mim][CF<sub>3</sub>SO<sub>3</sub>] > [C<sub>4</sub>mim][CH<sub>3</sub>SO<sub>3</sub>] ≈ [C<sub>4</sub>mim][CH<sub>3</sub>CO<sub>2</sub>].

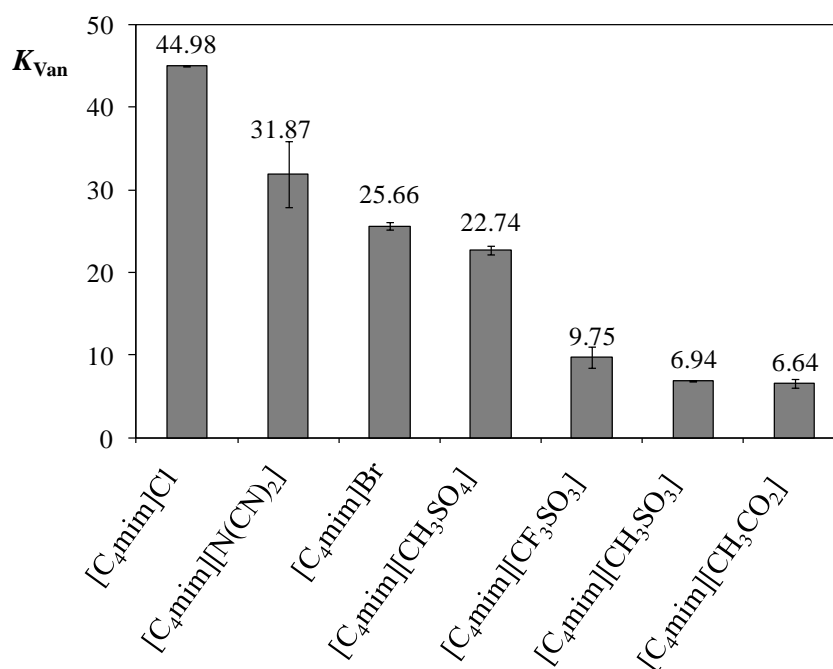


**Figure 11:** Partition coefficients of vanillin in [C<sub>4</sub>mim]-based ILs + K<sub>3</sub>PO<sub>4</sub> ATPS at 298.15 K.

Vanillin partitions preferentially for IL-rich phases composed by halogenated ions, such as Cl<sup>-</sup> or Br<sup>-</sup>, or for ILs comprising anions with a more hydrophobic character and a higher hydrogen

bonding accepting character, such as  $[\text{N}(\text{CN})_2]^-$ . In addition, the fluorination of  $[\text{C}_4\text{mim}][\text{CH}_3\text{SO}_3]$  to a more hydrophobic IL,  $[\text{C}_4\text{mim}][\text{CF}_3\text{SO}_3]$ , enhances the partition coefficients. Finally, the sulfate anion is more effective in extracting vanillin than the sulfonate and acetate anions. Indeed, methanesulfonate and acetate anions are strongly salting-out inducing ions, resulting therefore in lower partition coefficients, and as observed before.<sup>[32]</sup> In general it is observed that vanillin extraction becomes more efficient using IL anions with a salting-in inducing behavior. Ions that usually promote the solutes salting-in increase their partition coefficients in contrast to the salting-out inducing ions that tend to decrease them. Salting-out inducing ions (high charge density ions) have a greater tendency to form hydration complexes, increasing the surface tension of the cavity, and thus decreasing the vanillin partition coefficient. On the other hand, for salting-in inducing ions (low charge density ions) the tendency to form hydration complexes is marginal and thus they tend to stabilize the solutes in solution by specific ion binding to the solute.<sup>[62, 65]</sup>

### ***2.3.2. Effect of Temperature in Vanillin Partitioning***

The effect of temperature on the partition coefficients of vanillin was studied with four ILs:  $[\text{C}_4\text{mim}]\text{Cl}$ ,  $[\text{C}_4\text{mim}][\text{CH}_3\text{SO}_4]$ ,  $[\text{C}_7\text{H}_7\text{mim}]\text{Cl}$  and  $[\text{amim}]\text{Cl}$ . These ILs allowed to study whether the anion and cation suffer different influences under temperature variations. The temperatures evaluated were 288.15 K, 298.15 K, 308.15 K, 318.15 K and 328.15 K. Accordingly to previous studies,<sup>[11, 57, 112]</sup> using IL-based ATPS, the temperature was shown to be either a negligible or a significant factor in the extraction of various types of biomolecules. While He et al.<sup>[12]</sup> indicated that temperature had not significant influence on the distribution behavior of steroids, Pei et al.,<sup>[67]</sup> on the other hand, reported that the temperature greatly influences the extraction efficiency of proteins. As a result it can be established that the partition coefficients dependence on temperature will largely depends on the solute and ternary system under study. The results obtained for the temperature influence on the vanillin partitioning are shown in Figure 12.

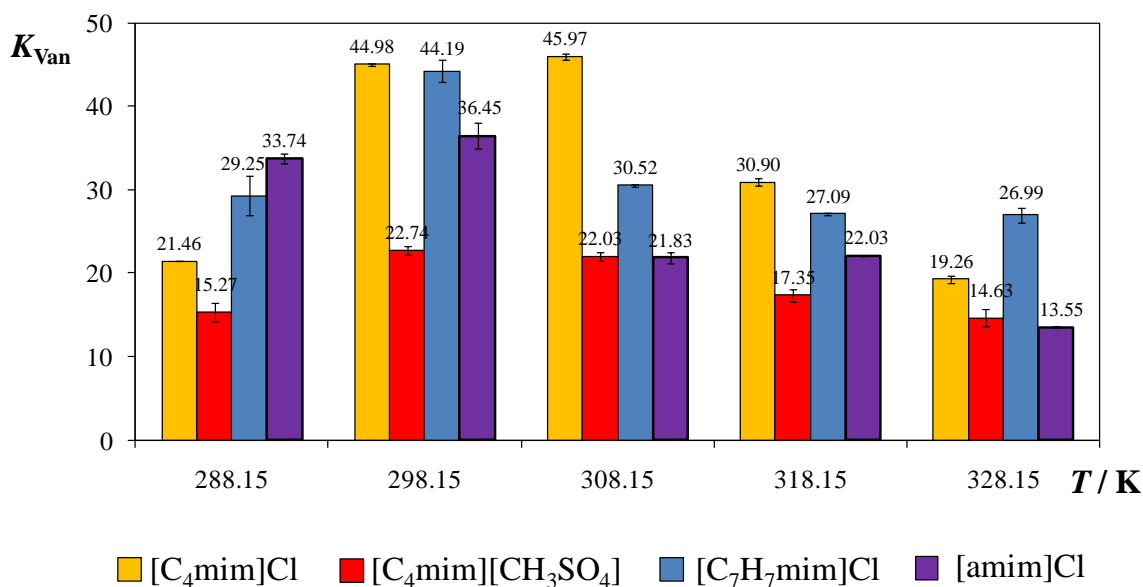


**Figure 12:** Partition coefficients of vanillin in IL + K<sub>3</sub>PO<sub>4</sub> ATPS as a function of temperature for the ILs: [C<sub>4</sub>mim]Cl, [C<sub>4</sub>mim][CH<sub>3</sub>SO<sub>4</sub>], [C<sub>7</sub>H<sub>7</sub>mim]Cl and [amim]Cl.

The results indicate that the temperature greatly influences the vanillin partition. This effect is less pronounced for systems containing the IL [C<sub>4</sub>mim][CH<sub>3</sub>SO<sub>4</sub>]. The [C<sub>4</sub>mim][CH<sub>3</sub>SO<sub>4</sub>], [C<sub>7</sub>H<sub>7</sub>mim]Cl and [amim]Cl systems have an optimum temperature for the extraction of vanillin at 298.15 K while for [C<sub>4</sub>mim]Cl the largest partition coefficient was observed at 308.15 K. Both IL cation and anion contribute for the differences observed in the partition coefficients and their dependence on temperature. The presence of maximum values in the partition coefficients as a function of temperature suggest that the partitioning of vanillin is driven by opposite effects that result from the temperature dependency of the energetic and entropic contributions.

For the systems studied the partition coefficients of vanillin are higher than those observed for the system octanol-water<sup>[72]</sup> that also show a decrease in the partition coefficients of vanillin with temperature in the range between (298.15 and 318.15) K.

In order to calculate the vanillin thermodynamic parameters of transfer, such as the standard molar Gibbs energy ( $\Delta_{tr}G_m^0$ ), the standard molar enthalpy ( $\Delta_{tr}H_m^0$ ), and the standard molar entropy of transfer ( $\Delta_{tr}S_m^0$ ) the van't Hoff approach was used. The plots of  $\ln(K_{Van})$  versus  $T^{-1}$  for the four ILs studied, in the temperature range from 298.15 K to 328.15 K, are provided in Appendix C.

These parameters reveal the association equilibrium between the vanillin composition in two different fluids. The following isochors were used to determine the molar thermodynamic functions of transfer (Eqs. 2 to 4),<sup>[113-114]</sup>

$$\ln(K_{\text{Van}}) = -\frac{\Delta_{\text{tr}}H_{\text{m}}^0}{R} \times \frac{1}{T} + \frac{\Delta_{\text{tr}}S_{\text{m}}^0}{R} \quad (2)$$

$$\Delta_{\text{tr}}G_{\text{m}}^0 = \Delta_{\text{tr}}H_{\text{m}}^0 - T\Delta_{\text{tr}}S_{\text{m}}^0 \quad (3)$$

$$\Delta_{\text{tr}}G_{\text{m}}^0 = -RT \ln(K_{\text{Van}}) \quad (4)$$

where  $K_{\text{Van}}$  is the partition coefficient of vanillin,  $R$  is the universal gas constant ( $8.314 \text{ J}\cdot\text{mol}^{-1}\cdot\text{K}^{-1}$ ),  $T$  is the temperature (K), and  $\Delta_{\text{tr}}H_{\text{m}}^0$ ,  $\Delta_{\text{tr}}S_{\text{m}}^0$  and  $\Delta_{\text{tr}}G_{\text{m}}^0$  are the standard molar enthalpy of transfer, the standard molar entropy of transfer and the standard molar Gibbs energy of vanillin transfer, respectively.

For the four systems, the plots of  $\ln(K_{\text{van}})$  versus  $T^{-1}$  exhibit linearity indicating that the molar enthalpy of transfer of vanillin is temperature independent. In Table 2, the obtained values of  $\Delta_{\text{tr}}G_{\text{m}}^0$ ,  $\Delta_{\text{tr}}H_{\text{m}}^0$  and  $\Delta_{\text{tr}}S_{\text{m}}^0$  at 298.15 K are summarized.

**Table 2:** Standard molar thermodynamic functions of transfer of vanillin at 298.15 K.

System	$\frac{\Delta_{\text{tr}}H_{\text{m}}^0}{\text{kJ}\cdot\text{mol}^{-1}}$	$\frac{\Delta_{\text{tr}}S_{\text{m}}^0}{\text{J}\cdot\text{mol}^{-1}\cdot\text{K}^{-1}}$	$\frac{\Delta_{\text{tr}}G_{\text{m}}^0}{\text{kJ}\cdot\text{mol}^{-1}}$	$\ln(K_{\text{Van}})$
[C <sub>4</sub> mim]Cl + K <sub>3</sub> PO <sub>4</sub> + water	-23.66	-46.51	-9.79	3.95
[C <sub>4</sub> mim][CH <sub>3</sub> SO <sub>4</sub> ] + K <sub>3</sub> PO <sub>4</sub> + water	-12.62	-15.93	-7.87	3.18
[C <sub>7</sub> H <sub>7</sub> mim]Cl + K <sub>3</sub> PO <sub>4</sub> + water	-13.19	-13.47	-9.17	3.70
[amim]Cl + K <sub>3</sub> PO <sub>4</sub> + water	-24.09	-51.30	-8.80	3.55

The calculated  $\Delta_{\text{tr}}G_{\text{m}}^0$  values are negative for all the systems evaluated reflecting thus the spontaneous and preferential partitioning of vanillin for the IL-rich phase and as indicated by the  $K_{\text{Van}} > 1$ .  $\Delta_{\text{tr}}H_{\text{m}}^0$  values are negative indicating that the transference of vanillin from the K<sub>3</sub>PO<sub>4</sub>-rich phase to the IL-rich phase is an exothermic process which further reflects the favorable vanillin-IL type interactions. The standard molar enthalpies of transfer largely depend on the IL anion while the effect of changing the IL cation is only relevant for cases where the chain side cation is highly complex, as for [C<sub>7</sub>H<sub>7</sub>mim]Cl. These results again suggest that the partitioning process is essentially controlled by the anion interactions with the solute.

The results here obtained show that the effect of temperature on the extraction of vanillin is highly significant and that it is necessary to control the temperature at which the extraction is performed to achieve the maximum efficiency.

### 2.3.3. Effect of Concentration in Vanillin Partitioning

Figure 13 shows the partition coefficients for different initial concentrations of vanillin. The ILs used to study this effect were  $[C_4mim]Cl$ ,  $[C_4mim][CH_3SO_4]$  and  $[C_7H_7mim]Cl$ . The range of vanillin concentrations in the water mass fraction at the ternary system varied between  $0.5 \text{ g}\cdot\text{dm}^{-3}$  ( $3.3 \times 10^{-3} \text{ mol}\cdot\text{dm}^{-3}$ ) and  $7.5 \text{ g}\cdot\text{dm}^{-3}$  ( $4.9 \times 10^{-2} \text{ mol}\cdot\text{dm}^{-3}$ ). It should be pointed out that the saturation of vanillin in water at 298.15 K is around  $10.0 \text{ g}\cdot\text{dm}^{-3}$  ( $6.5 \times 10^{-2} \text{ mol}\cdot\text{kg}^{-1}$ ).<sup>[1]</sup>

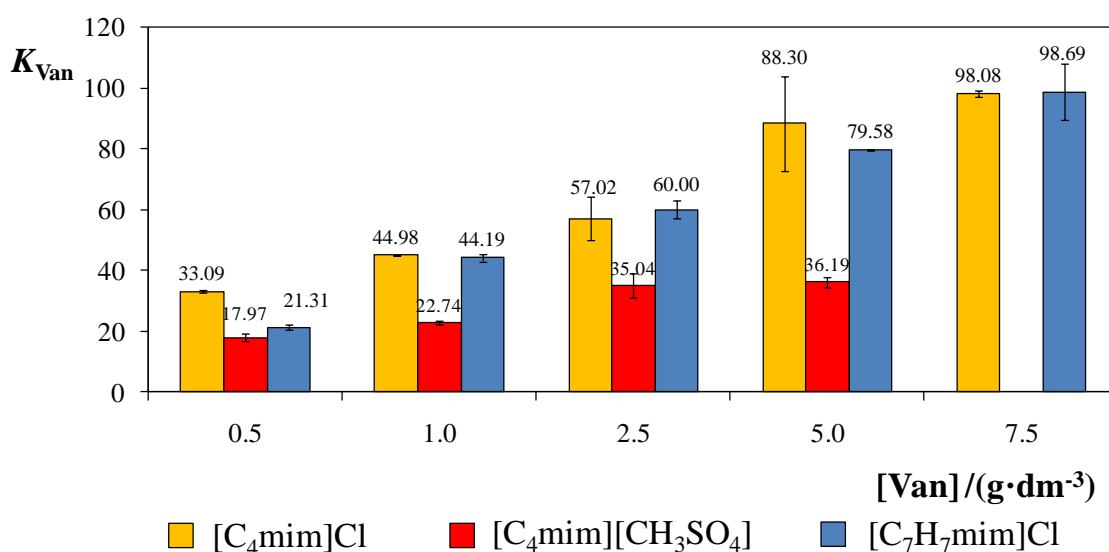


**Figure 13:** Partition coefficients of vanillin in IL +  $K_3PO_4$  ATPS as a function of initial vanillin concentration for the ILs:  $[C_4mim]Cl$ ,  $[C_4mim][CH_3SO_4]$  and  $[C_7H_7mim]Cl$ .

For the three ILs studied there is an increase in the vanillin partition coefficients with the initial concentration of the solute. Note that the value at  $7.5 \text{ g}\cdot\text{dm}^{-3}$  is not shown for  $[C_4mim][CH_3SO_4]$  since the precipitation of vanillin/ionic liquid mixture was observed at these conditions (as confirmed by NMR spectroscopic analysis). The precipitation of vanillin was found to be of 82 wt % and results from the salting-out inducing ability of  $[C_4mim][CH_3SO_4]$  as discussed before. The dependence on the initial concentration is less pronounced for the IL  $[C_4mim][CH_3SO_4]$ , while highly noticeable with  $[C_4mim]Cl$  and  $[C_7H_7mim]Cl$ . These results suggest that the IL cation starts to influence the dependency of the partitioning of vanillin with the solute content. Since anions are typically more polarizable than cations, due to their more diffuse valence electronic configuration, their hydration is usually stronger than that of cations and, as a result, their salting-out effects are more prominent.<sup>[62, 65]</sup> Thus, due to the stronger ability of anions for salting-out, and particularly of the methylsulfate anion, the presence of additional vanillin does not conduct to favourable interactions between IL anions and the solute. In contrast, methylsulfate preferentially forms hydration complexes. Therefore, when increasing the vanillin content, the

increase in the partition coefficients is more evident when changing the IL cation due to their higher aptitude for specific binding with the phenolic aldehyde (typical salting-in inducing ions).

#### ***2.3.4. Density and Viscosity***

The physical properties of the upper and lower phase in different ternary systems at various compositions and temperatures are required for the design and scale up of extraction processes. Therefore, densities and viscosities of all systems evaluated in this work, in the temperature range between 298.15 K and 328.15 K, were determined at the following ternary composition: 15 wt % of  $K_3PO_4$  + 25 wt % of IL + 60 wt % of water (except for [OHC<sub>2</sub>mim]Cl that was at 15 wt % of  $K_3PO_4$  + 40 wt % of IL + 45 wt % of water). Results are displayed in Figures 14 to 17 and the experimental data obtained are reported in Appendix B. In Figure 14, data for viscosities of the chloride-based ILs are presented.

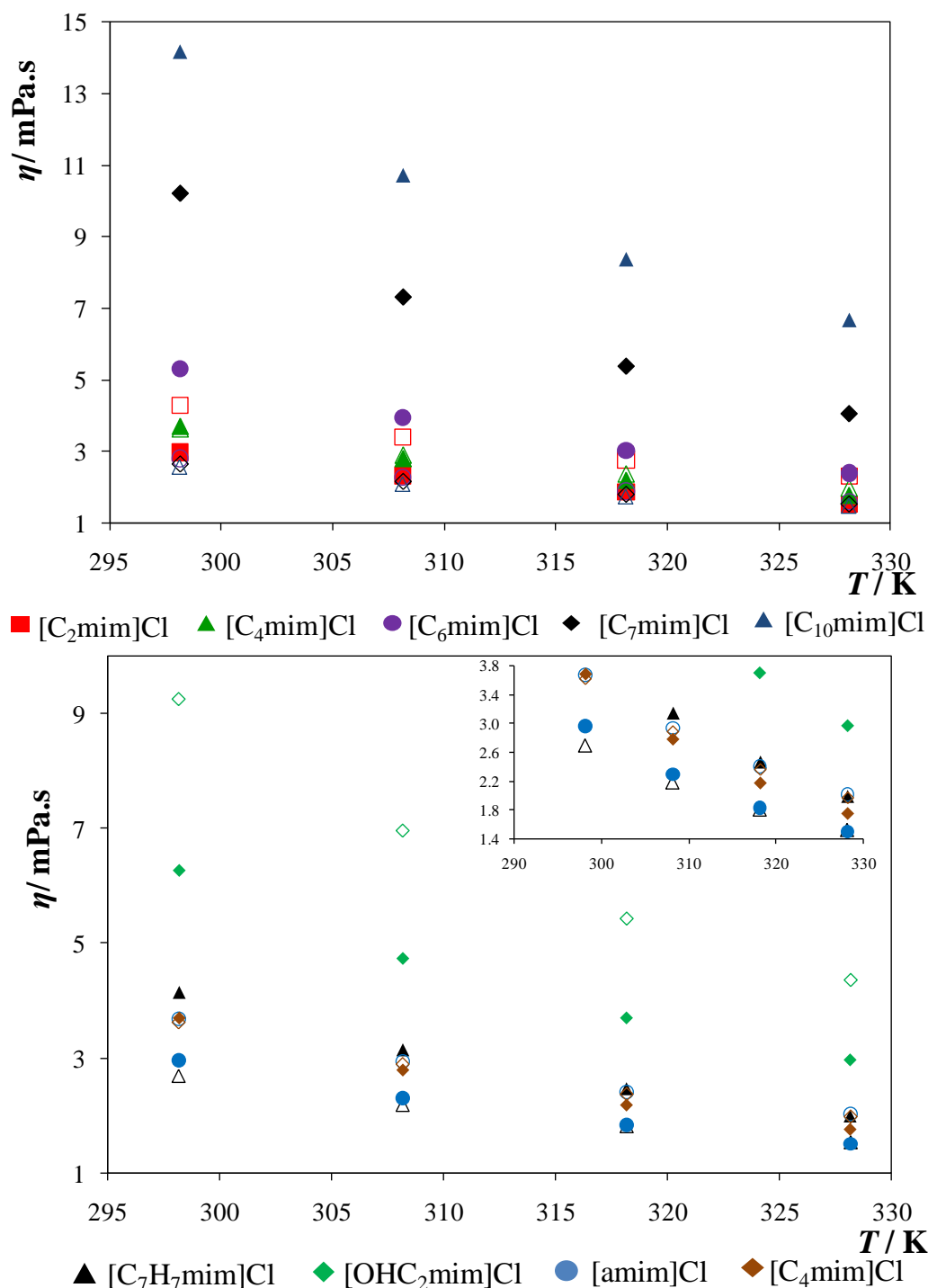


**Figure 14:** Experimental viscosity ( $\eta$ ) for the IL-rich phase (full symbols) and  $K_3PO_4$ -rich phase (open symbols) for systems composed by chloride-based ILs +  $K_3PO_4$  +  $H_2O$  as a function of temperature.

For the IL-rich phase the viscosities monotonically increase with the alkyl side chain length increase from [C<sub>2</sub>mim]Cl ( $\eta = 2.98$  mPa·s at 298.15 K) to [C<sub>10</sub>mim]Cl ( $\eta = 14.19$  mPa·s at 298.15 K). Concerning the influence of the functional groups inclusion, the viscosities of the IL-rich phase

decrease in the order: [OHC<sub>2</sub>mim]Cl ( $\eta = 6.27$  mPa.s at 298.15 K) > [C<sub>7</sub>H<sub>7</sub>mim]Cl > [C<sub>4</sub>mim]Cl > [amim]Cl ( $\eta = 2.96$  mPa.s at 298.15 K). Although [OHC<sub>2</sub>mim]Cl presents relatively high viscosity values it should be remarked that this system is richer in IL than the remaining systems so that a direct comparison is not indeed fair. Regarding the inorganic salt-rich phase for the systems with the chloride-based ILs the values of viscosities at 298.15 K range between 9.25 mPa.s for [OHC<sub>2</sub>mim]Cl and 2.56 mPa.s for [C<sub>10</sub>mim]Cl. An opposite trend with the ILs was observed for the viscosities at the K<sub>3</sub>PO<sub>4</sub>-rich phase. The opposite trends are in good agreement with each other since the most viscous ILs are also the least water soluble.

The viscosities of the IL-rich phases are surprisingly low for ATPS and also sometimes lower than the viscosities observed at the K<sub>3</sub>PO<sub>4</sub>-rich phase. This trend was observed for systems composed by [C<sub>2</sub>mim]Cl, [C<sub>4</sub>mim]Cl, [OHC<sub>2</sub>mim]Cl and [amim]Cl. In particular for [C<sub>4</sub>mim]Cl there is an inversion on the relative viscosities with the temperature.

The viscosity data for [C<sub>4</sub>mim]-based ILs are depicted in Figure 15.

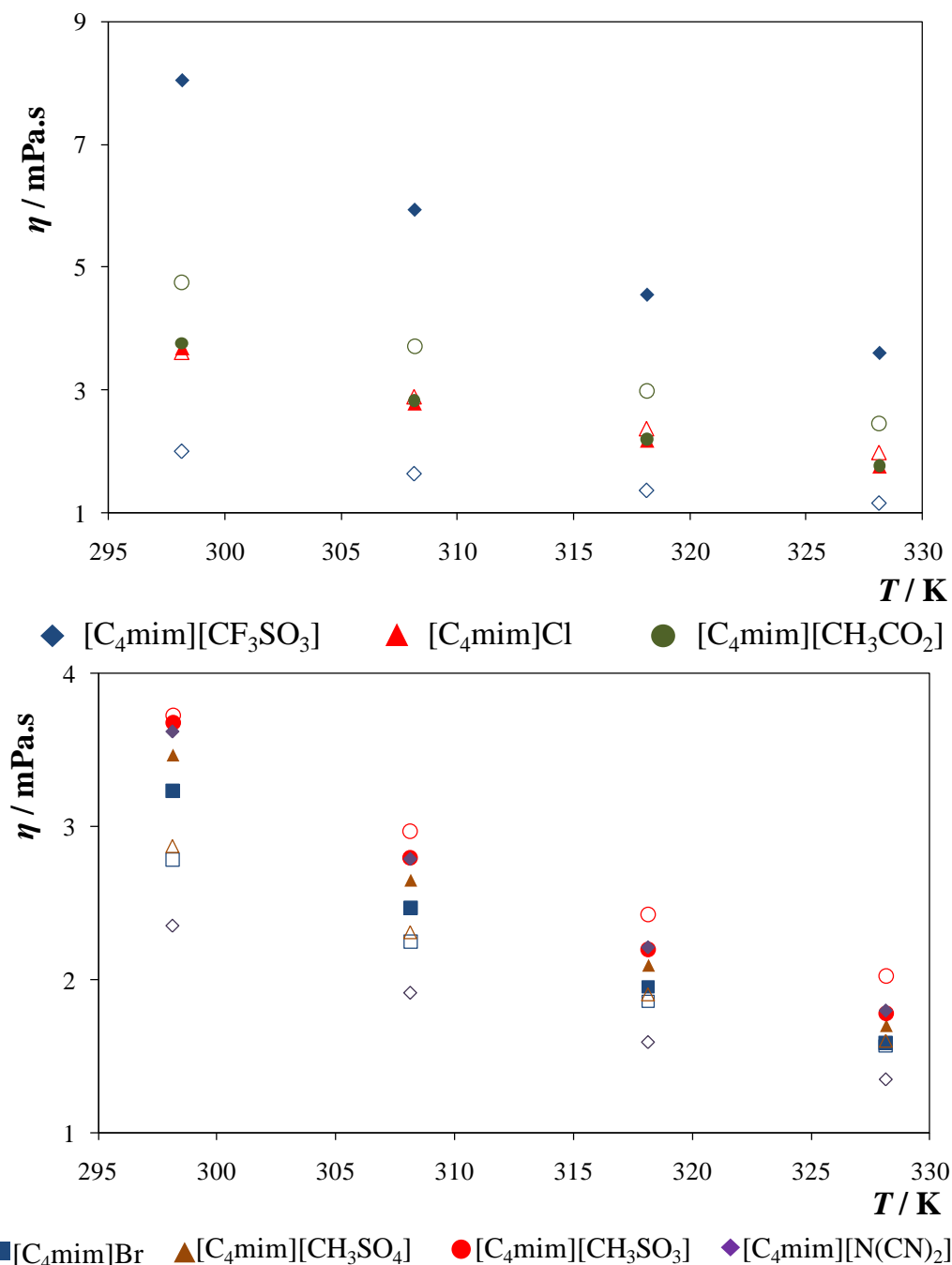


**Figure 15:** Experimental viscosity ( $\eta$ ) for the IL-rich phase (full symbols) and  $K_3PO_4$ -rich phase (open symbols) for systems composed by  $[C_4mim]$ -based ILs +  $K_3PO_4$  +  $H_2O$  as a function of temperature.

The results for the IL-rich phase show that the  $[C_4mim][CF_3SO_3]$  system ( $\eta = 8.05$  mPa·s at 298.15 K) presents the higher viscosity, while  $[C_4mim][Br]$  ( $\eta = 3.23$  mPa·s at 298.15 K) presents the lower viscosity values. The viscosity data at 298.15 K, and at the same mass fraction compositions, decrease in the following order:  $[C_4mim][CF_3SO_3] > [C_4mim][CH_3CO_2] > [C_4mim]Cl > [C_4mim][CH_3SO_3] > [C_4mim][N(CN)_2] > [C_4mim][CH_3SO_4] > [C_4mim]Br$ . The viscosities of the

salt-rich phase at 298.15 K range between 4.76 mPa·s for [C<sub>4</sub>mim][CH<sub>3</sub>CO<sub>2</sub>] and 2.00 mPa·s for [C<sub>4</sub>mim][CF<sub>3</sub>SO<sub>3</sub>]. Again, and as observed with the chloride-based ILs, the viscosity of the inorganic salt-rich phase is higher for the systems containing the ILs [C<sub>4</sub>mim][CH<sub>3</sub>SO<sub>3</sub>] and [C<sub>4</sub>mim][CH<sub>3</sub>CO<sub>2</sub>].

One of the critical problems related to the polymer-based ATPS is the high viscosity of the polymer-rich phases, for example, at 293.15 K, for an aqueous solution composed by 22 wt % of PEG2000 and 10 wt % of K<sub>3</sub>PO<sub>4</sub>, the viscosity takes the value of 18.94 mPa.s, while for an aqueous solution of 19 wt % of PEG4000 and 9 wt % of K<sub>3</sub>PO<sub>4</sub> the viscosity reaches 40.06 mPa.s.<sup>[115]</sup> It was previously shown<sup>[61]</sup> that phosphonium-based ATPS displayed lower viscosities than polymer-based ATPS. As shown here the imidazolium-based ATPS present even lower viscosity values which is highly beneficial in industrial processes. The low viscosity systems favors the mass transfer of the solute between the two phases, as well as in improving the phases handling.<sup>[116]</sup>

The density data for all the studied systems are presented in Figures 16 and 17, in the temperature range between 298.15 K and 328.15 K. In all equilibrated systems the density of the K<sub>3</sub>PO<sub>4</sub>-rich phase is higher than the density of the IL-rich phase. Only for the system containing [C<sub>4</sub>mim][CF<sub>3</sub>SO<sub>3</sub>] the densities of both phases are similar.

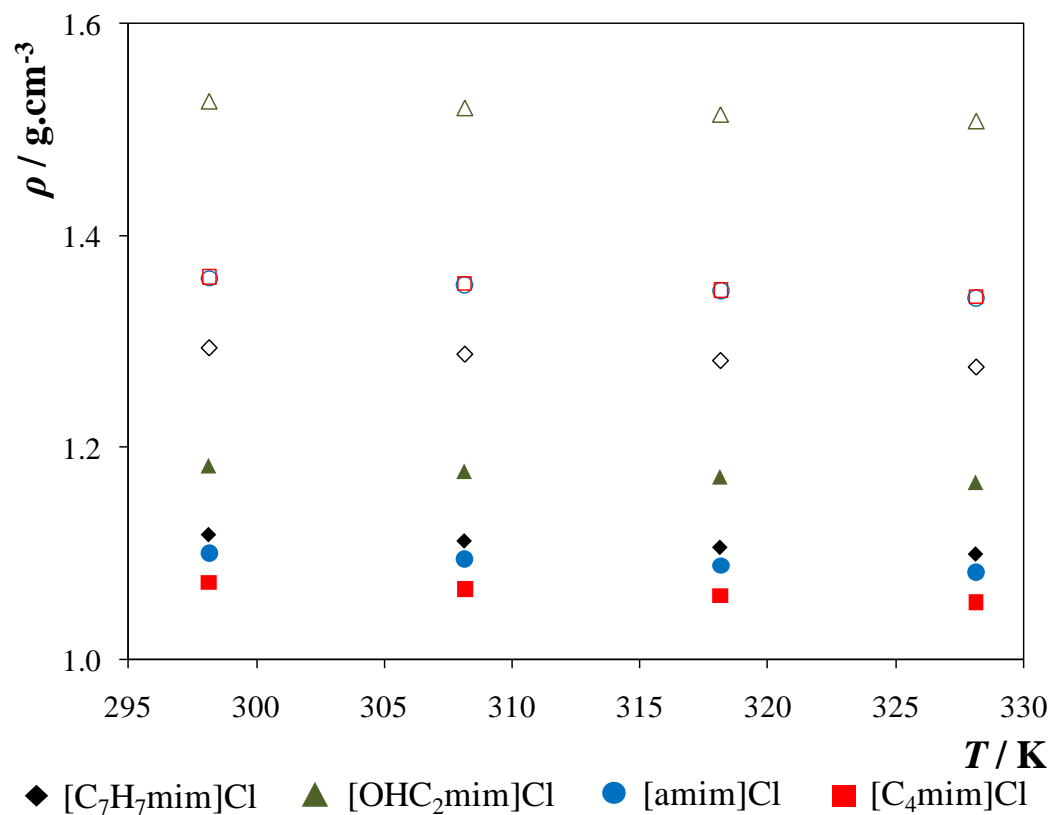
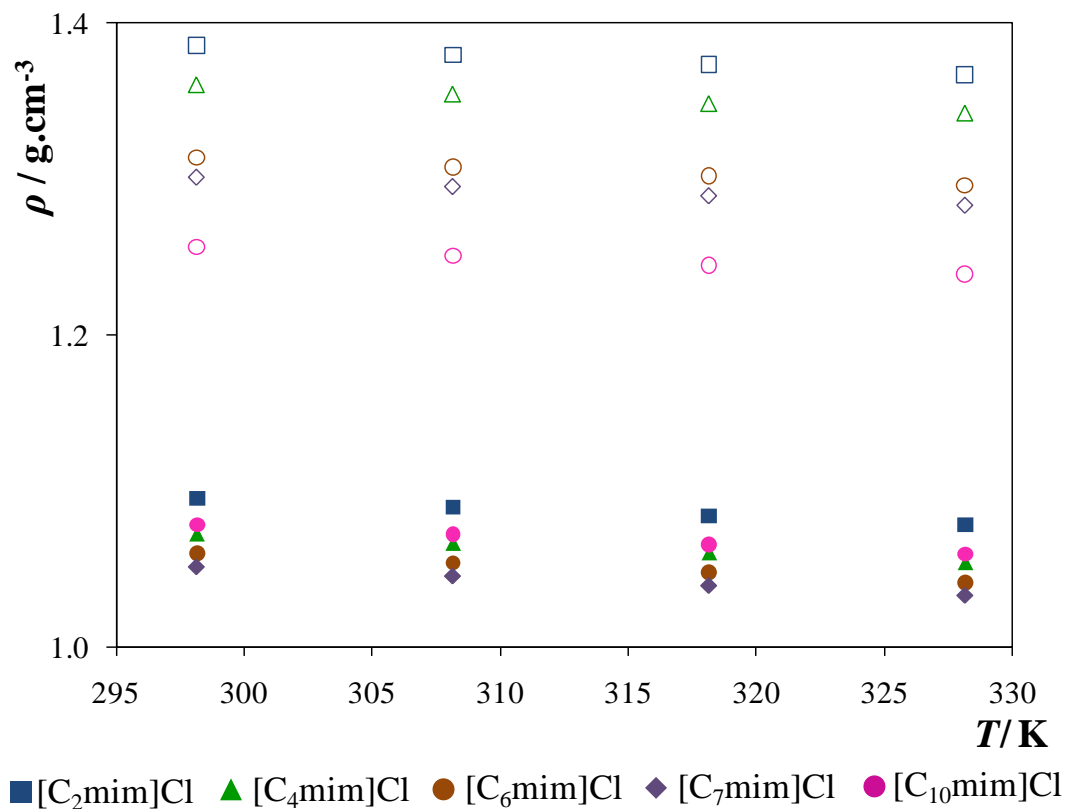


**Figure 16:** Experimental density ( $\rho$ ) for the IL-rich phase (full symbols) and  $\text{K}_3\text{PO}_4$ -rich phase (open symbols) for systems composed by chloride-based ILs +  $\text{K}_3\text{PO}_4$  +  $\text{H}_2\text{O}$  as a function of temperature.

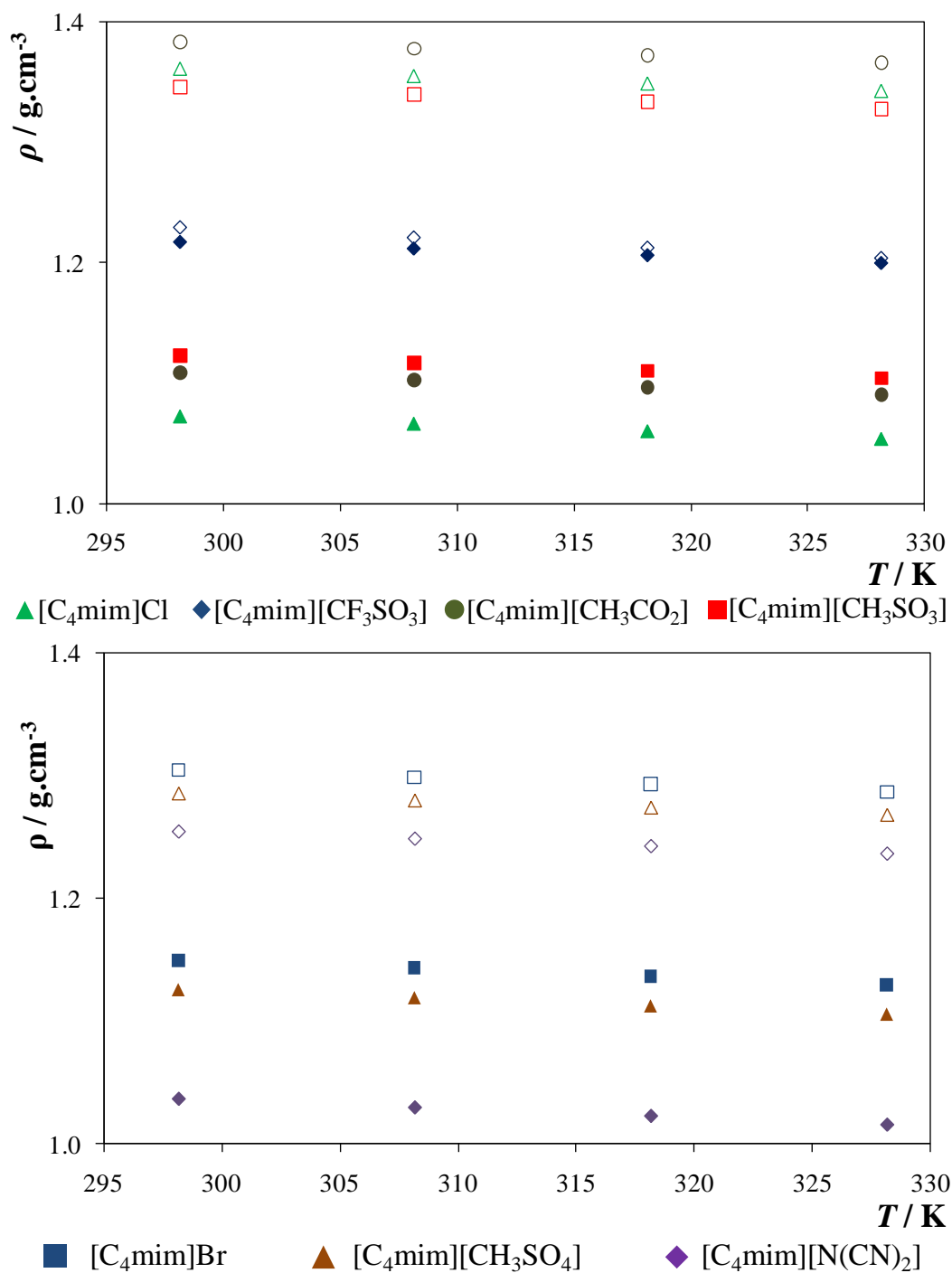


**Figure 17:** Experimental density ( $\rho$ ) for the IL-rich phase (full symbols) and  $\text{K}_3\text{PO}_4$ -rich phase (open symbols) for systems composed by  $[\text{C}_4\text{mim}]$ -based ILs +  $\text{K}_3\text{PO}_4$  +  $\text{H}_2\text{O}$  as a function of temperature.

For the IL-rich phase the values of densities at 298.15 K range between 1.0366  $\text{g}\cdot\text{cm}^{-3}$  for  $[\text{C}_4\text{mim}][\text{N}(\text{CN})_2]$  and 1.2169  $\text{g}\cdot\text{cm}^{-3}$  for  $[\text{C}_4\text{mim}][\text{CF}_3\text{SO}_3]$ . For the bottom phase ( $\text{K}_3\text{PO}_4$ -rich phase) the density values at 298.15 K range between 1.2291  $\text{g}\cdot\text{cm}^{-3}$  in the system with  $[\text{C}_4\text{mim}][\text{CF}_3\text{SO}_3]$  and 1.5265  $\text{g}\cdot\text{cm}^{-3}$  for the system composed by  $[\text{OHC}_2\text{mim}]\text{Cl}$ . Comparing IL-

based ATPS and typical polymer-inorganic salt ATPS<sup>[115]</sup> there are not significant differences in the density values. In both systems the top phase is the IL- or polymer-rich phase, while the bottom layer is the inorganic salt-rich phase.

## **2.4. Conclusions**

In this work the optimization of the IL structure for the improved extraction of vanillin was experimentally determined by measuring the partition coefficients on several IL-based ATPS. The effect of the IL cation and anion nature, the temperature of equilibrium and the concentration of the solute were evaluated. All the studied parameters have shown to influence the extraction of vanillin.

For all the studied systems, and at all the conditions analyzed, vanillin preferentially partitions for the IL-rich phase presenting  $K_{\text{van}} > 1$ . The partition coefficients dependency with the cation alkyl chain length displays a maximum for the system formed by [C<sub>6</sub>mim]Cl resulting from a decrease in the polar character of the IL cation and lower surface tension at the IL-rich phase. The introduction of features such as double bonds, benzyl and hydroxyl groups in ILs had only a marginal impact on the partition coefficients of vanillin. Regarding the IL anion, vanillin partitions preferentially for ILs composed by halogenated anions, such as Cl<sup>-</sup> or Br<sup>-</sup>, or by anions with a higher hydrogen bonding accepting character, such as [N(CN)<sub>2</sub>]<sup>-</sup>.

The influence of temperature in the partitioning of vanillin presented a maximum in the extraction efficiency at 298.15 K for [C<sub>4</sub>mim][CH<sub>3</sub>SO<sub>4</sub>], [C<sub>7</sub>H<sub>7</sub>mim]Cl and [amim]Cl and at 308.15 K for [C<sub>4</sub>mim]Cl. Moreover, the partition coefficients of vanillin increased monotonically with the initial concentration of the solute added to the global system. Variations in the partition coefficients as a function of the vanillin concentration were more dependent on the IL cation nature.

The viscosities of the IL-rich phase in all IL-based ATPS studied were found to be substantially lower than those observed in typical polymer-based ATPS what constitutes an additional advantage for industrial applications of the systems here studied.

### **3. Extraction of gallic acid in ATPS with ILs**

### 3.1. Gallic Acid

Gallic acid, 3,4,5-trihydroxybenzoic acid, with the chemical formula  $C_6H_2(OH)_3COOH$ , is a polar compound and its physical appearance is as yellowish-white crystals. Table 3 depicts some thermophysical properties of this phenolic compound.

**Table 3:** Thermophysical properties of gallic acid.<sup>[92, 117]</sup>

Molar mass ( $g \cdot mol^{-1}$ )	Density ( $g \cdot cm^{-3}$ )	Melting point (K)	Solubility in water ( $g \cdot dm^{-3}$ )	$pK_a$
170.12	1.7 at 298.15 K	523	11 at 293.15 K	4.41 at 298 K

Gallic acid, whose molecular structure is reported in Figure 18, is present in diverse natural products, such as fruits (grapes<sup>[118]</sup>), pomegranate husk,<sup>[119]</sup> vegetables,<sup>[75]</sup> green and black teas,<sup>[78]</sup> oak wood,<sup>[120]</sup> and some plants like *Plantae regnum*.<sup>[121]</sup> Besides its natural sources, gallic acid can also be found in residual waste. In olive mill effluents, gallic acid, protocatechuic acid and vanillic acid are the second major family of PhCs available<sup>[1]</sup>. Gallic acid can be either found in its free form or in the tannins constitution. Nevertheless, in wood, gallic acid is present in the form of gallotannins (hydrolysable tannins) and the further contact of such hydrolysable tannins with acidic media or hydrolytic enzymes (e.g. tannase) originate sugars and phenolic acids, such as gallic acid.<sup>[78, 122-123]</sup> The

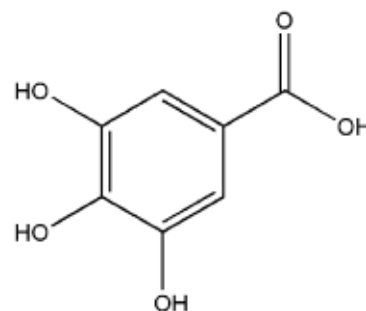


**Figure 18:** Chemical structure of gallic acid.

extraction of this biomolecule has a great practical interest because it has several important biological characteristics. It has properties of antioxidant, anti-inflammatory, antifungal, anti-tumor, diuretic, depurative, intestinal antiseptic, bacteriostatic and bactericidal, tonic, anti-arthritis and as a hydrogen carrier.<sup>[5, 118, 121, 124-125]</sup> Gallic acid also displays an important role as a metabolic inhibitor of some microorganisms (antimicrobial action). Due to these attractive characteristics associated to gallic acid, this biomolecule plays an essential position in the pharmaceutical industry in the treatment of gastric tonus problems, anorexia, bloating, gases, urinary diseases gout, haemostatic, skin repairer and sedative since it is well absorbed by humans.<sup>[75, 122]</sup> Moreover, gallic acid is commonly used as antioxidant in food additives.<sup>[4]</sup> It has a percentage antioxidant activity of 92.92 %.<sup>[74]</sup> The utilization of natural phenolic compounds for nutraceutical and cosmetic applications has proved to be highly advantageous compared to synthetic substitutes that could demonstrate adverse effects.<sup>[125]</sup>

Being an antioxidant, gallic acid in the presence of alkaline solutions gets a brownish color due to absorption of oxygen,<sup>[121]</sup> and can be further degraded during the extraction procedures. To prevent the degradation of gallic acid another antioxidant can be added to the system of extraction, such as ascorbic acid.

Gallic acid was found to be partially soluble in different solvents and the order of solubility in several solvents is as follows: methanol > ethanol > water > ethyl acetate.<sup>[122]</sup> This solubility in several common and molecular solvents represents an important advantage from the industrial point of view.<sup>[121-122]</sup> Furthermore, studies regarding the effect of salts on the solubility of phenolic compounds,<sup>[1]</sup> showed that there is a decrease in the solubility of gallic acid with increasing the salt molality, where the influence of the cation was shown to be highly noticeable.

## **3.2. Experimental section**

Before the studies of extraction of gallic acid by aqueous two-phase systems composed by Na<sub>2</sub>SO<sub>4</sub> and different ILs, it was necessary to determine the respective ternary phase diagrams due to their absence in literature. These diagrams are useful to know in which conditions was possible to form a biphasic mixture and at which ternary compositions the extraction can be performed.

### **3.2.1. Chemicals**

The ILs studied to determine the ternary phase diagrams were: 1-butyl-3-methylimidazolium chloride, [C<sub>4</sub>mim]Cl; 1-hexyl-3-methylimidazolium chloride, [C<sub>6</sub>mim]Cl; 1-heptyl-3-methylimidazolium chloride, [C<sub>7</sub>mim]Cl; 1-methyl-3-octylimidazolium chloride, [C<sub>8</sub>mim]Cl; 1-butyl-3-methylimidazolium bromide, [C<sub>4</sub>mim]Br; 1-butyl-3-methylimidazolium methanesulfonate, [C<sub>4</sub>mim][CH<sub>3</sub>SO<sub>3</sub>]; 1-butyl-3-methylimidazolium acetate, [C<sub>4</sub>mim][CH<sub>3</sub>CO<sub>2</sub>]; 1-butyl-3-methylimidazolium methylsulfate [C<sub>4</sub>mim][CH<sub>3</sub>SO<sub>4</sub>]; 1-butyl-3-methyl-imidazolium trifluoromethanesulfonate, [C<sub>4</sub>mim][CF<sub>3</sub>SO<sub>3</sub>]; 1-butyl-3-methylimidazolium dicyanamide, [C<sub>4</sub>mim][N(CN)<sub>2</sub>]; 1-butyl-3-methylimidazolium hydrogensulfate, [C<sub>4</sub>mim][HSO<sub>4</sub>]; 1-butyl-3-methylimidazolium tosylate, [C<sub>4</sub>mim][TOS]; 1-ethyl-3-methylimidazolium methylsulfate [C<sub>2</sub>mim][CH<sub>3</sub>SO<sub>4</sub>]; 1-ethyl-3-methyl-imidazolium trifluoromethanesulfonate, [C<sub>2</sub>mim][CF<sub>3</sub>SO<sub>3</sub>]; 1-benzyl-3-methylimidazolium chloride, [C<sub>7</sub>H<sub>7</sub>mim]Cl; 1-benzyl-3-methylimidazolium ethylsulfate, [C<sub>7</sub>H<sub>7</sub>mim][C<sub>2</sub>H<sub>5</sub>SO<sub>4</sub>]; 1-allyl-3-methylimidazolium ethylsulfate, [amim][C<sub>2</sub>H<sub>5</sub>SO<sub>4</sub>]; 1-butyl-3-methylimidazolium ethylsulfate, [C<sub>4</sub>mim][C<sub>2</sub>H<sub>5</sub>SO<sub>4</sub>]; 1-butyl-3-methylpyridinium chloride, [C<sub>4</sub>mpy]Cl(1,3); 1-butyl-3-methylpiperidinium chloride, [C<sub>4</sub>mpip]Cl; 1-butyl-3-methylpyrrolidinium chloride, [C<sub>4</sub>mpyrr]Cl; 1-octylpyridinium dicyanamide, [C<sub>8</sub>py][N(CN)<sub>2</sub>]. All ILs were supplied by Iolitec. To reduce the impurities content to negligible values, ILs individual samples were purified under constant agitation at vacuum and moderate temperature (353 K) for a minimum of 24 hours. After this step, the purity of each IL was checked by <sup>1</sup>H, <sup>13</sup>C and <sup>19</sup>F NMR spectra and found to be > 99 wt % for all samples. The inorganic salt Na<sub>2</sub>SO<sub>4</sub> was from LabSolve (purity > 99.8 wt %), and gallic acid, 99.5 wt % pure, was from Merck. The molecular structure of gallic acid is depicted in Figure 17. The water employed was double distilled, passed across a reverse osmosis system and further treated with a Milli-Q plus 185 water purification apparatus. The structures of ILs that were successful in the determination of the phase diagrams are shown in Figure 19.

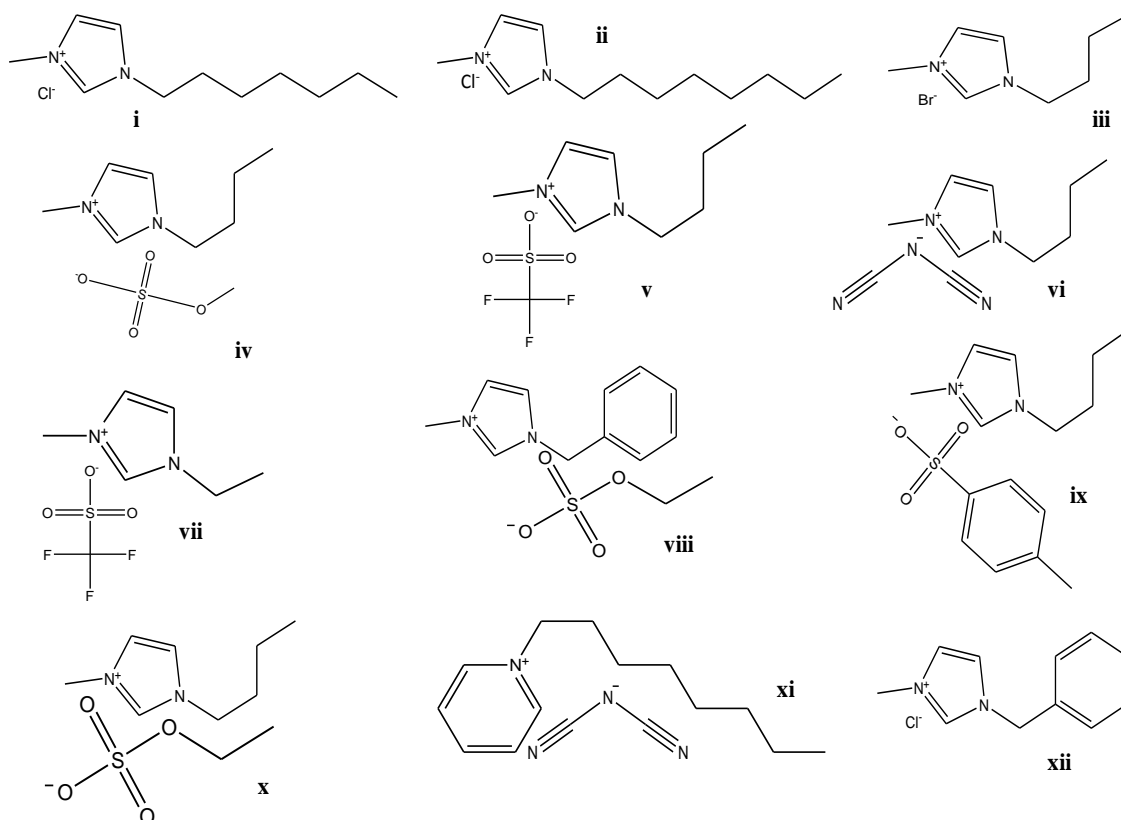


**Figure 19:** Chemical structure of the studied ILs: (i) [C<sub>7</sub>mim]Cl; (ii) [C<sub>8</sub>mim]Cl; (iii) [C<sub>4</sub>mim]Br; (iv) [C<sub>4</sub>mim][CH<sub>3</sub>SO<sub>4</sub>]; (v) [C<sub>4</sub>mim][CF<sub>3</sub>SO<sub>3</sub>]; (vi) [C<sub>4</sub>mim][N(CN)<sub>2</sub>]; (vii) [C<sub>2</sub>mim][CF<sub>3</sub>SO<sub>3</sub>]; (viii) [C<sub>7</sub>H<sub>7</sub>mim] [C<sub>2</sub>H<sub>5</sub>SO<sub>4</sub>]; (ix) [C<sub>4</sub>mim][TOS]; (x) [C<sub>4</sub>mim] [C<sub>2</sub>H<sub>5</sub>SO<sub>4</sub>]; (xi) [C<sub>8</sub>py][N(CN)<sub>2</sub>]; (xii) [C<sub>7</sub>H<sub>7</sub>mim]Cl.

### 3.2.2. Experimental procedure

#### 3.2.2.1. Preparation of Phase Diagrams

Aqueous solutions of  $\text{Na}_2\text{SO}_4$  and aqueous solutions of the different hydrophilic ILs were prepared gravimetrically as described in Appendix D. The phase diagrams were determined at 298 K ( $\pm 1$  K) and at atmospheric pressure through the cloud point titration method.<sup>[61]</sup> Drop-wise addition of the aqueous inorganic salt solution to each IL aqueous solution was carried out until the detection of a cloudy (biphasic solution), followed by drop-wise addition of ultra-pure water until the finding of a clear and limpid solution (monophasic region), as shown in Figure 20. Drop-wise additions were carried out under constant stirring. The ternary systems compositions were determined by the weight quantification of all components within an uncertainty of  $\pm 10^{-5}$  g.

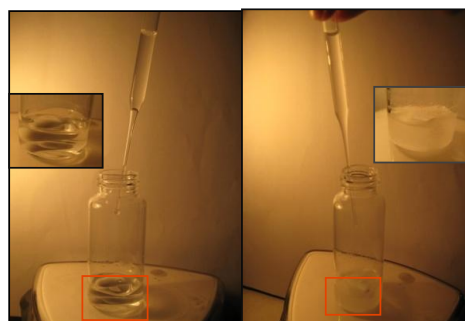


**Figure 20:** Experimental determination of the binodal curves for the aqueous systems IL- $\text{Na}_2\text{SO}_4$ : in the first picture it is shown a limpid and clear solution while in the second picture it denotes a cloudy solution.

For  $[\text{C}_8\text{mim}]\text{Cl}$  it was not possible to determine the complete binodal curve using the described method, so the turbidometric titration method was used in parallel.<sup>[126]</sup> Test tubes at the biphasic region with different compositions of known weight of IL, salt and water were prepared. Then, it was drop-wise added pure water, under continuous stirring, until reaching a limpid solution (single-phase region). The total amount of added water was determined gravimetrically and the mass fraction of each component in the mixture was recalculated.

#### 3.2.2.2. Determination of Tie-Lines

Tie-lines (TLs) were determined by a gravimetric method originally proposed by Merchuck et al.<sup>[127]</sup> For the determination of TLs, a mixture at the biphasic region was gravimetrically prepared with  $\text{Na}_2\text{SO}_4$  + water + IL, vigorously agitated, and left to equilibrate for at least 12 h at 298 K, aiming at completing separating both phases. After a careful separation step, both top and bottom phases were weighed. Finally, each TL was determined by mass balance through the application of the lever rule to the relationship between the top mass phase composition and the overall system composition. The experimental binodal curves were fitted using Equation 5.<sup>[127]</sup>

$$Y = A \exp[(BX^{0.5}) - (CX^3)] \quad (5)$$

where  $Y$  and  $X$  are the IL and salt weight percentages, respectively, and  $A$ ,  $B$  and  $C$  are constants obtained by the regression.

For the TL determination the following system of four equations (Equations 6 to 9) and four unknown values ( $Y_T$ ,  $Y_B$ ,  $X_T$  and  $X_B$ ) was solved:<sup>[127]</sup>

$$Y_T = A \exp[(BX_T^{0.5}) - (CX_T^3)] \quad (6)$$

$$Y_B = A \exp[(BX_B^{0.5}) - (CX_B^3)] \quad (7)$$

$$Y_T = \frac{Y_M}{\alpha} - \frac{1-\alpha}{\alpha} \times Y_B \quad (8)$$

$$X_T = \frac{X_M}{\alpha} - \frac{1-\alpha}{\alpha} \times X_B \quad (9)$$

where  $T$ ,  $B$  and  $M$  designate the top phase, the bottom phase and the mixture, respectively.  $X$  and  $Y$  represent, respectively, the weight fraction of inorganic salt and IL, and  $\alpha$  is the ratio between the mass of the top phase and the total mass of the mixture. The system solution results in the concentration (wt %) of the IL and inorganic salt in the top and bottom phases, and thus, TLs can be simply represented.

For the calculation of the tie-lines length (TLL) it was employed Equation 10:

$$\text{TLL} = \sqrt{(X_T - X_B)^2 - (Y_T - Y_B)^2} \quad (10)$$

where  $T$  and  $B$  symbolize, respectively, the top and bottom phases, and  $X$  and  $Y$  are the weight fraction of inorganic salt and IL, respectively.

### **3.2.2.3. Partitioning of Biomolecules**

The ternary mixtures compositions were chosen based on the determined phase diagrams containing each of the ILs. A ternary mixture was prepared within the biphasic region containing 15 wt % of inorganic salt, 60 wt % of an aqueous solution of gallic acid with  $0.5 \text{ g}\cdot\text{dm}^{-3}$  ( $3.06 \times 10^{-3}$ ) and 25 wt % of selected ILs. The ternary compositions were prepared by weight with an uncertainty of  $\pm 10^{-5}$  g. Each ternary mixture (IL, inorganic salt and aqueous solution of gallic acid) was prepared in small ampoules ( $10 \text{ cm}^3$ ) especially built for such extraction procedures and vigorously stirred. After such step, the ampoules were kept in rest for at least 12 h, and at  $298.15 \pm 0.01 \text{ K}$  in an air bath equipped with a Pt 100 probe and a temperature controller, to reach the equilibrium and the separation of both phases. A preliminary study showed that the equilibration of gallic acid was completely attained after a period of 12 h. The time required to establish the equilibrium of gallic

acid was experimentally determined by measuring the concentration of gallic acid in each phase at different times until reproducible data were obtained.

After a gentle separation of both phases, the amount of gallic acid at each aqueous phase was quantified through UV-spectroscopy, using a SHIMADZU UV-1700, Pharma-Spec Spectrometer, at wavelength of 262 nm. Calibration curves were properly established and are reported in Appendix A. At least three individual samples of each phase were quantified in order to determine the gallic acid partition coefficients and the respective standard deviations. Possible interferences of both inorganic salts and all ILs with the analytical method were investigated and found to be slightly significant at the wavelength of 262 nm and at the magnitude of the dilutions carried. Mixtures at the same fraction composition were prepared, for each of the ILs, using pure water instead of an aqueous solution of gallic acid, and the proper discount in the analytical quantification was performed.

The partition coefficients of gallic acid,  $K_{GA}$ , were determined as the ratio of the concentration of gallic acid in the IL and in the inorganic salt ( $\text{Na}_2\text{SO}_4$ ,  $\text{K}_3\text{PO}_4$  or  $\text{K}_2\text{HPO}_4/\text{KH}_2\text{PO}_4$ ) aqueous-rich phases, accordingly to:

$$K_{GA} = \frac{[\text{GA}]_{\text{IL}}}{[\text{GA}]_{\text{X}}} \quad (11)$$

where  $[\text{GA}]_{\text{IL}}$  and  $[\text{GA}]_{\text{X}}$  are the concentration of gallic acid in the IL and in each of the inorganic salt aqueous-rich phases, respectively. At the compositions used, the top layer is the IL-rich phase while the bottom phase is the inorganic salt-rich phase. The only exceptions are the specific case of the  $[\text{C}_2\text{mim}][\text{CF}_3\text{SO}_3]-\text{K}_3\text{PO}_4$ ,  $[\text{C}_4\text{mim}][\text{CF}_3\text{SO}_3]-\text{K}_3\text{PO}_4$  and  $[\text{C}_4\text{mim}][\text{CF}_3\text{SO}_3]-\text{Na}_2\text{SO}_4$  systems where it was observed an inversion on the density of both phases.

#### **3.2.2.4. *pH measurement***

The pH of the both IL and inorganic salt-rich phases was measured at 298 K using an HI 9321 Microprocessor pH meter (HANNA instruments) within an uncertainty of  $\pm 0.01$ .

### **3.3. Results and Discussion**

#### **3.3.1. Phase Diagrams**

Since the partitioning of gallic acid could be somewhat affected by the pH of the solutions, several inorganic salts in combination with distinct IL-based ATPS were investigated. The inorganic salt most used was  $\text{Na}_2\text{SO}_4$  because it is normally used in the acidic hydrolysis for breaking the hemicellulose fraction of lignocellulose into monosaccharides of vegetal biomass (wood), aiming at *a posteriori* extract value-added compounds such as phenolic compounds, furfural and others. Partial depolymerization of lignin and lignin-hemicellulose linkages occur through acid hydrolysis and the acid-soluble lignin fraction is mainly identified with the presence of PhCs. In order to know the degree of extraction with ILs in acidic systems, the extraction of gallic acid with  $\text{Na}_2\text{SO}_4$ -based ATPS was studied more extensively.<sup>[128-129]</sup>

Due to the absence in literature of the ternary phase diagrams for IL- $\text{Na}_2\text{SO}_4$ -water systems, they were here determined. Table 4 represents all the evaluated systems. It should be pointed out that with  $\text{Na}_2\text{SO}_4$  it was not possible to determine the phase diagrams of all the proposed ILs due to the lack of an immiscibility region. All systems signed with ✖ means that it was not possible to observe a two phase region in the conditions studied. The systems with ✓ indicate the phase diagrams studied. In some cases it was found a solid-liquid region instead of a liquid-liquid region.

**Table 4:** Initial weight fraction compositions for the determination of the phase diagrams and indication of the possibility of existing liquid-liquid equilibrium.

IL + Na <sub>2</sub> SO <sub>4</sub> + Water system	Weight fraction composition / wt %		LLE
	IL	Na <sub>2</sub> SO <sub>4</sub>	
[C <sub>2</sub> mim][CH <sub>3</sub> SO <sub>4</sub> ]	59.94	27.00	✗
[C <sub>2</sub> mim][CF <sub>3</sub> SO <sub>3</sub> ]	59.17	24.89	✓
	79.61	29.98	✗
	78.38	29.98	✗
	69.70	29.98	✗
[C <sub>4</sub> mim]Cl	79.43	24.17	✗
	70.05	24.17	✗
	63.73	24.08	✗
	54.80	24.08	✗
	49.69	24.08	✗
[C <sub>4</sub> mim]Br	59.40	24.89	✓
[C <sub>4</sub> mim][CH <sub>3</sub> CO <sub>2</sub> ]	62.06	24.89	✗
[C <sub>4</sub> mim][CF <sub>3</sub> SO <sub>3</sub> ]	59.41	29.98	✓
[C <sub>4</sub> mim][N(CN) <sub>2</sub> ]	60.45	30.26	✓
[C <sub>4</sub> mim][HSO <sub>4</sub> ]	60.05	26.64	✗
[C <sub>4</sub> mim][CH <sub>3</sub> SO <sub>4</sub> ]	59.46	30.26	✓
[C <sub>4</sub> mim][C <sub>2</sub> H <sub>5</sub> SO <sub>4</sub> ]	60.83	27.00	✓
[C <sub>4</sub> mim][TOS]	59.43	30.26	✓
[C <sub>6</sub> mim]Cl	61.52	24.89	✗
[C <sub>7</sub> mim]Cl	59.27	26.12	✓
[C <sub>8</sub> mim]Cl	60.15	24.89	✓
[amim][C <sub>2</sub> H <sub>5</sub> SO <sub>4</sub> ]	63.51	24.89	✗
[C <sub>7</sub> H <sub>7</sub> mim]Cl	78.64	29.98	✗
	60.68	24.50	✓
[C <sub>7</sub> H <sub>7</sub> mim][C <sub>2</sub> H <sub>5</sub> SO <sub>4</sub> ]	60.36	24.50	✓
[C <sub>4</sub> mim][DMphosp]	58.74	26.64	✗
[C <sub>4</sub> mpyrr]Cl	59.85	30.26	✗
	46.60	30.26	✗
[C <sub>4</sub> mpip]Cl	59.19	26.64	✗
[C <sub>4</sub> mpy]Cl	59.58	24.89	✗
[C <sub>8</sub> py][N(CN) <sub>2</sub> ]	60.42	26.12	✓

From an inspection to Table 4, it is visible that anions or cations with more hydrophobic characteristics have a greater capacity to promote ATPS. Examples are those systems with IL containing the anions  $[N(CN)_2]^-$  and  $[CF_3SO_3]^-$  or larger alkyl side chains at the cation. Figure 21 depicts the experimental phase diagrams, at 298 K and at atmospheric pressure, for the biphasic systems determined with  $Na_2SO_4$  + water + different ILs. The phase diagrams are presented in molality units for a more comprehensive perception of the impact of distinct ILs through ATPS formation.

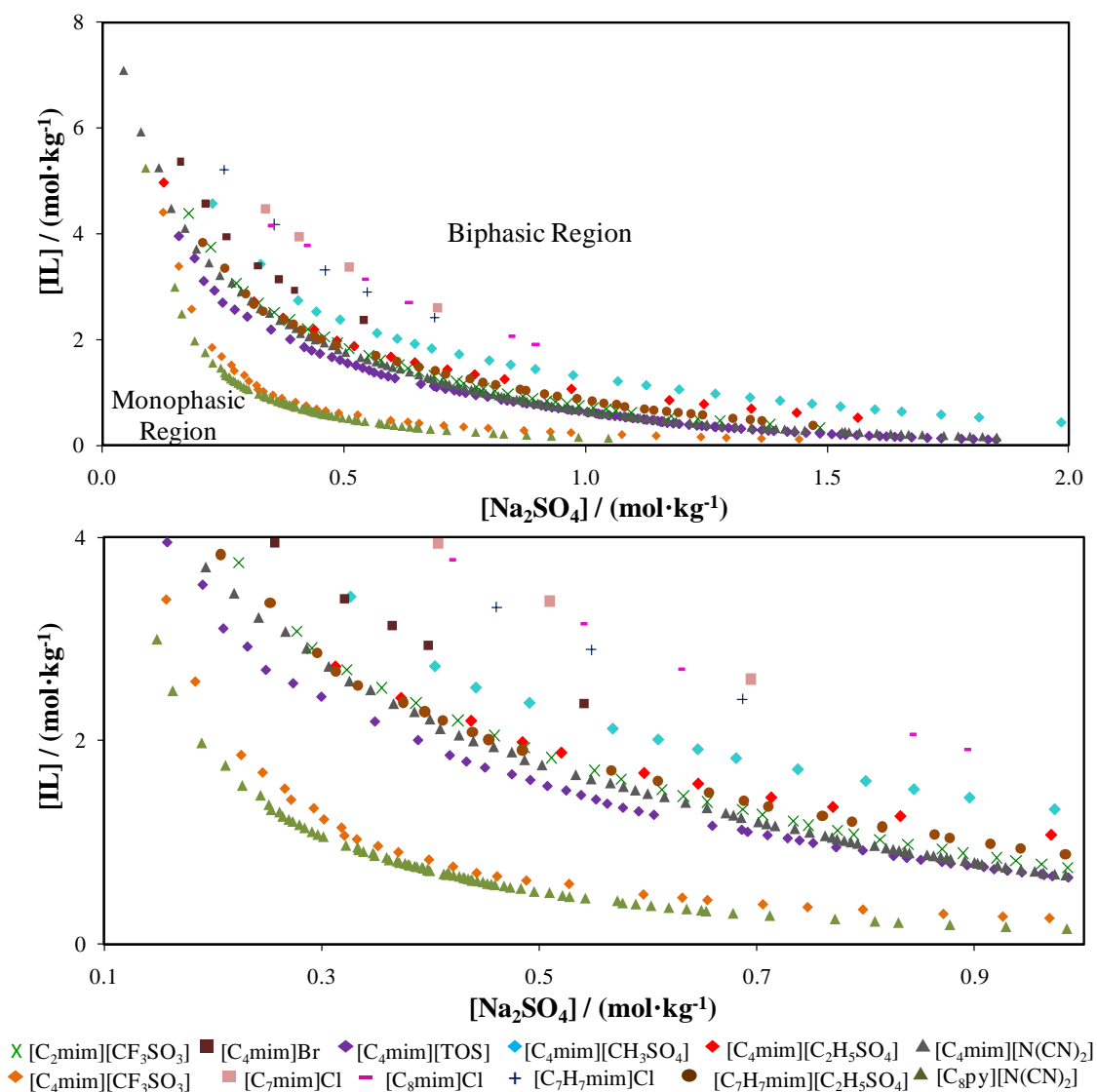


**Figure 21:** Ternary phase diagrams for all the ILs studied at 298 K and atmospheric pressure.

The presence of inorganic salt/IL combinations turns ATPS more complex than typical PEG-based ATPS. Thus a more complex equilibrium is expected taking into account that ion exchange and ion-pairing phenomena may occur.<sup>[32, 49]</sup> Although, it was previously found that electroneutrality is

maintained in such systems and that the ion partitioning is in the order of the deviation aroused from the cloud point titration method.<sup>[69]</sup>

Binodal curves with a larger biphasic region are an indication of the higher capability by ILs to promote ATPS, that is, ILs with stronger salting-in inducing behavior. From Figure 21 the tendency of ILs to promote ATPS with Na<sub>2</sub>SO<sub>4</sub> follows the order: [C<sub>8</sub>py][N(CN)<sub>2</sub>] > [C<sub>4</sub>mim][CF<sub>3</sub>SO<sub>3</sub>] > [C<sub>4</sub>mim][TOS] > [C<sub>4</sub>mim][N(CN)<sub>2</sub>] > [C<sub>2</sub>mim][CF<sub>3</sub>SO<sub>3</sub>] ≈ [C<sub>7</sub>H<sub>7</sub>mim][C<sub>2</sub>H<sub>5</sub>SO<sub>4</sub>] > [C<sub>4</sub>mim][C<sub>2</sub>H<sub>5</sub>SO<sub>4</sub>] > [C<sub>4</sub>mim][CH<sub>3</sub>SO<sub>4</sub>] ≈ [C<sub>4</sub>mim]Br > [C<sub>7</sub>H<sub>7</sub>mim]Cl > [C<sub>7</sub>mim]Cl ≈ [C<sub>3</sub>mim]Cl. Analyzing the anion influence, when fixing the cation [C<sub>4</sub>mim]<sup>+</sup>, the ability of the IL anions to promote ATPS follows the rank: [CF<sub>3</sub>SO<sub>3</sub>]<sup>-</sup> > [TOS]<sup>-</sup> > [N(CN)<sub>2</sub>]<sup>-</sup> > [C<sub>2</sub>H<sub>5</sub>SO<sub>4</sub>]<sup>-</sup> > [CH<sub>3</sub>SO<sub>4</sub>]<sup>-</sup> > Br<sup>-</sup>. Similarly, with the common cation [C<sub>7</sub>H<sub>7</sub>mim]<sup>+</sup>, [C<sub>2</sub>H<sub>5</sub>SO<sub>4</sub>]<sup>-</sup> shows a higher ability to induce ATPS than Cl<sup>-</sup>. In spite of a different inorganic salt, this trend on the IL anions agrees with the one reported previously.<sup>[32]</sup> This rank reflects the competition between the inorganic salt and the IL ions for the formation of water-ion hydration complexes. Thus, the ability of the anions' hydrogen bonding accepting strength is determinant for the ATPS formation. Indeed, in a previous work it was shown that the IL inducing capacity to promote ATPS follows the anion hydrogen bond basicity<sup>[32]</sup>, and additionally corroborated by this work, employing a different inorganic salt.

Moreover, an increase in the alkyl chain length in both the IL cation or anion enhances the ability of the IL for ATPS formation, as deduced when comparing the two following pairs of ILs: [C<sub>2</sub>mim][CF<sub>3</sub>SO<sub>3</sub>] and [C<sub>4</sub>mim][CF<sub>3</sub>SO<sub>3</sub>], and [C<sub>4</sub>mim][CH<sub>3</sub>SO<sub>4</sub>] and [C<sub>4</sub>mim][C<sub>2</sub>H<sub>5</sub>SO<sub>4</sub>]. Obviously, this trend can be justified due to an increase in the IL hydrophobicity generated by an increase in the alkyl chain lengths. Nevertheless, for systems with longer alkyl chains, [C<sub>7</sub>mim]Cl and [C<sub>8</sub>mim]Cl, the tendency of ILs for ATPS formation is very close, although [C<sub>8</sub>mim]Cl is slightly more favorable to create ATPS. This small difference with longer alkyl chain lengths can be related with the formation of IL aggregates in aqueous solutions increasing thus the ILs affinity for water.<sup>[110]</sup> Comparing both [C<sub>4</sub>mim][C<sub>2</sub>H<sub>5</sub>SO<sub>4</sub>] and [C<sub>7</sub>H<sub>7</sub>mim][C<sub>2</sub>H<sub>5</sub>SO<sub>4</sub>], it is verified that the former presents a higher ability to promote ATPS, and which is in agreement with literature when using a different anion.<sup>[49]</sup>

The manipulation of the phase diagrams through the IL cation/anion combinations clearly reflects the ILs character of "designer solvents". Therefore, an appropriate selection of cation or anion could provide ATPS with specific phase behavior.

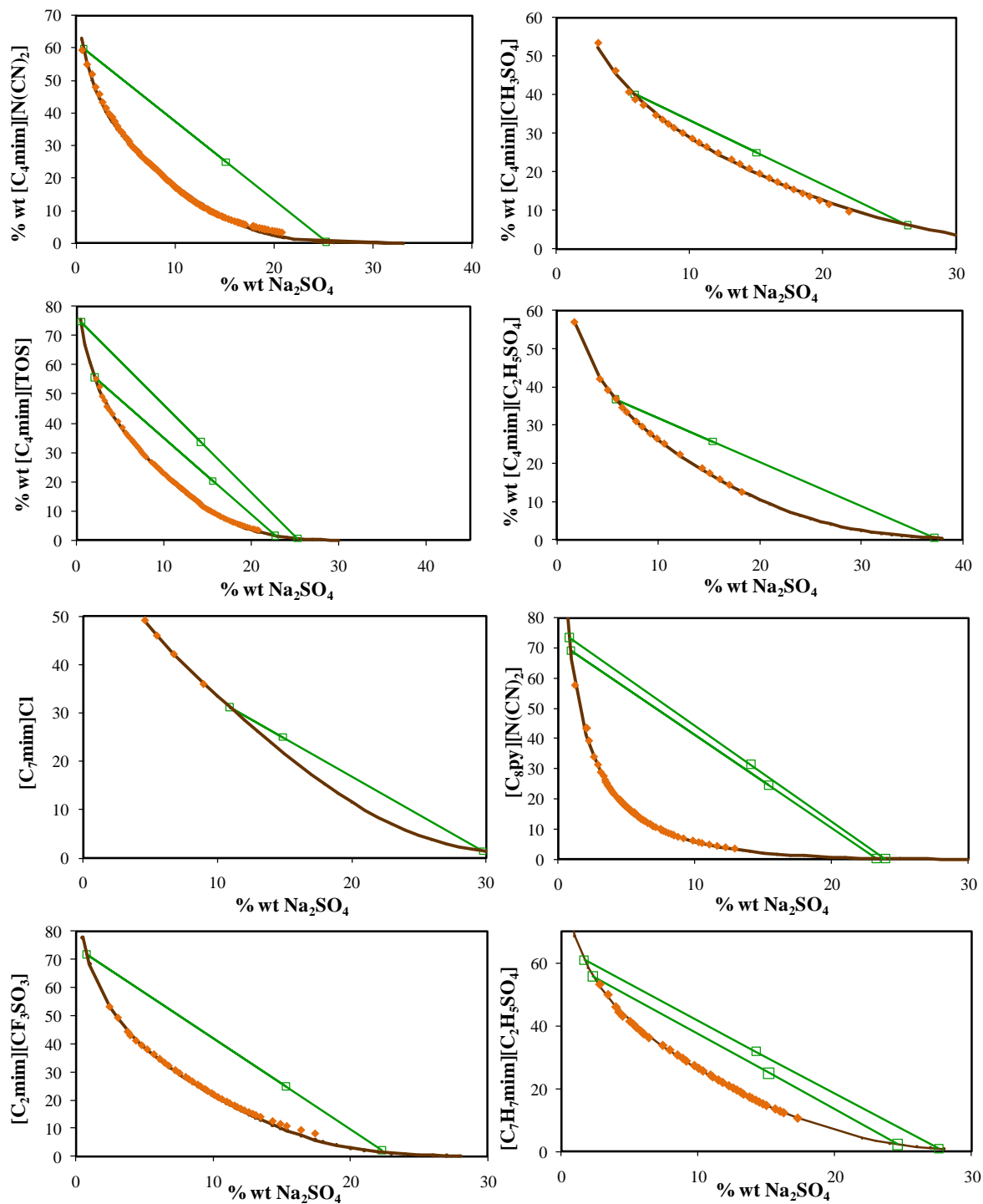
All experimental data were correlated by Equation 5. The adjusted parameters for all ternary systems studied are presented in Table 5.

**Table 5:** Adjusted Parameters used to describe the experimental binodal data by Equation 5.

<b>IL + Na<sub>2</sub>SO<sub>4</sub> + Water system</b>	<b>A</b>	<b>B</b>	<b>10<sup>5</sup>C</b>	<b>R<sup>2</sup></b>
[C <sub>2</sub> mim][CF <sub>3</sub> SO <sub>3</sub> ]	106.1 ± 2.1	-0.439 ± 0.010	16.2 ± 2.0	0.9990
[C <sub>4</sub> mim][CF <sub>3</sub> SO <sub>3</sub> ]	130.0 ± 15.7	-0.760 ± 0.066	30.0 ± 10.0	0.9616
[C <sub>4</sub> mim]Br	97.5 ± 2.6	-0.393 ± 0.016	1.0 ± 5.8	0.9989
[C <sub>4</sub> mim][N(CN) <sub>2</sub> ]	88.8 ± 1.0	-0.446 ± 0.006	20.2 ± 0.7	0.9963
[C <sub>4</sub> mim][CH <sub>3</sub> SO <sub>4</sub> ]	105.4 ± 2.4	-0.396 ± 0.009	4.4 ± 0.4	0.9980
[C <sub>4</sub> mim][C <sub>2</sub> H <sub>5</sub> SO <sub>4</sub> ]	95.4 ± 0.7	-0.393 ± 0.004	5.7 ± 0.2	0.9997
[C <sub>4</sub> mim][TOS]	101.5 ± 0.7	-0.417 ± 0.003	18.7 ± 0.2	0.9995
[C <sub>7</sub> mim]Cl	91.6 ± 2.0	-0.287 ± 0.011	9.9 ± 1.5	1.0000
[C <sub>7</sub> H <sub>7</sub> mim]Cl	104.7 ± 7.4	-0.372 ± 0.036	4.9 ± 6.6	0.9982
[C <sub>7</sub> H <sub>7</sub> mim][C <sub>2</sub> H <sub>5</sub> SO <sub>4</sub> ]	100.6 ± 1.6	-0.383 ± 0.007	12.9 ± 0.5	0.9997
[C <sub>8</sub> mim]Cl	84.6 ± 6.2	-0.245 ± 0.033	13.7 ± 3.1	0.9984
[C <sub>8</sub> py][N(CN) <sub>2</sub> ]	195.2 ± 2.4	-1.079 ± 0.008	9.9 ± 2.3	0.9984

The correlation of the experimental data through the application of Equation 5, as well as the graphical representation of the TLs measured, are presented in Figure 22. Experimental data with the phases composition at equilibrium, and respective TLLs, are reported in Appendix E.

Extraction of Phenolic Compounds with Aqueous Two Phase Systems



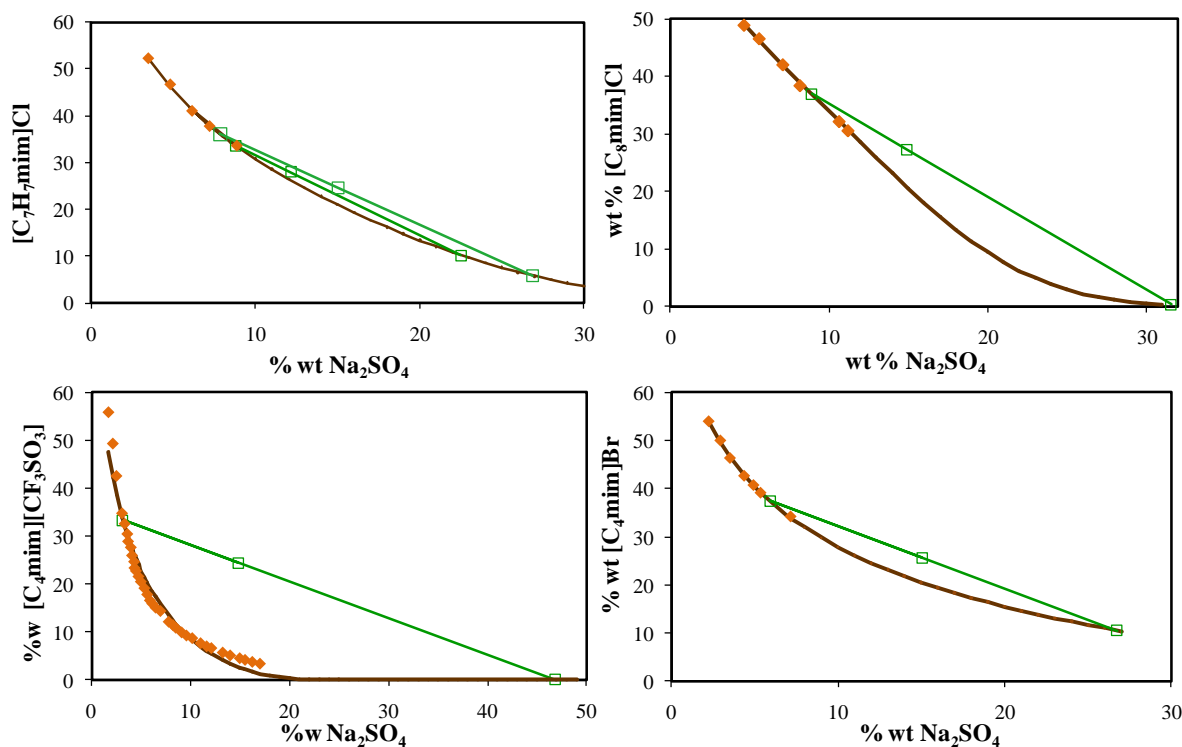


**Figure 22:** Phase diagrams for the different ternary systems composed by IL+ Na<sub>2</sub>SO<sub>4</sub>+ H<sub>2</sub>O at 298 K and atmospheric pressure: ◆, experimental binodal data; □, TL data; — fitting of experimental data by the method proposed by Merchuck et al.<sup>[127]</sup>

For all systems represented, except for [C<sub>4</sub>mim][CF<sub>3</sub>SO<sub>3</sub>], the top-rich phase is the IL-rich phase while the bottom phase is the Na<sub>2</sub>SO<sub>4</sub>-rich phase. Observing all the binodal curves and respective tie-lines it can be seen that the IL concentration in the bottom phase is very small, and in some cases, the IL is almost completely excluded from that phase. Additionally, for systems with more than one TL, the TLs slope are not strictly parallel. Although, these deviations in the TLs slopes are in conformity with literature.<sup>[49]</sup> This fact occurs particularly for longer TLLs.

### 3.3.2. Effect of IL ions and pH in the acid gallic partitioning

The extraction of a molecule in ATPS based on ILs depends on its ability to migrate for the IL-rich phase. In this study it was assessed the selectivity of gallic acid for different ILs and how the pH of the medium influences the respective partition coefficients. In order to evaluate the IL ions influence in the extraction of gallic acid, several combinations between cations and anions were performed. In addition, to evaluate the pH of the medium several inorganic salts combinations were used. The mass fraction compositions used for the determination of each partition coefficient,

partition coefficients values and respective standard deviations, and pH values are reported in Appendix F.

For all the studied systems it was observed that specific interactions between gallic acid and imidazolium-based ILs are favorable since gallic acid preferentially migrates for the IL-rich phase ( $K_{GA} > 1$ ). However, in general the partition coefficients were lower than those obtained with vanillin for the same systems (Chapter 2 of this thesis).

The partition coefficients of gallic acid in aqueous biphasic systems composed by  $\text{Na}_2\text{SO}_4$  and distinct ILs were measured at 298.15 K and are presented in Figure 23. From the inspection of Figure 23 it can be seen that  $K_{GA}$  ranges between 10.25 and 29.58 and thus depend on the IL used. The partition coefficients decrease in the following order:  $[\text{C}_4\text{mim}][\text{C}_2\text{H}_5\text{SO}_4] \gg [\text{C}_7\text{mim}]\text{Cl} > [\text{C}_4\text{mim}][\text{N}(\text{CN})_2] > [\text{C}_4\text{mim}][\text{CH}_3\text{SO}_4] \approx [\text{C}_4\text{mim}][\text{CF}_3\text{SO}_3] > [\text{C}_8\text{mim}]\text{Cl} > [\text{C}_4\text{mim}]\text{Br} \gg [\text{C}_2\text{mim}][\text{CF}_3\text{SO}_3]$ .

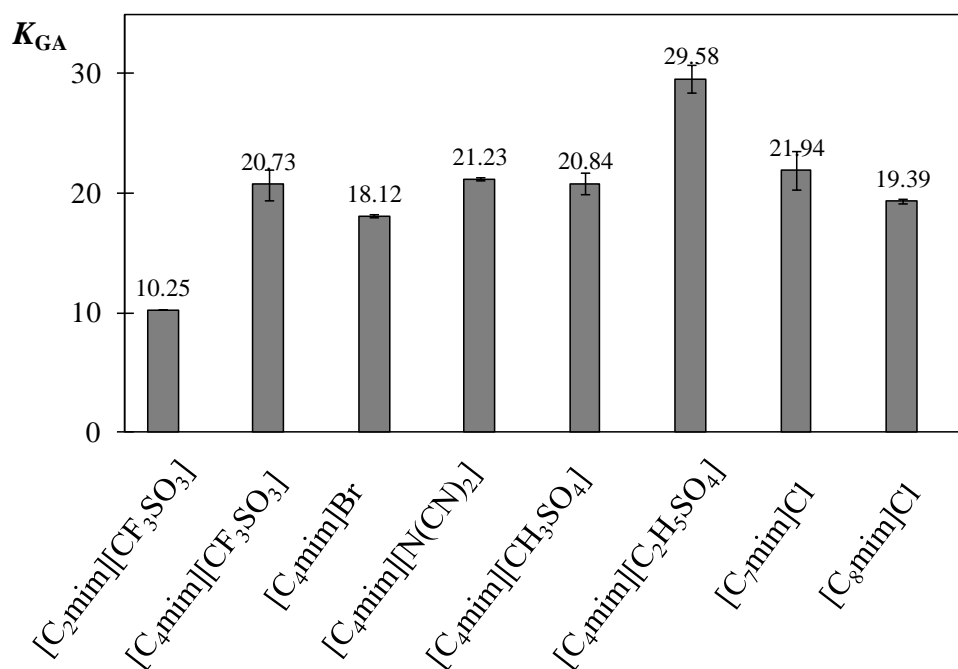


**Figure 23:** Partition coefficients of gallic acid for different ILs +  $\text{Na}_2\text{SO}_4$  ATPS at 298.15 K.

Ranging from  $[\text{C}_2\text{mim}][\text{CF}_3\text{SO}_3]$ - to  $[\text{C}_4\text{mim}][\text{CF}_3\text{SO}_3]$ -based systems (increase of size of the alkyl side chain of the imidazolium cation) leads to an increase in the partition coefficient values. This fact results from the concomitant increase of the IL free volume while decreasing the surface tension of the system.<sup>[49, 109]</sup> In parallel, an increase in the alkyl chain at the anion, from  $[\text{C}_4\text{mim}][\text{CH}_3\text{SO}_4]$  to  $[\text{C}_4\text{mim}][\text{C}_2\text{H}_5\text{SO}_4]$ , promotes the increase of the partition coefficients for gallic acid. For the systems composed by  $[\text{C}_7\text{mim}]\text{Cl}$  and  $[\text{C}_8\text{mim}]\text{Cl}$  it was found a smaller decrease on the partition coefficient values. Longer alkyl chains lead to a decrease in the coulombic and polar interactions and to an increase in dispersive-type interactions between the IL ions.<sup>[42, 111]</sup>

Fixing the  $[C_4mim]^+$  cation, the IL anion effect on the gallic acid extraction follows the rank:  $[C_4mim][C_2H_5SO_4] > [C_4mim][N(CN)_2] \approx [C_4mim][CH_3SO_4] \approx [C_4mim][CF_3SO_3] > [C_4mim]Br$ . Therefore, based on those data, anions with longer alkyl chains or higher hydrogen bond accepting strength present higher extraction abilities for gallic acid. Nevertheless, the effect of the anion is marginal and the higher influence was mainly observed with the increase of the alkyl chain length in  $[C_4mim][C_2H_5SO_4]$ .

The pH of the aqueous medium in the extraction of gallic acid was evaluated using different inorganic salts. The gallic acid partition coefficients obtained are depicted in Figure 24. The pH of each aqueous rich phase are presented in Table 6. In addition, the mass fraction compositions used for the determination of each partition coefficient, partition coefficients values and respective standard deviations, and pH values are presented in Appendix F.

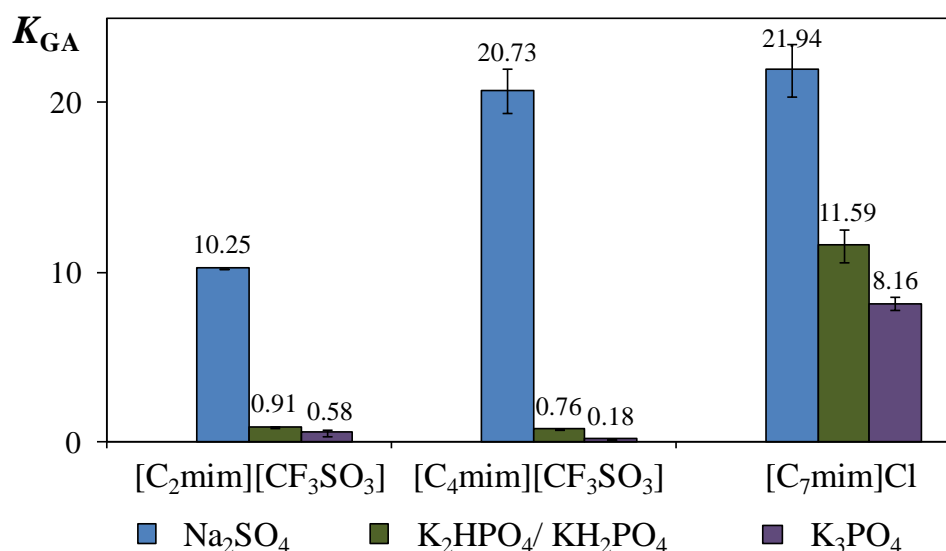


**Figure 24:** Partition coefficients of gallic acid in IL + different inorganic salt ATPS for the ILs:  $[C_2mim][CF_3SO_3]$ ,  $[C_4mim][CF_3SO_3]$  and  $[C_7mim]Cl$ .

From Figure 24, the choice of the inorganic salt employed, and hence of the pH of the system, is highly important and shows to be more significant than the IL used. Although  $K_3PO_4$  is a stronger salting-out agent than  $Na_2SO_4$  it is here obvious that the influence of the pH of the aqueous medium plays a major role since higher partition coefficients of gallic acid are attained with ATPS employing  $Na_2SO_4$ . For instance, focusing on the partition coefficients of the extraction system composed by  $[C_4mim][CF_3SO_3]$  the partition coefficients range between 0.18 and 20.73 for salts  $K_3PO_4$  and  $Na_2SO_4$ , respectively.

For all the studied inorganic salts, the IL that presents an higher ability for extracting gallic acid is  $[C_7mim]Cl$ . Nevertheless, since the biphasic region for the system  $[C_7mim]Cl + K_2HPO_4/KH_2PO_4 +$

water is smaller than for the outstanding ILs, the concentration of this ILs was slightly higher and a direct comparison between [C<sub>7</sub>mim]Cl and the remaining ILs is not strictly accurate. While for the ILs [C<sub>2</sub>mim][CF<sub>3</sub>SO<sub>3</sub>] and [C<sub>4</sub>mim][CF<sub>3</sub>SO<sub>3</sub>] their mass composition was around 25 wt %, for the [C<sub>7</sub>mim]Cl + K<sub>2</sub>HPO<sub>4</sub>/KH<sub>2</sub>PO<sub>4</sub> system the IL was at approximately 30 wt %. Therefore, aiming at better understanding the effect of the IL concentration, the system [C<sub>4</sub>mim][CF<sub>3</sub>SO<sub>3</sub>] + K<sub>2</sub>HPO<sub>4</sub>/KH<sub>2</sub>PO<sub>4</sub> was also evaluated with the IL at 30 wt % (Figure 25).

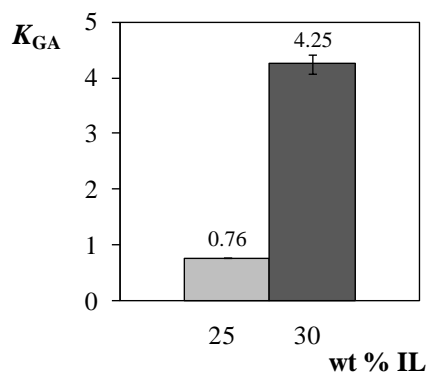


**Figure 25:** Partition coefficients of gallic acid in IL + K<sub>2</sub>HPO<sub>4</sub>/KH<sub>2</sub>PO<sub>4</sub> ATPS for [C<sub>4</sub>mim][CF<sub>3</sub>SO<sub>3</sub>] at 25 wt % and 30 wt %.

Actually there is an increase of the gallic acid partition coefficient with the increase of 5 wt % of IL. However, at 30 wt % of IL, it is observed that the [C<sub>7</sub>mim]Cl has indeed a significantly higher partition coefficient. From the inspection of Table 6, and from the results depicted in Figure 24 and Figure 25, the acidity of the medium largely influences the gallic acid partitioning and favors the solute migration for the IL-rich phase.

**Table 6:** pH values as function the different systems performed.

IL+inorganic salt + water		Na <sub>2</sub> SO <sub>4</sub>	K <sub>2</sub> HPO <sub>4</sub> /KH <sub>2</sub> PO <sub>4</sub>	K <sub>3</sub> PO <sub>4</sub>
[C <sub>2</sub> mim][CF <sub>3</sub> SO <sub>3</sub> ]	Salt-rich phase	3.32	7.28	13.09
	IL-rich phase	2.71	7.57	13.15
[C <sub>4</sub> mim][CF <sub>3</sub> SO <sub>3</sub> ]	Salt-rich phase	3.04	7.10	12.85
	IL-rich phase	3.12	7.37	13.10
[C <sub>7</sub> mim]Cl	Salt-rich phase	4.16	7.22	12.85
	IL-rich phase	4.15	7.45	12.99

The pK<sub>a</sub> of gallic acid is 4.41, which means that in the system with salt Na<sub>2</sub>SO<sub>4</sub>, gallic acid is in its anionic form. As a result, the anionic form preferentially migrates for IL-rich phases.

From the inspection of Table 6, it can be seen that there are no major deviations in the aqueous phases pH at the salt-rich phase and IL-rich phase for the same system or IL. Comparing the pH values for systems composed by [C<sub>2</sub>mim][CF<sub>3</sub>SO<sub>3</sub>] or [C<sub>4</sub>mim][CF<sub>3</sub>SO<sub>3</sub>] there are not large differences in the pH values. Thus, the cation alkyl chain length does not significantly contributes for differences in the pH values at the two aqueous phases in equilibrium. Nevertheless, changing the anion from [CF<sub>3</sub>SO<sub>3</sub>]<sup>-</sup> to Cl<sup>-</sup> guides to slightly differences in the acidity of both aqueous phases.

### **3.4. Conclusions**

In this part of the work ternary phase diagrams employing diverse ILs, water and Na<sub>2</sub>SO<sub>4</sub> were determined due to their absence in literature. Generally, it was observed that anions or cations with more hydrophobic characteristics, ILs with stronger salting-in inducing behavior, have a greater capability to promote ATPS. Additionally, all phase diagrams were adjusted through the equation proposed by Merchuck et al.<sup>[127]</sup> and supplementary TLs and TLLs for each system were determined.

The ability to extract gallic acid of several IL-based ATPS was studied. For aqueous systems composed by Na<sub>2</sub>SO<sub>4</sub> and IL, it was verified that the increase of the alkyl side chain length, in both cation and anion, leads to an increase in the partition coefficient values. Moreover, ILs presenting anions with higher hydrogen bond accepting strength present higher extraction abilities for gallic acid.

Comparing the extractions performed with ATPS containing different inorganic salts (Na<sub>2</sub>SO<sub>4</sub>, K<sub>2</sub>HPO<sub>4</sub>/KH<sub>2</sub>PO<sub>4</sub>, K<sub>3</sub>PO<sub>4</sub>) it can be concluded that the Na<sub>2</sub>SO<sub>4</sub> provides enhanced recovery of gallic acid for the IL-rich phase. Therefore, the choice of the inorganic salt employed in IL-based ATPS, and hence of the system pH, is highly important and shows to be more significant than the IL used.

## **4. Future work**

In the future it would be interesting to extend this type of study to other phenolic compounds and test more conditions in order to optimize extraction routes.

In order to better evaluate the effect of pH on the phenolic compounds extraction it will be important to extend the study for more systems based on different ILs beyond those demonstrated here. Also it is important to determine the pH of both rich phases for some systems already evaluated in this work.

It would also be of utmost importance to use the knowledge acquired in this work to proceed to more practical and real experiments attempting direct extractions from biomass, such as the extraction of phenolic compounds from wood, plants or wastewater effluents.

## **5. References**

1. Noubigh, A.; Mgaidi, A.; Abderrabba, M.; Provost, E.; and Furst, W., *Effect of salts on the solubility of phenolic compounds: experimental measurements and modelling*. Journal of the Science of Food and Agriculture, 2007. 87(5): p. 783-788.
2. Noubigh, A.; Cherif, M.; Provost, E. and Abderrabba, M. *Solubility of gallic acid, vanillin, syringic acid, and protocatechuic acid in aqueous sulfate solutions from (293.15 to 318.15) K*. Journal of Chemical and Engineering Data, 2008. 53(7): p. 1675-1678.
3. RiceEvans, C.A.; Miller, N.J.; and Paganga, G., *Structure-antioxidant activity relationships of flavonoids and phenolic acids*. Free Radical Biology and Medicine, 1996. 20(7): p. 933-956.
4. Sergediene, E.; Jonsson, K.; Szymusiak, H.; Tyrakowska, B.; Rietjens, I. and Cenas, N., *Prooxidant toxicity of polyphenolic antioxidants to HL-60 cells: description of quantitative structure-activity relationships*. Febs Letters, 1999. 462(3): p. 392-396.
5. Du, F.Y., Xiao, X.H.; Luo, X.J. and Li, G.K., *Application of ionic liquids in the microwave-assisted extraction of polyphenolic compounds from medicinal plants*. Talanta, 2009. 78(3): p. 1177-1184.
6. Sanza, M.D.; Domniguez, I.N.; Carcel, L.M.C. and Gracia, L.N., *Analysis for low molecular weight phenolic compounds in a red wine aged in oak chips*. Analytica Chimica Acta, 2004. 513(1): p. 229-237.
7. Martinez-Aragon, M.; Burghoff, S.; Goetheer, E.L.V., and de Haan, A.B., *Guidelines for solvent selection for carrier mediated extraction of proteins*. Separation and Purification Technology, 2009. 65(1): p. 65-72.
8. Domínguez-Pérez, M.; Tomé, L.I.N.; Freire, M.G.; Marrucho, I.M.; Cabeza, O. and Coutinho, J.A.P., *(Extraction of biomolecules using) aqueous biphasic systems formed by ionic liquids and aminoacids*. Separation and Purification Technology, 2010. 72(1): p. 85-91.
9. Earle, M.J.; Esperança, J. M. S. S.; Gilea, M. A.; Canongia Lopes, J. N.; Rebelo, L. P. N.; Magee, J. W.; Seddon, K. R.; Widgren, J. A., *The distillation and volatility of ionic liquids*. Nature, 2006. 439(7078): p. 831-834.
10. Santos, L. M. N. B. F.; Canongia Lopes, J. N.; Coutinho, J. A. P.; Esperança, J. M. S. S.; Gomes, L. R.; Marrucho, I. M.; Rebelo, L. P. N. J., *Ionic liquids: First direct determination of their cohesive energy*. Journal of the American Chemical Society, 2007. 129(2): p. 284-285.
11. Wang, J.J.; Pei, Y.C.; Zhao, Y. and Hu, Z.G. *Recovery of amino acids by imidazolium based ionic liquids from aqueous media*. Green Chemistry, 2005. 7(4): p. 196-202.
12. He, C.Y.; Li, S.H.; Liu, H.W.; Li, K. and Liu, F. *Extraction of testosterone and epitestosterone in human urine using aqueous two-phase systems of ionic liquid and salt*. Journal of Chromatography A, 2005. 1082(2): p. 143-149.
13. Visser, A.E.; Swatloski, R.P.; Reichert, W.M.; Mayton, R.; Sheff, S.; Wierzbicki, A.; Davis, J.H. and Rogers, R.D., *Task-specific ionic liquids incorporating novel cations for the coordination and extraction of Hg<sup>2+</sup> and Cd<sup>2+</sup>: Synthesis, characterization, and extraction studies*. Environmental Science & Technology, 2002. 36(11): p. 2523-2529.
14. Wasserscheid, P. and Keim, W.; *Ionic liquids - New "solutions" for transition metal catalysis*. Angewandte Chemie-International Edition, 2000. 39(21): p. 3773-3789.
15. Plechkova, N.V. and Seddon, K.R., *Applications of ionic liquids in the chemical industry*. Chemical Society Reviews, 2008. 37(1): p. 123-150.
16. Walden, P., Bulletin de l'Académie Impériale des Sciences de St.-Petersbourg, 1914. 8: p. 405-422.
17. Graenacher, C., *Cellulose solution*. U.S. Patent 1943176, 1934.
18. Hurley, F.H. U.S. Patent 4446331, 1948.
19. Wier, T.P.; Hurley, F.H., U.S. Patent 4446349, 1948.
20. Ventura, S.P.M.; Gonçalves, A.M.M.; Gonçalves, F. and Coutinho, J.A.P. *Assessing the toxicity on [C3mim][Tf2N] to aquatic organisms of different trophic levels*. Aquatic Toxicology, 2010. 96(4): p. 290-297.
21. Welton, T., *Room-temperature ionic liquids. Solvents for synthesis and catalysis*. Chemical Reviews, 1999. 99(8): p. 2071-2083.

22. Park, S. and Kazlauskas, R.J., *Biocatalysis in ionic liquids - advantages beyond green technology*. Current Opinion in Biotechnology, 2003. 14(4): p. 432-437.
23. van Rantwijk, F. and Sheldon, R.A. *Biocatalysis in ionic liquids*. Chemical Reviews, 2007. 107(6): p. 2757-2785.
24. Dreyer, S. and Kragl, U., *Ionic liquids for aqueous two-phase extraction and stabilization of enzymes*. Biotechnology and Bioengineering, 2008. 99(6): p. 1416-1424.
25. Holbrey, J.D. and Seddon, K.R., *Ionic Liquids*. Clean Technologies and Environmental Policy, 1999. 1(4): p. 223-236.
26. Dupont, J., de Souza, R.F. and Suarez, P.A.Z. *Ionic liquid (molten salt) phase organometallic catalysis*. Chemical Reviews, 2002. 102(10): p. 3667-3691.
27. Cull, S.G.; Holbrey, J.D.; Vargas-Mora, V.; Seddon, K.R. and Lye, G.J., *Room-temperature ionic liquids as replacements for organic solvents in multiphase bioprocess operations*. Biotechnology and Bioengineering, 2000. 69(2): p. 227-233.
28. Zhao, F.; Wu, X.; Wang, M.K.; Liu, Y.; Gao, L.X. and Dong, S.J. *Electrochemical and bioelectrochemistry properties of room-temperature ionic liquids and carbon composite materials*. Analytical Chemistry, 2004. 76(17): p. 4960-4967.
29. Ding, J.; Welton, T. and Armstrong, D.W., *Chiral ionic liquids as stationary phases in gas chromatography*. Analytical Chemistry, 2004. 76(22): p. 6819-6822.
30. Mank, M.; Stahl, B. and Boehm, G., *2,5-Dihydroxybenzoic acid butylamine and other ionic liquid matrixes for enhanced MALDI-MS analysis of biomolecules*. Analytical Chemistry, 2004. 76(10): p. 2938-2950.
31. Brennecke, J.F. and Maginn, E.J., *Ionic liquids: Innovative fluids for chemical processing*. Aiche Journal, 2001. 47(11): p. 2384-2389.
32. Ventura, S.P.M.; Neves, C.; Freire, M.G.; Marrucho, I.M.; Oliveira, J. and Coutinho, J.A.P., *Evaluation of Anion Influence on the Formation and Extraction Capacity of Ionic-Liquid-Based Aqueous Biphasic Systems*. Journal of Physical Chemistry B, 2009. 113(27): p. 9304-9310.
33. Visser, A.E.; Swatloski, R.P.; Reichert, W.M.; Mayton, R.; Sheff, S.; Wierzbicki, A.; Davis, J.H. and Rogers, R.D., *Task-specific ionic liquids for the extraction of metal ions from aqueous solutions*. Chemical Communications, 2001(01): p. 135-136.
34. Holbrey, J.D.; Visser, A.E.; Spear, S.K.; Reichert, W.M.; Swatloski, R.P.; Broker, G.A. and Rogers, R.D., *Mercury(II) partitioning from aqueous solutions with a new, hydrophobic ethylene-glycol functionalized bis-imidazolium ionic liquid*. Green Chemistry, 2003. 5(2): p. 129-135.
35. Bosmann, A.; Datsevich, L.; Jess, A.; Lauter, A.; Schmitz, C. and P. Wasserscheid, *Deep desulfurization of diesel fuel by extraction with ionic liquids*. Chemical Communications, 2001(23): p. 2494-2495.
36. Branco, L.C.; Crespo, J. G.; Afonso, C. A. M., *Highly selective transport of organic compounds by using supported liquid membranes based on ionic liquids*. Angewandte Chemie-International Edition, 2002. 41(15): p. 2771.
37. Huddleston, J.G.; Willauer, H.D.; Swatloski, R.P. ; Visser, A.E. and Rogers, R.D. *Room temperature ionic liquids as novel media for 'clean' liquid-liquid extraction*. Chemical Communications, 1998(16): p. 1765-1766.
38. Zhao, H.; Xia, S.Q. and Ma, P.S. *Use of ionic liquids as 'green' solvents for extractions*. Journal of Chemical Technology and Biotechnology, 2005. 80(10): p. 1089-1096.
39. Couling, D.J.; Bernot, R.J.; Docherty, K.M.; Dixon, J.K. and Maginn, E.J., *Assessing the factors responsible for ionic liquid toxicity to aquatic organisms via quantitative structure-property relationship modeling*. Green Chemistry, 2006. 8(1): p. 82-90.
40. Docherty, K.M. and Kulpa, C.F. *Toxicity and antimicrobial activity of imidazolium and pyridinium ionic liquids*. Green Chemistry, 2005. 7(4): p. 185-189.
41. Freire, M.G.; Carvalho, P.J. ; Gardas, R.L.; Marrucho, I.M.; Santos, L. M. N. B. F.; and Coutinho, J.A.P., *Mutual solubilities of water and the C(n)mim Tf2N hydrophobic ionic liquids*. Journal of Physical Chemistry B, 2008. 112(6): p. 1604-1610.

42. Freire, M.G., Neves, C., Carvalho, P.J.; Gardas, R.L.; Fernandes, A.M.; Marrucho, I.M.; Santos, L. M. N. B. F. and Coutinho, J.A.P., *Mutual Solubilities of water and hydrophobic ionic liquids*. Journal of Physical Chemistry B, 2007. 111(45): p. 13082-13089.
43. Ranke, J.; Muller, A.; Bottin-Weber, U.; Stock, F.; Stolte, S.; Arning, J.; Stormann, R. and B. Jastorff, *Lipophilicity parameters for ionic liquid cations and their correlation to in vitro cytotoxicity*. Ecotoxicology and Environmental Safety, 2007. 67(3): p. 430-438.
44. Seddon, K.R., Stark, A. and Torres, M.J. *Influence of chloride, water, and organic solvents on the physical properties of ionic liquids*. Pure and Applied Chemistry, 2000. 72(12): p. 2275-2287.
45. Huddleston, J.G.; Visser, A.E.; Reichert, W.M.; Willauer, H.D.; Broker, G.A. and Rogers, R.D., *Characterization and comparison of hydrophilic and hydrophobic room temperature ionic liquids incorporating the imidazolium cation*. Green Chemistry, 2001. 3(4): p. 156-164.
46. Daugulis, A.J., Axford, D.B. Cizek, B. and Malinowski, J.J. *Continuous fermentation of high-strength glucose feeds to ethanol*. Biotechnology Letters, 1994. 16(6): p. 637-642.
47. Rydberg, J.; Musikas, C.; Choppin, G.R., *Principles and Practices of Solvent Extraction*. 1992, New York: Marcel Dekker, Inc.
48. Albertsson, P.A., *Partition of proteins in liquid polymer-polymer 2-phase systems*. Nature, 1958. 182(4637): p. 709-711.
49. Neves, C.; Ventura, S.P.M.; Freire, M.G.; Marrucho, I.M. and Coutinho, J.A.P., *Evaluation of Cation Influence on the Formation and Extraction Capability of Ionic-Liquid-Based Aqueous Biphasic Systems*. Journal of Physical Chemistry B, 2009. 113(15): p. 5194-5199.
50. Hatti-Kaul, R., *Aqueous Two-Phase Systems Methods and Protocols*. 2000, Totowa, New Jersey: Humana Press.
51. Albertsson, P.A., *Chromatography and partition of cells and cell fragments*. Nature, 1956. 177(4513): p. 771-774.
52. Albertsson, P.A., *Particle fractionation in liquid two-phase systems - The composition of some phase systems and the behaviour of some model particles in them application to the isolation of cell walls from microorganisms*. Biochimica Et Biophysica Acta, 1958. 27(2): p. 378-395.
53. Albertsson, P.A., *Partitioning of cell particles and macromolecules*. 3rd ed. 1986, New York Wiley.
54. Albertsson, P.A. and E.J. Nyns, *Counter-current distribution of proteins in aqueous polymer phase systems*. Nature, 1959. 184(4697): p. 1465-1468.
55. Baskir, J.N., Hatton, T.A. and Suter, U.W. *Protein partitioning in two-phase aqueous polymer systems*. Biotechnology and Bioengineering, 1989. 34(4): p. 541-558.
56. Walter, H.; Brooks, D. E., and Fisher, D., *Partition in Aqueous Two-Phase Systems. Theory, Methods, Uses and Applications to Biotechnology*. 1985, Orlando, FL: Academic.
57. Li, S.H.; He, C.Y.; Liu, H.W.; Li, K. and Liu, F. *Ionic liquid-based aqueous two-phase system, a sample pretreatment procedure prior to high-performance liquid chromatography of opium alkaloids*. Journal of Chromatography B-Analytical Technologies in the Biomedical and Life Sciences, 2005. 826(1-2): p. 58-62.
58. Lima, A.S.; Alegre, R.M. and Meirelles, A.J.A., *Partitioning of pectinolytic enzymes in polyethylene glycol/potassium phosphate aqueous two-phase systems*. Carbohydrate Polymers, 2002. 50(1): p. 63-68.
59. Tomé, L.I.N., Catambas, V.R.; Teles, A.R.R.; Freire, M.G.; Marrucho, I.M. and Coutinho, J.A.P., *Tryptophan extraction using hydrophobic ionic liquids*. Separation and Purification Technology, 2010. 72(2): p. 167-173.
60. Gutowski, K.E.; Broker, G.A.; Willauer, H.D.; Huddleston, J.G.; Swatloski, R.P.; Holbrey, J.D. and Rogers, R.D., *Controlling the aqueous miscibility of ionic liquids: Aqueous biphasic systems of water-miscible ionic liquids and water-structuring salts for recycle, metathesis, and separations*. Journal of the American Chemical Society, 2003. 125(22): p. 6632-6633.
61. Louros, C.L.S., Cláudio, A.F.M.; Neves, C.M.S.S.; Freire, M.G.; Marrucho, I.M.; Pauly, J.; and Coutinho, J.A.P., *Extraction of Biomolecules Using Phosphonium-Based Ionic Liquids +*

- K<sub>3</sub>PO<sub>4</sub> Aqueous Biphasic Systems*. International Journal of Molecular Sciences, 2010. 11(4): p. 1777-1791.
62. Freire, M.G.; Carvalho, P.J.; Silva, A.M.S.; Santos, L. M. N. B. F.; Rebelo, L.P.N.; Marrucho, I.M. and Coutinho, J.A.P., *Ion Specific Effects on the Mutual Solubilities of Water and Hydrophobic Ionic Liquids*. Journal of Physical Chemistry B, 2009. 113(1): p. 202-211.
63. Tome, L.I.N., Varanda, F.R. , Freire, M.G.; Marrucho, I.M. and Coutinho, J.A.P. *Towards an Understanding of the Mutual Solubilities of Water and Hydrophobic Ionic Liquids in the Presence of Salts: The Anion Effect*. Journal of Physical Chemistry B, 2009. 113(9): p. 2815-2825.
64. Tomé, L.I.N.; Dominguez-Perez, M; Cláudio , A.F.M; Freire, M.G.; Marrucho, I.M.; Cabeza, O., and Coutinho, J.A.P., *On the Interactions between Amino Acids and Ionic Liquids in Aqueous Media*. Journal of Physical Chemistry B, 2009. 113(42): p. 13971-13979.
65. Freire, M.G., Neves, C.; Silva, A.M.S.; Santos, L. M. N. B. F.; Marrucho, I.M.; Rebelo, L.P.N.; Shah, J.K.; Maginn, E.J. and Coutinho, J.A.P., *H-1 NMR and Molecular Dynamics Evidence for an Unexpected Interaction on the Origin of Salting-In/Salting-Out Phenomena*. Journal of Physical Chemistry B, 2010. 114(5): p. 2004-2014.
66. Soto, A.; Arce, A. and Khoshkbarchi, M.K., *Partitioning of antibiotics in a two-liquid phase system formed by water and a room temperature ionic liquid*. Separation and Purification Technology, 2005. 44(3): p. 242-246.
67. Pei, Y.C.; Wang, J.J.; Wu, K.; Xuan; X.P. and Lu, X.J., *Ionic liquid-based aqueous two-phase extraction of selected proteins*. Separation and Purification Technology, 2009. 64(3): p. 288-295.
68. Liu, Q.F.; Yu, J.; Li, W.L.; Hu, X.S.; Xia, H.S.; Liu, H.Z. and Yang, P., *Partitioning behavior of penicillin G in aqueous two phase system formed by ionic liquids and phosphate*. Separation Science and Technology, 2006. 41(12): p. 2849-2858.
69. Bridges, N.J.; Gutowski, K.E. and Rogers, R.D., *Investigation of aqueous biphasic systems formed from solutions of chaotropic salts with kosmotropic salts (salt-salt ABS)*. Green Chemistry, 2007. 9(2): p. 177-183.
70. Deng, Y.F.; Chen, J. and Zhang, D.L. *Phase diagram data for several salt plus salt aqueous biphasic systems at 298.15 K*. Journal of Chemical and Engineering Data, 2007. 52(4): p. 1332-1335.
71. Hofmeister, F., *Arch. Exp. Pathol. Pharmacol.* . Vol. XXV. 1888.
72. Noubigh, A.; Mgaidi, A. and Abderrabba, M. *Temperature Effect on the Distribution of Some Phenolic Compounds: An Experimental Measurement of 1-Octanol/Water Partition Coefficients*. Journal of Chemical and Engineering Data, 2010. 55(1): p. 488-491.
73. Lacombe, A., Wu, V.C.H.; Tyler, S. and Edwards, K., *Antimicrobial action of the American cranberry constituents; phenolics, anthocyanins, and organic acids, against Escherichia coli O157:H7*. International Journal of Food Microbiology, 2010. 139(1-2): p. 102-107.
74. Habila, J.D.; Bello, I.A. Dzikwi, A.A. Musa, H. and Abubakar, N. *Total phenolics and antioxidant activity of Tridax procumbens Linn*. African Journal of Pharmacy and Pharmacology, 2010. 4(3): p. 123-126.
75. Gil-Longo, J. and Gonzalez-Vazquez, C., *Vascular pro-oxidant effects secondary to the autoxidation of gallic acid in rat aorta*. Journal of Nutritional Biochemistry, 2010. 21(4): p. 304-309.
76. Duthie, S.J.; Collins, A.R.; Duthie, G.G. and Dodson, V.L., *Quercetin and myricetin protect against hydrogen peroxide-induced DNA damage (strand breaks and oxidised pyrimidines) in human lymphocytes*. Mutation Research-Genetic Toxicology and Environmental Mutagenesis, 1997. 393(3): p. 223-231.
77. Skaper, S.D., Fabris, M.; Ferrari, V.; Carbonare, M.D. and Leon, A. *Quercetin protects cutaneous tissue-associated cell types including sensory neurons from oxidative stress induced by glutathione depletion: Cooperative effects of ascorbic acid*. Free Radical Biology and Medicine, 1997. 22(4): p. 669-678.

78. Zuo, Y.; Chen, H. and Deng, Y., *Simultaneous determination of catechins, caffeine and gallic acids in green, Oolong, black and pu-erh teas using HPLC with a photodiode array detector*. *Talanta*, 2002. 57(2): p. 307-316.
79. Sjöström, E., *Wood Chemistry- Fundamentals and applications* 2ed. 1993: Academic Press.
80. Adrian, T.; Freitag, J. and Maurer, G., *High pressure multiphase equilibria in aqueous systems of carbon dioxide, a hydrophilic organic solvent and biomolecules*. *Fluid Phase Equilibria*, 1999. 160: p. 685-693.
81. Brudi, K.; Dahmen, N. and Schmieder, H., *Partition coefficients of organic substances in two-phase mixtures of water and carbon dioxide at pressures of 8 to 30 MPa and temperatures of 313 to 333 K*. *Journal of Supercritical Fluids*, 1996. 9(3): p. 146-151.
82. Hasmann, F.A.; Santos, V.C.; Gurpilhares, D.B.; Pessoa-Junior, A. and Roberto, I.C. *Aqueous two-phase extraction using thermoseparating copolymer: a new system for phenolic compounds removal from hemicelulosic hydrolysate*. *Journal of Chemical Technology and Biotechnology*, 2008. 83(2): p. 167-173.
83. Hayouni, E.; Abedrabba, M.; Bouix, M. and Hamdi, M. *The effects of solvents and extraction method on the phenolic contents and biological activities in vitro of Tunisian Quercus coccifera L. and Juniperus phoenicea L. fruit extracts*. *Food Chemistry*, 2007. 105(3): p. 1126-1134.
84. Hertog, M.G.L.; Feskens, E.J.M.; Hollman, P.C.H.; Katan, M.B. and Kromhout, D., *Dietary antioxidant flavonoids and risk of coronary heart-disease - the Zutphen elderly study*. *Lancet*, 1993. 342(8878): p. 1007-1011.
85. Horax, R.; Hettiarachchy, N. and Chen, P.Y., *Extraction, Quantification, and Antioxidant Activities of Phenolics from Pericarp and Seeds of Bitter Melons (Momordica charantia) Harvested at Three Maturity Stages (Immature, Mature, and Ripe)*. *Journal of Agricultural and Food Chemistry*, 2010. 58(7): p. 4428-4433.
86. Jadhav, D.; Rekha, B.N.; Gogate, P.R. and Rathod, V.K., *Extraction of vanillin from vanilla pods: A comparison study of conventional soxhlet and ultrasound assisted extraction*. *Journal of Food Engineering*, 2009. 93(4): p. 421-426.
87. Kim, J.W. and Mazza, G. *Optimization of extraction of phenolic compounds from flax shives by pressurized low-polarity water*. *Journal of Agricultural and Food Chemistry*, 2006. 54(20): p. 7575-7584.
88. Siddhuraju, P. and Becker, K. *Antioxidant properties of various solvent extracts of total phenolic constituents from three different agroclimatic origins of drumstick tree (Moringa oleifera Lam.) leaves*. *Journal of Agricultural and Food Chemistry*, 2003. 51(8): p. 2144-2155.
89. Tarabanko, V.E.; Chelbina, Y.V.; Sokolenko, V.A. and Tarabanko, N.V., *A study of vanillin extraction by octylamine*. *Solvent Extraction and Ion Exchange*, 2007. 25(1): p. 99-107.
90. Trabelsi, N.; Megdiche, W.; Ksouri, R.; Falleh, H.; Oueslati, S.; Soumaya, B.; Hajlaoui, H. and Abdelly, C. *Solvent effects on phenolic contents and biological activities of the halophyte Limoniastrum monopetalum leaves*. *Lwt-Food Science and Technology*, 2010. 43(4): p. 632-639.
91. Khokhar, S. and Magnusdottir, S.G.M., *Total phenol, catechin, and caffeine contents of teas commonly consumed in the United Kingdom*. *Journal of Agricultural and Food Chemistry*, 2002. 50(3): p. 565-570.
92. *Diadem Public 1.2, The DIPPR Information and Data Evolution Manager*. 2000, AIChE: New York.
93. *Royal Society Catalog of Scientific Papers; Royal Society of London*. Vol. 2. 1868, London.
94. *Beilstein's Handbuch der Organischen Chemie*. 4 ed. Vol. 8. 1925, Berlin: Springer.
95. Goble, M., *Jahresberichte über die Fortschritte der Chemie*. 1858.
96. Goble, M., *J. Pharmacie*, 1858(34): p. 401-405.
97. Esposito, L.J., Formanek, K., Kientz, G., Mauger, F., Maureaux, V., Robert, G. and Truchet, F., *Vanillin, Kirk-Othmer Encyclopedia of Chemical Technology*. 4 ed. 1997, New York: John Wiley & Sons.

98. Hocking, M.B., *Vanillin: Synthetic flavoring from spent sulfite liquor*. Journal of Chemical Education, 1997. 74(9): p. 1055-1059.
99. Diddams, D.G., Krum, J. K., *In Kirk–Othmer Encyclopedia of Chemical Technology*. 2 ed. Vol. 21. 1970, New York: Interscience.
100. Anon, Dinglers Polytech J., 1875. 216(372).
101. Grafe, V., Monatsh. Chem. Wissen., 1904(25): p. 987.
102. Howard, G.C. U.S. Patent 1551882, 1925:
103. Tomlinson, G.H. and Hibbert, H. *Studies on lignin and related compounds. XXIV. The formation of vanillin from waste sulfite liquor*. Journal of the American Chemical Society, 1936. 58: p. 345-348.
104. Freudenberg, K.; Lautsch, W. and Brenek, H., German, Patent 947402, 1956.
105. Sandborn, L.R.; Salvesen, J. R. and Howard, G. C., U.S., Patent 2057117, 1936.
106. Hibbert, H. and Tomlinson, G., U.S., Patent 2069185, 1937.
107. Hearon, W.M. U.S., Patent 4208350, 1980:
108. Flory, P.J., *Principles of Polymer Chemistry*. 1953, Ithaca, NY: Cornell University Press.
109. Carvalho, P.J.; Freire, M.G.; Marrucho, I.M.; Queimada, A.J. and Coutinho, J.A.P., *Surface tensions for the 1-alkyl-3-methylimidazolium bis(trifluoromethylsulfonyl)imide ionic liquids*. Journal of Chemical and Engineering Data, 2008. 53(6): p. 1346-1350.
110. Blesic, M.; Marques, M.H.; Plechkova, N.V.; Seddon, K.R.; Rebelo, L.P.N. and Lopes, A. *Self-aggregation of ionic liquids: micelle formation in aqueous solution*. Green Chemistry, 2007. 9(5): p. 481-490.
111. Canongia Lopes, J.N.A. and Pádua, A.A.H., *Nanostructural Organization in Ionic Liquids*. The Journal of Physical Chemistry B, 2006. 110(7): p. 3330-3335.
112. Du, Z., Yu, Y.L. and Wang, J.H. *Extraction of proteins from biological fluids by use of an ionic liquid/aqueous two-phase system*. Chemistry-a European Journal, 2007. 13(7): p. 2130-2137.
113. Boddu, V.M., Abburi, K.; Maloney, S.W. and Damavarapu, R., *Physicochemical properties of an insensitive munitions compound, N-methyl-4-nitroaniline (MNA)*. Journal of Hazardous Materials, 2008. 155(1-2): p. 288-294.
114. Ottiger, C. and Wunderli-Allenspach, H., *Immobilized artificial membrane (IAM)-HPLC for partition studies of neutral and ionized acids and bases in comparison with the liposomal partition system*. Pharmaceutical Research, 1999. 16(5): p. 643-650.
115. Mei, L.H.; Lin, D.Q.; Zhu, Z.Q. and Han, Z.X., *Densities and viscosities of polyethylene-glycol plus salt plus water-systems at 20 degrees - C*. Journal of Chemical and Engineering Data, 1995. 40(6): p. 1168-1171.
116. Perumalsamy, M. and Murugesan, T. *Phase Compositions, Molar Mass, and Temperature Effect on Densities, Viscosities, and Liquid-Liquid Equilibrium of Polyethylene Glycol and Salt-Based Aqueous Two-Phase Systems*. Journal of Chemical and Engineering Data, 2009. 54(4): p. 1359-1366.
117. Chuysinuan, P., Chimnoi, N. ; Techasakul, S. and Supaphol, P. *Galic Acid-Loaded Electrospun Poly(L-Lactic Acid) Fiber Mats and their Release Characteristic*. Macromolecular Chemistry and Physics, 2009. 210(10): p. 814-822.
118. Yilmaz, Y. and Toledo, R.T., *Major Flavonoids in Grape Seeds and Skins: Antioxidant Capacity of Catechin, Epicatechin, and Gallic Acid*. Journal of Agricultural and Food Chemistry, 2003. 52(2): p. 255-260.
119. Lu, J.J.; Wei, Y. and Yuan, Q.P. *Preparative separation of gallic acid from Chinese traditional medicine by high-speed counter-current chromatography and followed by preparative liquid chromatography*. Separation and Purification Technology, 2007. 55(1): p. 40-43.
120. Mammela, P.; Tuomainen, A.; Savolainen, H.; Kangas, J.; Vartiainen, T. and Lindroos, L. *Determination of gallic acid in wood dust as an indicator of oak content*. Journal of Environmental Monitoring, 2001. 3(5): p. 509-511.
121. Condrat, D.; Mosoarca, C.; Zamfir, A.D.; Crisan, F.; Szabo, M.R. and Lupea, A.X., *Qualitative and quantitative analysis of gallic acid in Alchemilla vulgaris, Allium ursinum, Acorus calamus and Solidago virga-aurea by chip-electrospray ionization mass spectrometry and high*

- performance liquid chromatography*. Central European Journal of Chemistry, 2010. 8(3): p. 530-535.
122. Daneshfar, A., Ghaziaskar, H.S. and Homayoun, N., *Solubility of gallic acid in methanol, ethanol, water, and ethyl acetate*. Journal of Chemical and Engineering Data, 2008. 53(3): p. 776-778.
123. Ossipov, V.; Loponen, J.; Ossipova, S.; Haukioja, E. and Pihlaja, K. *Gallotannins of birch Betula pubescens leaves: HPLC separation and quantification*. Biochemical Systematics and Ecology, 1997. 25(6): p. 493-504.
124. Alberto, M.R.; Farias, M.E. and Manca de Nadra, M.C., *Effect of Gallic Acid and Catechin on Lactobacillus hilgardii 5w Growth and Metabolism of Organic Compounds*. Journal of Agricultural and Food Chemistry, 2001. 49(9): p. 4359-4363.
125. Santos, S.A.O.; Pinto, P.; Silvestre, A.J.D. and Neto, C.P., *Chemical composition and antioxidant activity of phenolic extracts of cork from Quercus suber L*. Industrial Crops and Products, 2010. 31(3): p. 521-526.
126. I.-M. a. C. Chu, W.-Y., *Methods in biotechnology 11*. 2000, Totowa, N.J.: R. Hatti-Kaul, Humana Press.
127. Merchuk, J.C., Andrews, B.A. and Asenjo, J.A., *Aqueous two-phase systems for protein separation Studies on phase inversion*. Journal of Chromatography B, 1998. 711(1-2): p. 285-293.
128. Gonzalez, J.; Cruz, J.M.; Dominguez, H. and Parajo, J.C., *Production of antioxidants from Eucalyptus globulus wood by solvent extraction of hemicellulose hydrolysates*. Food Chemistry, 2004. 84(2): p. 243-251.
129. Huang, H.J.; Ramaswamy, S.; Tschirner, U.W. and Ramarao, B.V., *A review of separation technologies in current and future biorefineries*. Separation and Purification Technology, 2008. 62(1): p. 1-21.

# **List of Publications**

Co-author in

- Tomé, L.I.N.; Dominguez-Perez, M; Cláudio , A.F.M; Freire, M.G.; Marrucho, I.M.; Cabeza, O.,and Coutinho, J.A.P., *On the Interactions between Amino Acids and Ionic Liquids in Aqueous Media*. Journal of Physical Chemistry B, 2009. **113**(42): p. 13971-13979.
- Louros, C.L.S; Cláudio , A.F.M; Neves ,C.M.S.S.; Freire, M.G.; Marrucho, I.M.; Pauly, J.; and Coutinho, J.A.P., *Extraction of Biomolecules Using Phosphonium-Based Ionic Liquids + K<sub>3</sub>PO<sub>4</sub> Aqueous Biphasic Systems*. International Journal of Molecular Sciences, 2010. **11**(4): p. 1777-1791
- Cláudio, A.F.M.; Freire ,M.G.; Freire, C. S. R.; Silvestre, A. J. D.and Coutinho, J.A.P. *Extraction of Vanillin using Ionic-Liquid-Based Aqueous Two-Phase Systems*, Separation and Purification Technology, 2010, accepted for publication.
- Neves, C. M. S. S.; Batista, M. L. S.; Cláudio, A. F. M.; Santos, L. M. N. B. F.; Marrucho, I. M; Freire, M G. and Coutinho, J A. P., *Thermophysical Properties and Water Saturation of [PF<sub>6</sub>]-based Ionic Liquids*, Journal of Chemical & Engineering Data, 2010, accepted for publication.
- Cláudio, A. F. M.; Soto, A. M.; Freire, M.G. and Coutinho, J.A.P., *Extraction of gallic acid using Ionic-Liquid-Based Aqueous Two-Phase Systems*, in preparation.

# **Appendix A**

### A.1. Calibration curve for vanillin

In order to know the amount of vanillin in each phase, it is necessary to draw a calibration curve. For this, 7 standards of different known concentrations were prepared (Table A 1) from the initial stock solution ( $[\text{Van}] = 0.513 \text{ g}\cdot\text{dm}^{-3}$ ). Absorbance was measured at a wavelength of 280 nm.

**Table A 1:** Concentration of vanillin and respective absorbance at  $\lambda = 280 \text{ nm}$ .

Standard	$[\text{Van}] / (\text{g}\cdot\text{dm}^{-3})$	Abs
1	$2.57 \times 10^{-2}$	1.694
2	$2.05 \times 10^{-2}$	1.377
3	$1.03 \times 10^{-2}$	0.707
4	$5.13 \times 10^{-3}$	0.372
5	$4.10 \times 10^{-3}$	0.281
6	$6.16 \times 10^{-3}$	0.432
7	$8.21 \times 10^{-3}$	0.570

The calibration curve obtained is displayed in Figure A1.

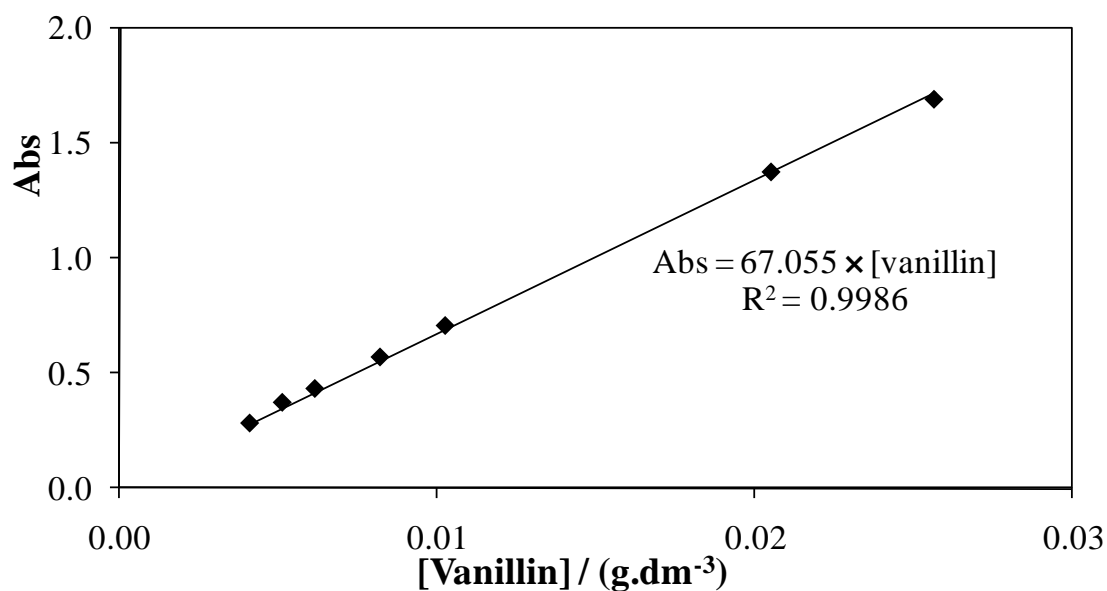


**Figure A 1:** Calibration curve for vanillin at  $\lambda = 280 \text{ nm}$ .

## A.2. Calibration curve for gallic acid

To quantify gallic acid in each of the aqueous phases it was established the respective calibration curve. As a result, 7 standards of different known concentrations were prepared (Table A 2) from the initial stock solution ( $[GA] = 0.521 \text{ g}\cdot\text{dm}^{-3}$ ). Absorbance was measured at a wavelength of 262 nm.

**Table A 2:** Concentration of gallic acid and respective absorbance at  $\lambda = 262 \text{ nm}$ .

standard	$[GA] / (\text{g}\cdot\text{dm}^{-3})$	Abs
1	$2.08 \times 10^{-3}$	0.095
2	$2.61 \times 10^{-3}$	0.113
3	$3.47 \times 10^{-3}$	0.157
4	$5.21 \times 10^{-3}$	0.227
5	$1.04 \times 10^{-2}$	0.474
6	$1.56 \times 10^{-2}$	0.683
7	$2.08 \times 10^{-2}$	0.907

The calibration curve obtained is displayed in Figure A2.

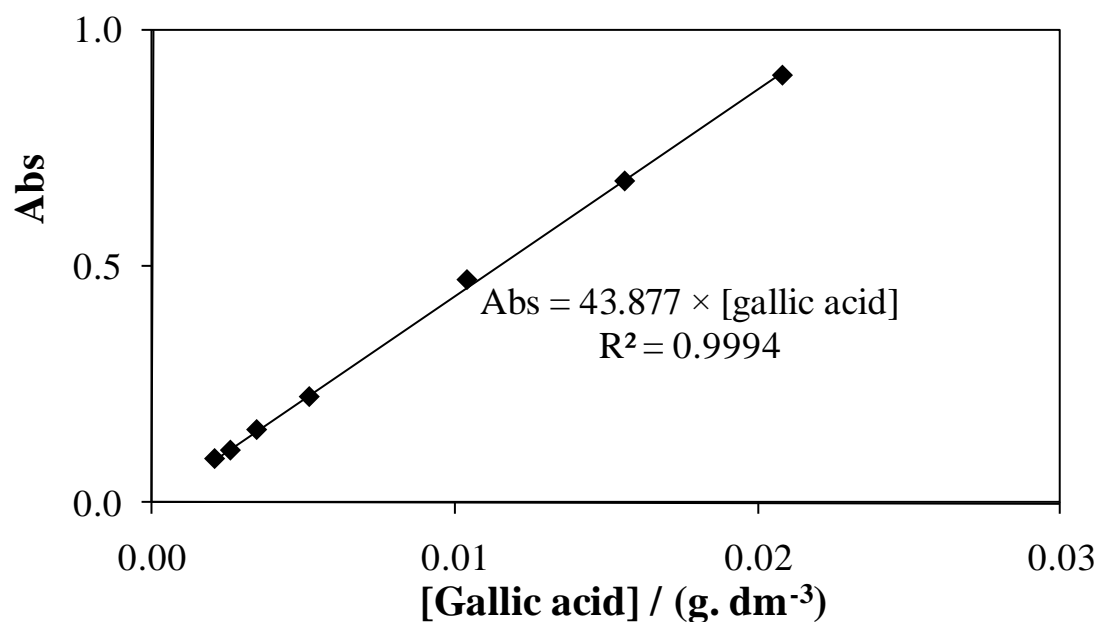


**Figure A 2:** Calibration curve for gallic acid at  $\lambda = 262 \text{ nm}$ .

# **Appendix B**

## Experimental data for the vanillin partition coefficients, density and viscosity

**Table B 1:** Experimental weight fraction composition and partition coefficients of vanillin in ILs + K<sub>3</sub>PO<sub>4</sub> ATPS at 298.15 K.

IL + K <sub>3</sub> PO <sub>4</sub> + water system	Weight fraction composition / wt %		$K_{\text{van}} \pm \sigma^{\text{a}}$
	IL	K <sub>3</sub> PO <sub>4</sub>	
[C <sub>2</sub> mim]Cl	24.83	15.28	36.49 ± 0.61
[C <sub>4</sub> mim]Cl	25.00	15.02	44.98 ± 0.10
[C <sub>6</sub> mim]Cl	25.66	14.62	49.59 ± 1.12
[C <sub>7</sub> mim]Cl	24.61	14.88	42.39 ± 1.35
[C <sub>10</sub> mim]Cl	24.80	15.33	2.72 ± 0.22
[amim]Cl	24.75	15.86	36.45 ± 1.60
[OHC <sub>2</sub> mim]	40.66	14.92	22.95 ± 0.12
[C <sub>7</sub> H <sub>7</sub> mim]Cl	24.54	14.78	44.18 ± 1.34
[C <sub>4</sub> mim][CH <sub>3</sub> CO <sub>2</sub> ]	24.63	14.88	6.64 ± 0.54
[C <sub>4</sub> mim][N(CN) <sub>2</sub> ]	24.63	14.77	31.87 ± 3.97
[C <sub>4</sub> mim]Br	24.74	15.55	25.66 ± 0.40
[C <sub>4</sub> mim][CH <sub>3</sub> SO <sub>3</sub> ]	24.82	15.23	6.94 ± 0.05
[C <sub>4</sub> mim][CF <sub>3</sub> SO <sub>3</sub> ]	24.67	15.16	9.75 ± 1.34
[C <sub>4</sub> mim][CH <sub>3</sub> SO <sub>4</sub> ]	25.05	15.16	22.74 ± 0.55

<sup>a</sup>standard deviation

**Table B 2:** Experimental weight fraction composition and partition coefficients of vanillin in IL + K<sub>3</sub>PO<sub>4</sub> ATPS as a function of temperature.

<i>T</i> / K	Weight fraction composition / wt %		<i>K</i> <sub>Van±</sub> σ <sup>a</sup>
	IL	K <sub>3</sub> PO <sub>4</sub>	
[C <sub>4</sub> mim]Cl			
288.15	24.64	15.06	21.46 ± 0.01
298.15	25.00	15.02	44.98 ± 0.10
308.15	24.68	14.94	45.97 ± 0.37
318.15	25.02	15.08	30.90 ± 0.47
328.15	24.98	14.99	19.26 ± 0.42
[C <sub>4</sub> mim][CH <sub>3</sub> SO <sub>4</sub> ]			
288.15	24.90	15.20	15.27 ± 1.12
298.15	25.05	15.16	22.74 ± 0.55
308.15	24.76	15.70	22.03 ± 0.49
318.15	24.71	15.06	17.35 ± 0.74
328.15	24.89	15.07	14.63 ± 1.07
[C <sub>7</sub> H <sub>7</sub> mim]Cl			
288.15	24.90	15.28	29.25 ± 2.35
298.15	24.54	14.78	44.19 ± 1.34
308.15	24.59	14.76	30.52 ± 0.15
318.15	25.15	14.94	27.09 ± 0.20
328.15	24.55	14.96	26.99 ± 0.90
[amim]Cl			
288.15	24.80	14.90	33.74 ± 0.53
298.15	24.76	15.86	36.45 ± 1.60
308.15	24.77	14.95	21.83 ± 0.64
318.15	24.78	15.42	22.03 ± 0.01
328.15	24.96	15.16	13.55 ± 0.13

<sup>a</sup>standard deviation

**Table B 3:** Experimental weight fraction composition and partition coefficients of vanillin in IL + K<sub>3</sub>PO<sub>4</sub> ATPS as a function of the initial vanillin concentration.

IL + K <sub>3</sub> PO <sub>4</sub> + Water system with different concentrations	Weight fraction composition / wt %		$K_{\text{van}} \pm \sigma^a$
	IL	K <sub>3</sub> PO <sub>4</sub>	
	[C <sub>4</sub> mim]Cl		
0.5 g·dm <sup>-3</sup> = 3.3 × 10 <sup>-3</sup> mol·dm <sup>-3</sup>	25.05	15.14	33.09 ± 0.49
1.0 g·dm <sup>-3</sup> = 6.6 × 10 <sup>-3</sup> mol·dm <sup>-3</sup>	25.00	15.20	44.98 ± 0.10
2.5 g·dm <sup>-3</sup> = 1.6 × 10 <sup>-2</sup> mol·dm <sup>-2</sup>	24.73	15.48	57.02 ± 7.26
5.0 g·dm <sup>-3</sup> = 3.3 × 10 <sup>-2</sup> mol · dm <sup>-2</sup>	25.05	15.00	88.30 ± 15.50
7.5 g·dm <sup>-3</sup> = 4.9 × 10 <sup>-2</sup> mol · dm <sup>-2</sup>	24.96	14.99	98.08 ± 1.00
	[C <sub>4</sub> mim][CH <sub>3</sub> SO <sub>4</sub> ]		
0.5 g·dm <sup>-3</sup> = 3.3 × 10 <sup>-3</sup> mol·dm <sup>-3</sup>	25.02	15.19	17.97 ± 1.28
1.0 g·dm <sup>-3</sup> = 6.6 × 10 <sup>-3</sup> mol·dm <sup>-3</sup>	25.05	15.16	22.74 ± 0.55
2.5 g·dm <sup>-3</sup> = 1.6 × 10 <sup>-2</sup> mol·dm <sup>-2</sup>	24.86	15.30	35.04 ± 4.03
5.0 g·dm <sup>-3</sup> = 3.3 × 10 <sup>-2</sup> mol · dm <sup>-2</sup>	24.14	15.75	36.19 ± 1.65
	[C <sub>7</sub> H <sub>7</sub> mim]Cl		
0.5 g·dm <sup>-3</sup> = 3.3 × 10 <sup>-3</sup> mol·dm <sup>-3</sup>	24.95	14.97	21.31 ± 0.97
1.0 g·dm <sup>-3</sup> = 6.6 × 10 <sup>-3</sup> mol·dm <sup>-3</sup>	24.54	14.78	44.19 ± 1.34
2.5 g·dm <sup>-3</sup> = 1.6 × 10 <sup>-2</sup> mol·dm <sup>-2</sup>	24.94	15.07	60.00 ± 2.86
5.0 g·dm <sup>-3</sup> = 3.3 × 10 <sup>-2</sup> mol · dm <sup>-2</sup>	24.61	14.71	79.58 ± 0.24
7.5 g·dm <sup>-3</sup> = 4.9 × 10 <sup>-2</sup> mol · dm <sup>-2</sup>	24.86	14.90	98.69 ± 9.12

<sup>a</sup>standard deviation

**Table B 4:** Density and viscosity dependence on temperature of the IL-rich phase (Top phase, *T*) and salt-rich phase (Bottom phase, *B*) for systems composed by chloride-based ILs + K<sub>3</sub>PO<sub>4</sub> + H<sub>2</sub>O equilibrated at 298.15 K.

<i>T</i> / K	IL / wt %	K <sub>3</sub> PO <sub>4</sub> / wt %	$\eta_T$ / mPa.s	$\eta_B$ / mPa.s	$\rho_T$ / g.cm <sup>-3</sup>	$\rho_B$ / g.cm <sup>-3</sup>
[C <sub>2</sub> mim]Cl + water + K <sub>3</sub> PO <sub>4</sub>						
298.15			2.9785	4.2829	1.0951	1.3857
308.15	24.58	15.92	2.3209	3.4014	1.0896	1.3796
318.15			1.8597	2.7726	1.0840	1.3734
328.15			1.5261	2.3107	1.0781	1.3671
[C <sub>4</sub> mim]Cl + water + K <sub>3</sub> PO <sub>4</sub>						
298.15			3.6868	3.6160	1.0725	1.3609
308.15	24.80	15.46	2.7839	2.8889	1.0664	1.3549
318.15			2.1767	2.3672	1.0602	1.3488
328.15			1.7540	1.9775	1.0538	1.3427
[C <sub>6</sub> mim]Cl + water + K <sub>3</sub> PO <sub>4</sub>						
298.15			5.3025	2.8001	1.0597	1.3138
308.15	25.11	14.99	3.9496	2.2715	1.0536	1.3078
318.15			3.0351	1.8827	1.0476	1.3019
328.15			2.3933	1.5901	1.0413	1.2959
[C <sub>7</sub> mim]Cl + water + K <sub>3</sub> PO <sub>4</sub>						
298.15			10.208	2.6509	1.0515	1.3012
308.15	24.84	15.59	7.3087	2.1566	1.0455	1.2953
318.15			5.3741	1.7924	1.0393	1.2895
328.15			4.0472	1.5179	1.0329	1.2835
[C <sub>10</sub> mim]Cl + water + K <sub>3</sub> PO <sub>4</sub>						
298.15			14.187	2.5565	1.0782	1.2565
308.15	24.18	16.54	10.7300	2.0785	1.0721	1.2507
318.15			8.3817	1.7303	1.0658	1.2449
328.15			6.6833	1.4676	1.0594	1.2389
[C <sub>7</sub> H <sub>7</sub> mim]Cl + water + K <sub>3</sub> PO <sub>4</sub>						
298.15			4.1457	2.6911	1.1172	1.2939
308.15	25.09	14.97	3.1450	2.1835	1.1113	1.2880
318.15			2.4672	1.8106	1.1053	1.2821
328.15			1.9919	1.5302	1.0990	1.2761
[amim]Cl + water + K <sub>3</sub> PO <sub>4</sub>						
298.15			2.9621	3.6759	1.1002	1.3596
308.15	24.98	15.13	2.2977	2.9377	1.0945	1.3535
318.15			1.8362	2.4095	1.0887	1.3475
328.15			1.5055	2.018	1.0827	1.3413

*Extraction of Phenolic Compounds with Aqueous Two Phase Systems*

[OHC <sub>2</sub> mim]Cl + water + K <sub>3</sub> PO <sub>4</sub>						
298.15			6.2735	9.2536	1.1832	1.5265
308.15	39.64	15.76	4.7395	6.9621	1.1779	1.5201
318.15			3.7035	5.4289	1.1727	1.5138
328.15			2.9719	4.359	1.1675	1.5075

**Table B 5:** Density and viscosity dependence on temperature of the IL-rich phase (Top phase, *T*) and salt-rich phase (Bottom phase, *B*) for systems composed by [C<sub>4</sub>mim]-based ILs + K<sub>3</sub>PO<sub>4</sub> + H<sub>2</sub>O equilibrated at 298.15 K.

<i>T</i> / K	IL / wt %	K <sub>3</sub> PO <sub>4</sub> / wt %	$\eta_T$ / mPa.s	$\eta_B$ / mPa.s	$\rho_T$ / g.cm <sup>-3</sup>	$\rho_B$ / g.cm <sup>-3</sup>
[C <sub>4</sub> mim]Cl + water + K <sub>3</sub> PO <sub>4</sub>						
298.15			3.6868	3.616	1.0725	1.3609
308.15	24.80	15.46	2.7839	2.8889	1.0664	1.3549
318.15			2.1767	2.3672	1.0602	1.3488
328.15			1.754	1.9775	1.0538	1.3427
[C <sub>4</sub> mim]Br + water + K <sub>3</sub> PO <sub>4</sub>						
298.15			3.2282	2.7799	1.1496	1.3046
308.15	24.95	15.06	2.4675	2.2463	1.1432	1.2986
318.15			1.9501	1.8565	1.1368	1.2927
328.15			1.5839	1.5644	1.1299	1.2866
[C <sub>4</sub> mim][CH <sub>3</sub> SO <sub>4</sub> ] + water + K <sub>3</sub> PO <sub>4</sub>						
298.15			3.4649	2.8726	1.1254	1.2854
308.15	25.04	14.97	2.6485	2.3089	1.119	1.2796
318.15			2.0936	1.9023	1.1125	1.2737
328.15			1.7000	1.5985	1.1059	1.2677
[C <sub>4</sub> mim][CH <sub>3</sub> SO <sub>3</sub> ] + water + K <sub>3</sub> PO <sub>4</sub>						
298.15			3.6729	3.7196	1.1230	1.3459
308.15	24.11	16.49	2.7913	2.9666	1.1168	1.3397
318.15			2.1968	2.4258	1.1105	1.3335
328.15			1.7773	2.0240	1.1041	1.3273
[C <sub>4</sub> mim][CF <sub>3</sub> SO <sub>3</sub> ] + water + K <sub>3</sub> PO <sub>4</sub>						
298.15			8.0471	2.0015	1.2169	1.2291
308.15	24.98	15.02	5.9335	1.6372	1.2115	1.2208
318.15			4.5461	1.3656	1.2060	1.2125
328.15			3.5951	1.1594	1.1996	1.2041
[C <sub>4</sub> mim][CH <sub>3</sub> CO <sub>2</sub> ] + water + K <sub>3</sub> PO <sub>4</sub>						
298.15			3.7596	4.7622	1.1087	1.3830
308.15	24.98	14.93	2.8228	3.7208	1.1027	1.3774
318.15			2.2007	2.988	1.0966	1.3718
328.15			1.7677	2.4591	1.0903	1.3658
[C <sub>4</sub> mim][N(CN) <sub>2</sub> ] + water + K <sub>3</sub> PO <sub>4</sub>						
298.15			3.6187	2.3530	1.0366	1.2542
308.15	24.96	15.10	2.7869	1.9138	1.0297	1.2485
318.15			2.2100	1.5907	1.0229	1.2426
328.15			1.7969	1.3469	1.0159	1.2366

# **Appendix C**

van't Hoff plots

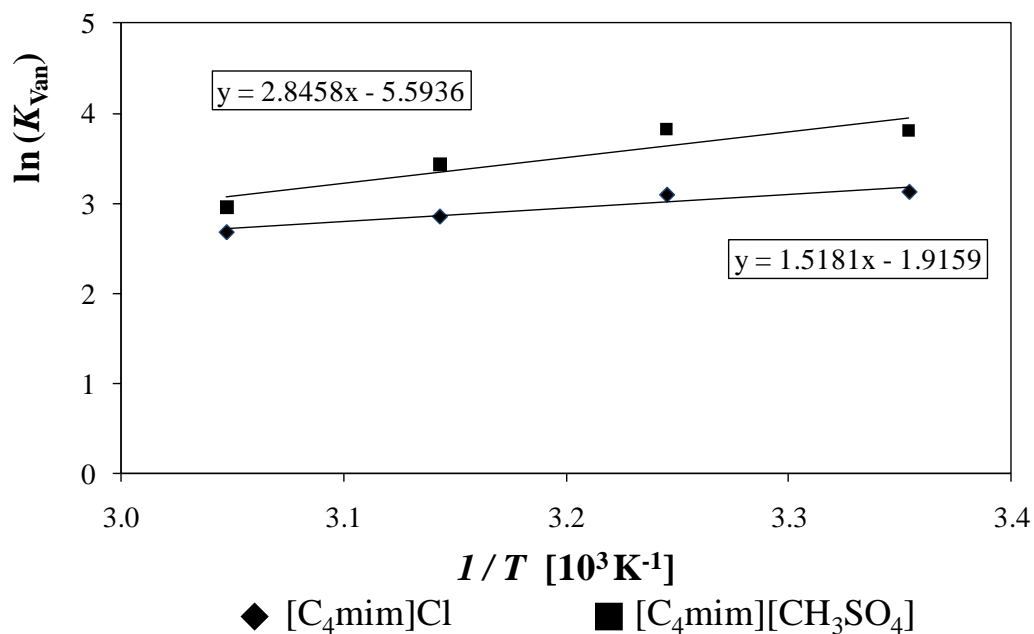


Figure C 1: van't Hoff plot of  $\ln(K_{\text{van}})$  versus inverse absolute temperature for  $[\text{C}_4\text{mim}]\text{Cl}$  and  $[\text{C}_4\text{mim}][\text{CH}_3\text{SO}_4]$  systems.

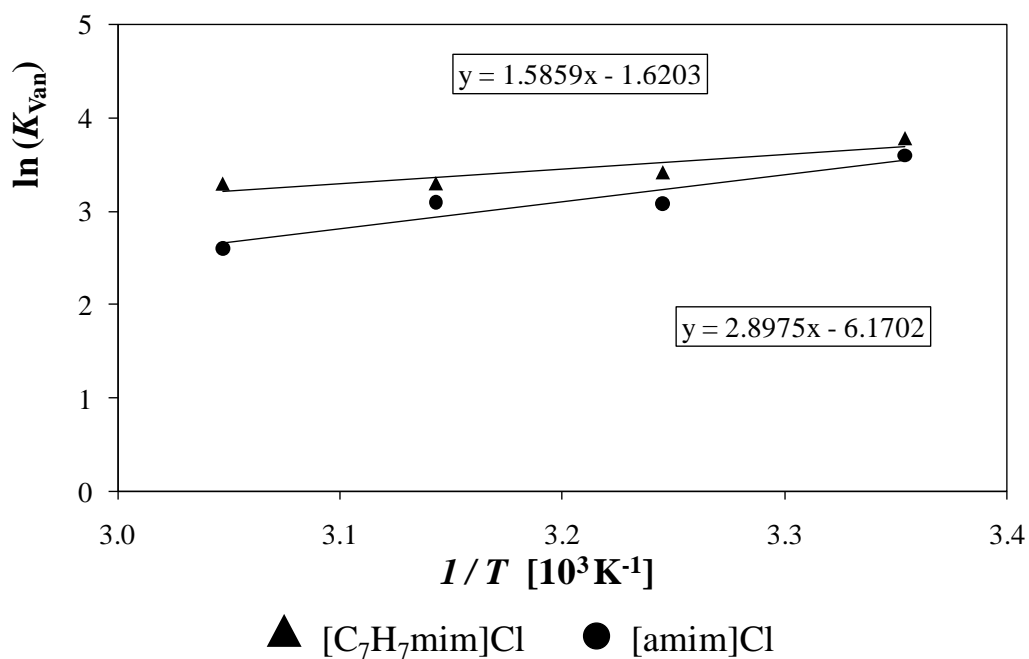


Figure C 2: van't Hoff plot of  $\ln(K_{\text{van}})$  versus inverse absolute temperature for  $[\text{C}_7\text{H}_7\text{mim}]\text{Cl}$  and  $[\text{amim}]\text{Cl}$  systems.

# **Appendix D**

## Experimental binodal curve mass fraction compositions

**Table D 1:** Experimental binodal curve and mass fraction compositions for the system IL + Na<sub>2</sub>SO<sub>4</sub> + H<sub>2</sub>O at 298 K.

[C <sub>4</sub> mim]Br <i>Mr</i> = 219.12		[C <sub>7</sub> mim]Cl <i>Mr</i> = 216.58		[C <sub>8</sub> mim]Cl <i>Mr</i> = 230.78	
100 w1	100 w2	100 w1	100 w2	100 w1	100 w2
54.039	2.245	49.164	4.570	48.964	4.640
50.037	2.943	46.036	5.467	46.616	5.599
46.376	3.518	42.213	6.747	42.090	7.098
42.669	4.363	36.094	8.979	38.460	8.185
40.734	4.920			32.220	10.669
39.139	5.343			30.624	11.230
34.186	7.139				

**Table D 2:** Experimental binodal curve and mass fraction compositions for the system IL + Na<sub>2</sub>SO<sub>4</sub> + H<sub>2</sub>O at 298 K.

[C <sub>4</sub> mim][CF <sub>3</sub> SO <sub>3</sub> ] <i>Mr</i> = 288.29				[C <sub>7</sub> H <sub>7</sub> mim]Cl <i>Mr</i> = 208.69	
100 w1	100 w2			100 w1	100 w2
55.957	1.742	15.200	6.486	52.119	3.459
49.416	2.184	14.489	6.971	46.554	4.804
42.662	2.545	12.249	7.804	40.895	6.141
34.874	3.111	11.548	8.233	37.642	7.216
32.697	3.374	11.010	8.508	33.469	8.885
30.563	3.644	10.031	9.111		
29.011	3.720	9.383	9.590		
27.770	3.993	8.829	10.178		
26.080	4.116	7.781	11.017		
24.786	4.326	7.124	11.627		
23.475	4.361	6.758	12.100		
22.857	4.509	5.826	13.242		
21.694	4.761	5.235	13.992		
20.616	5.001	4.646	14.956		
19.258	5.361	4.297	15.492		
17.943	5.642	3.879	16.222		
16.705	5.914	3.503	16.992		
16.043	6.150				

**Table D 3:** Experimental binodal curve and mass fraction compositions for the system IL + Na<sub>2</sub>SO<sub>4</sub> + H<sub>2</sub>O at 298 K.

[C <sub>4</sub> mim][TOS] <i>Mr</i> = 310.42					
100 w1	100 w2	100 w1	100 w2	100 w1	100 w2
55.113	2.197	19.397	11.255	11.239	14.492
52.339	2.637	19.050	11.426	10.871	14.705
49.096	2.892	18.596	11.531	10.518	14.874
47.612	3.188	18.292	11.668	10.371	14.978
45.586	3.412	17.971	11.814	10.175	15.076
44.347	3.743	17.611	12.010	10.010	15.244
43.047	4.083	17.409	12.038	9.880	15.272
40.476	4.722	17.182	12.123	9.662	15.403
38.394	5.230	16.891	12.282	9.453	15.540
36.588	5.600	16.415	12.469	9.254	15.664
35.800	5.793	16.224	12.492	9.037	15.805
35.029	6.008	15.925	12.663	8.619	16.041
34.144	6.317	15.735	12.708	8.326	16.232
33.392	6.527	15.576	12.744	8.095	16.367
32.564	6.722	15.416	12.805	7.905	16.481
31.945	6.934	15.174	12.936	7.528	16.753
31.286	7.103	15.006	12.972	7.282	16.904
30.643	7.271	14.792	13.091	6.957	17.135
30.008	7.396	14.579	13.207	6.621	17.415
29.402	7.572	14.360	13.312	6.282	17.651
28.845	7.747	14.230	13.329	6.077	17.823
28.312	7.915	13.999	13.472	5.963	17.927
26.539	8.557	13.879	13.496	5.751	18.148
25.875	8.877	13.686	13.595	5.454	18.389
25.520	8.940	13.382	13.720	5.253	18.597
24.958	9.155	13.258	13.751	5.101	18.727
24.438	9.372	13.157	13.797	4.919	18.887
24.047	9.498	12.971	13.907	4.830	18.997
23.591	9.644	12.854	13.933	4.644	19.210
22.808	9.888	12.692	14.030	4.339	19.514
22.245	10.169	12.526	14.122	4.087	19.777
21.207	10.492	12.247	14.097	3.834	20.156
20.842	10.630	12.133	14.133	3.621	20.379
20.465	10.777	11.768	14.237	3.433	20.652
20.058	10.996	11.466	14.366	3.283	20.802
19.751	11.086				

**Table D 4:** Experimental binodal curve and mass fraction compositions for the system IL + Na<sub>2</sub>SO<sub>4</sub> + H<sub>2</sub>O at 298 K.

[C <sub>4</sub> mim][N(CN) <sub>2</sub> ]					
<i>Mr</i> = 205.26					
100 w1	100 w2	100 w1	100 w2	100 w1	100 w2
59.251	0.599	18.934	9.451	6.790	16.014
54.869	1.101	18.450	9.610	6.549	16.284
51.855	1.614	17.981	9.775	6.431	16.386
47.900	1.966	17.765	9.848	6.320	16.525
45.730	2.355	14.851	11.048	6.138	16.701
43.248	2.673	14.693	11.088	5.950	16.907
41.487	3.022	14.471	11.236	5.749	17.110
39.764	3.322	14.196	11.335	5.319	17.916
38.715	3.649	14.063	11.367		
37.412	3.904	13.923	11.410		
35.952	4.171	13.717	11.571		
34.708	4.418	13.462	11.652		
33.951	4.670	13.165	11.809		
32.711	4.942	12.856	11.949		
31.958	5.187	12.657	12.036		
31.263	5.369	12.421	12.151		
30.331	5.489	12.274	12.262		
29.697	5.708	11.913	12.463		
29.112	5.874	11.740	12.511		
28.518	6.109	11.604	12.599		
27.970	6.317	11.387	12.720		
27.152	6.463	11.165	12.837		
26.597	6.661	10.965	12.953		
25.517	7.044	10.554	13.290		
25.039	7.217	10.260	13.381		
24.580	7.433	10.117	13.426		
24.157	7.579	10.015	13.506		
23.747	7.710	9.819	13.641		
23.333	7.849	9.624	13.790		
22.959	8.034	9.370	13.967		
22.275	8.267	9.047	14.168		
21.612	8.501	8.893	14.261		
20.968	8.706	8.710	14.426		
20.680	8.790	8.321	14.722		
20.373	8.873	8.082	14.868		
19.829	9.060	7.843	15.085		
19.565	9.148	7.451	15.400		
19.312	9.240	7.125	15.694		

**Table D 5:** Experimental binodal curve and mass fraction compositions for the system IL + Na<sub>2</sub>SO<sub>4</sub> + H<sub>2</sub>O at 298 K.

[C <sub>8</sub> py][N(CN) <sub>2</sub> ] <i>Mr</i> = 258.36				[C <sub>2</sub> mim][CF <sub>3</sub> SO <sub>3</sub> ] <i>Mr</i> = 260.24	
100 w1	100 w2	100 w1	100 w2	100 w1	100 w2
57.558	1.239	15.158	5.532	53.316	2.464
43.629	2.068	15.007	5.564	49.414	3.075
39.144	2.265	14.894	5.646	44.443	3.783
33.813	2.626	14.708	5.713	43.102	3.971
31.218	2.919	14.503	5.761	41.236	4.388
28.714	3.126	14.366	5.775	39.598	4.803
27.437	3.349	14.246	5.815	38.152	5.206
26.157	3.450	14.119	5.851	36.404	5.693
25.445	3.479	13.914	5.865	34.797	6.112
25.118	3.579	13.850	5.920	33.440	6.455
24.499	3.619	13.677	5.986	32.291	6.768
24.054	3.692	13.358	6.037	30.753	7.254
23.770	3.739	13.244	6.083	29.663	7.553
23.281	3.821	13.109	6.125	28.334	8.005
22.810	3.883	12.893	6.229	27.493	8.240
22.215	3.971	12.617	6.301	26.666	8.506
21.786	4.041	12.408	6.423	25.586	8.888
21.447	4.109	11.815	6.574	24.893	9.102
20.057	4.378	11.590	6.749	23.973	9.430
19.746	4.518	11.010	6.896	23.318	9.598
19.335	4.530	10.783	6.976	22.517	9.907
19.043	4.586	10.488	7.154	21.925	10.074
18.807	4.702	9.947	7.513	21.142	10.351
18.363	4.719	9.491	7.571	20.381	10.643
18.054	4.862	9.273	7.718	19.550	10.997
17.623	4.891	8.923	7.888	18.920	11.214
17.432	4.987	8.521	8.084	18.138	11.560
17.171	5.013	8.225	8.280	17.601	11.756
17.042	5.079	7.965	8.441	17.010	12.015
16.860	5.118	7.761	8.494	16.426	12.279
16.703	5.133	7.288	8.787	15.778	12.605
16.548	5.193	6.801	9.184	15.186	12.893
16.435	5.218	6.045	9.881	14.698	13.116
16.328	5.278	5.523	10.302	14.093	13.452
16.171	5.292	5.229	10.548	12.572	14.329
16.038	5.346	4.734	11.083	11.590	14.898
15.836	5.343	4.281	11.658	10.825	15.358
15.719	5.370	3.829	12.274	9.410	16.401
15.471	5.586	3.403	12.947	8.169	17.421

**Table D 6:** Experimental binodal curve and mass fraction compositions for the system IL + Na<sub>2</sub>SO<sub>4</sub> + H<sub>2</sub>O at 298 K.

[C <sub>7</sub> H <sub>7</sub> mim][C <sub>2</sub> H <sub>5</sub> SO <sub>4</sub> ] <i>Mr</i> = 298.36		[C <sub>4</sub> mim][CH <sub>3</sub> SO <sub>4</sub> ] <i>Mr</i> = 250.32		[C <sub>4</sub> mim][C <sub>2</sub> H <sub>5</sub> SO <sub>4</sub> ] <i>Mr</i> = 265.35	
100 <i>w</i> 1	100 <i>w</i> 2	100 <i>w</i> 1	100 <i>w</i> 2	100 <i>w</i> 1	100 <i>w</i> 2
53.325	2.856	53.318	3.127	56.885	1.750
50.037	3.461	46.121	4.436	41.987	4.250
46.107	4.032	40.626	5.431	39.097	5.030
44.440	4.251	38.709	5.907	36.809	5.847
43.172	4.520	37.260	6.521	34.510	6.438
41.480	5.053	34.647	7.461	33.315	6.880
40.560	5.306	33.481	7.965	30.874	7.808
39.592	5.515	32.400	8.401	29.510	8.403
38.323	5.862	31.375	8.818	27.694	9.197
37.513	6.048	30.064	9.483	26.378	9.856
36.273	6.435	28.620	10.203	25.056	10.566
33.795	7.444	27.569	10.706	22.221	12.114
32.349	7.958	26.467	11.281	18.628	14.283
30.732	8.520	24.877	12.146	17.313	15.024
29.664	8.897	23.222	13.149	15.724	16.019
28.767	9.163	22.076	13.776	14.248	16.951
27.353	9.743	20.872	14.489	12.380	18.173
26.479	10.055	19.588	15.258		
25.609	10.373	18.421	15.985		
24.307	10.924	17.405	16.602		
23.738	11.076	16.376	17.251		
22.720	11.495	15.476	17.820		
21.949	11.805	14.471	18.498		
20.877	12.255	13.697	19.017		
20.147	12.574	12.642	19.770		
19.486	12.846	11.653	20.482		
18.838	13.117	9.759	21.980		
18.180	13.320				
17.289	13.752				
16.819	13.952				
16.220	14.228				
15.662	14.468				
15.092	14.739				
14.573	14.996				
13.458	15.634				
12.753	15.986				
12.249	16.246				
10.512	17.270				

# **Appendix E**

## Experimental data of TL

**Table E1:** Weight fraction compositions for the coexisting phases at the TLs, and respective values of  $\alpha$  and TLL.

IL + Na <sub>2</sub> SO <sub>4</sub> + Water system	Weight fraction composition / wt%						$\alpha$	TLL
	Y <sub>T</sub>	X <sub>T</sub>	Y <sub>M</sub>	X <sub>M</sub>	Y <sub>B</sub>	X <sub>B</sub>		
[C <sub>2</sub> mim][CF <sub>3</sub> SO <sub>3</sub> ]	71.67	0.80	24.88	15.28	2.22	22.30	0.33	72.70
[C <sub>4</sub> mim]Br	37.42	5.91	25.66	15.03	10.57	26.73	0.56	33.98
[C <sub>4</sub> mim][TOS]	55.58	2.07	20.24	15.59	1.54	22.74	0.35	57.86
	74.68	0.54	33.65	14.24	0.61	25.26	0.45	78.09
[C <sub>4</sub> mim][CH <sub>3</sub> SO <sub>4</sub> ]	40.10	5.85	24.99	14.99	6.20	26.37	0.55	39.62
[C <sub>4</sub> mim][C <sub>2</sub> H <sub>5</sub> SO <sub>4</sub> ]	36.82	5.74	25.71	15.36	0.47	37.19	0.69	48.07
[C <sub>4</sub> mim][N(CN) <sub>2</sub> ]	59.77	0.79	24.94	15.14	0.37	25.26	0.41	64.25
[C <sub>4</sub> mim][CF <sub>3</sub> SO <sub>3</sub> ]	33.31	3.16	24.46	14.77	2.91×10 <sup>-14</sup>	46.84	0.73	54.93
[C <sub>7</sub> mim]Cl	31.29	10.89	25.03	14.85	1.43	29.75	0.79	35.32
[C <sub>8</sub> mim]Cl	36.91	8.91	27.24	14.89	0.28	31.58	0.74	43.08
[C <sub>7</sub> H <sub>7</sub> mim]Cl	33.63	8.77	27.90	12.13	10.22	22.49	0.51	27.13
	36.06	7.84	24.62	15.05	5.82	26.90	0.62	35.74
[C <sub>7</sub> H <sub>7</sub> mim][C <sub>2</sub> H <sub>5</sub> SO <sub>4</sub> ]	55.86	2.34	24.92	15.18	2.22	24.60	0.42	58.08
	60.95	1.70	31.82	14.26	0.91	27.58	0.51	65.39
[C <sub>8</sub> py][N(CN) <sub>2</sub> ]	69.11	0.93	24.57	15.36	0.31	23.23	0.35	72.32
	73.41	0.82	31.46	14.07	0.26	23.92	0.51	76.71

<sup>a</sup>standard deviation

# **Appendix F**

## Experimental data for the gallic acid partition coefficients

**Table F 1:** Experimental weight fraction composition and partition coefficients of gallic acid in ILs + Na<sub>2</sub>SO<sub>4</sub> ATPS at 298.15 K.

IL + Na <sub>2</sub> SO <sub>4</sub> + water system	Weight fraction composition / wt %		$K_{GA} \pm \sigma^a$
	IL	Na <sub>2</sub> SO <sub>4</sub>	
[C <sub>2</sub> mim][CF <sub>3</sub> SO <sub>3</sub> ]	24.88	15.28	10.25 ± 0.01
[C <sub>4</sub> mim][CF <sub>3</sub> SO <sub>3</sub> ]	24.46	15.37	20.73 ± 1.33
[C <sub>4</sub> mim]Br	24.99	15.04	18.12 ± 0.10
[C <sub>4</sub> mim][N(CN) <sub>2</sub> ]	24.94	15.14	21.23 ± 0.14
[C <sub>4</sub> mim][CH <sub>3</sub> SO <sub>4</sub> ]	24.99	14.99	20.84 ± 0.95
[C <sub>4</sub> mim][C <sub>2</sub> H <sub>5</sub> SO <sub>4</sub> ]	25.71	15.36	29.58 ± 1.19
[C <sub>7</sub> mim]Cl	25.03	14.85	21.94 ± 1.57
[C <sub>8</sub> mim]Cl	26.50	15.06	19.39 ± 0.19

<sup>a</sup>standard deviation

**Table F 2:** Experimental weight fraction composition and partition coefficients of gallic acid in ILs + K<sub>3</sub>PO<sub>4</sub> ATPS at 298.15 K.

IL + K <sub>3</sub> PO <sub>4</sub> + water system	Weight fraction composition / wt %		$K_{GA} \pm \sigma^a$
	IL	K <sub>3</sub> PO <sub>4</sub>	
[C <sub>2</sub> mim][CF <sub>3</sub> SO <sub>3</sub> ]	24.92	15.03	0.576 ± 0.191
[C <sub>4</sub> mim][CF <sub>3</sub> SO <sub>3</sub> ]	25.09	15.00	0.175 ± 0.007
[C <sub>7</sub> mim]Cl	24.74	14.96	8.162 ± 0.362

<sup>a</sup>standard deviation

**Table F 3:** Experimental weight fraction composition and partition coefficients of gallic acid in ILs + K<sub>2</sub>HPO<sub>4</sub>/ KH<sub>2</sub>PO<sub>4</sub> ATPS at 298.15 K.

IL + K <sub>2</sub> HPO <sub>4</sub> /KH <sub>2</sub> PO <sub>4</sub> + water system	Weight fraction composition / wt %		$K_{GA} \pm \sigma^a$
	IL	K <sub>2</sub> HPO <sub>4</sub> /KH <sub>2</sub> PO <sub>4</sub>	
[C <sub>2</sub> mim][CF <sub>3</sub> SO <sub>3</sub> ]	25.01	15.00	0.909 ± 0.052
[C <sub>4</sub> mim][CF <sub>3</sub> SO <sub>3</sub> ]	24.99	15.13	0.763 ± 0.003
	30.01	15.05	4.253 ± 0.172
[C <sub>7</sub> mim]Cl	29.97	15.00	11.586 ± 1.000

<sup>a</sup>standard deviation